Modelling Markovian epidemic and information diffusion over adaptive networks

Massimo Achterberg

TU Delft
Delft University of Technology

TU Delft

Modelling Markovian epidemic and information diffusion over adaptive networks

by

Massimo Alessandro Achterberg

to obtain the degree of Master of Science
at the Delft University of Technology,
to be defended publicly on July 9, 2019 at 10:00.

Student number:	4391136	
Project duration:	December 15, 2018 – July 9, 2019	
Thesis committee:	dr. J. L. A. Dubbeldam,	TU Delft, supervisor
	dr. Y. van Gennip,	TU Delft
	Prof. dr. ir. P. Van Mieghem,	TU Delft

Preface

I would like to thank a few people that mean a lot to me. I would like to thank my study mates Carlos, Rick, Marco, Pieter, Roel and Mike for making the student life a more enjoyable period. Especially the lunch-break card playing sessions were fun while writing my master thesis. Also, I would like to thank Rick Hegeman, Carlos Hermans and my parents for proofreading my thesis and Dennis van Duin for his design of the front page of my thesis.

Furthermore, I would like to thank my supervisor Johan Dubbeldam for his tremendous support throughout this period. His enthusiasm motivated me to continue working on the project, which was very nice. Also many thanks to Piet Van Mieghem from the faculty of Electrical Engineering for his effortless proofreading of chapter 3 of my thesis, what is planned to become my first scientific paper.

Finally, I wish to thank my family for their support throughout my study. Without their help, studying mathematics would not have been such a wonderful experience.

Delft, July 2019

Abstract

Modelling the spread of contagious diseases among people has been a research topic for over a hundred years. However, the increase in computation power in the recent years allows for more advanced scientific models. The well-known susceptible-infected-susceptible model is used to describe the spreading of a disease among a group of people. This is modelled as a network, where persons are represented by nodes and their connections are links in the network. In this thesis, instead of a typical static network, the network itself changes structure based on the disease states of the nodes. In other words, there are two independent processes; the spreading of the disease over the network (state of the nodes) and the adaption of the network to the disease (state of the links). As a spreading model, the Markovian adaptive susceptible-infected-susceptible model (ASIS model for short) is introduced. It is shown that the model has one steady state, named the trivial steady state, in which all individuals are healthy. When the infection rate is sufficiently high, the system undergoes a phase transition from the disease-free state to an endemic state, where most nodes are infected. The state where most nodes are infected is named the metastable state. After being in the metastable state for a long time, the system collapses to the trivial steady state.

The spreading of contagious processes is not just limited to disease spreading. Other relevant examples, such as opinion, gossip, fake news, neuron transmittance in the brain, etc. can be modelled using adaptive models as well. In this thesis, the ASIS model is extended by allowing different rules for the link-breaking and link-creation processes in what we call the Generalised ASIS framework. In total 36 models have been analysed simultaneously. Out of the 36 models, 9 showed a partially unstable metastable state. This resulted in rapid oscillations of the number of infected nodes just above the epidemic threshold. The relation between the epidemic threshold and the effective link-breaking rate was also determined. For 5 cases, the epidemic threshold is independent of the effective link-breaking rate. In 18 cases, the epidemic threshold scales linearly in the link-breaking rate. The remaining 13 cases are bounded between a constant and a linear link-breaking rate, however, its exact dependence remains unclear.

In the G-ASIS framework, it was conjectured that the metastable state of the Markov process can be accurately approximated by the steady state of the mean-field approximation. It was shown this is not true for every model. However in the ASIS model, the mean-field approximation showed close resemblance to the averaged stochastic results. This may be caused by a positive correlation between the nodes. For the other models, the deviation from the mean field approximation can probably be contributed to the fact that nodes are not positively correlated. Other higher order mean field approximations should be examined to approximate the averaged behaviour of the Markov process.

Contents

Introduction

The current healthcare system originates from several centuries ago. The ancient Romans already knew how diseases could be prevented. Their aqueducts were very famous, bringing fresh water to the large cities in the empire for public baths, latrines (toilets) and others [1]. By the availability of fresh water, these aqueducts prevented the spreading of many contagious diseases. Nowadays, many advances have been made in the healthcare system, including the development of all types of medicine, vaccinations, hospitals, and much more. Still, many contagious diseases occasionally result into epidemics where a large part of the population is infected with the disease. For example, in 2009 the swine flu broke out in Mexico, and it quickly spread to the entire world. In total, thousands of people lost their lives and millions have been infected [2]. To be able to prevent outbreaks in the future, it is highly important to investigate how and at which rate a disease spreads amongst people.

Already in 1766, Daniel Bernoulli invented mathematical tools to model the spread of infectious diseases [3]. The main aim of this field of research, named epidemiology, is to model the spreading of the disease and to discover how effective vaccinations, quarantines, and other measures are in preventing the spread of the disease [4]. A very basic model has been invented in 1932 by Kermack and McKendrick [5]. They split up the population in various compartments. Each compartment is assumed to be perfectly mixed, making all individuals in this group equal and indistinguishable, and each individual has the same connect pattern. They introduced the susceptible-infected-resistant model (SIR model) in which there is a compartment (group) of healthy, but susceptible people (S), a group of people who are infected with the disease and can spread it to susceptible (I) and a group who have become resistant to the disease (R). People transfer from one group to another by two processes: infected people infect susceptible people with a certain rate and infected people become resistant to the disease with a certain rate. Diseases like measles and whooping cough are known to be modelled accurately using the SIR model [6]. A related model is the susceptible-infected-susceptible (SIS) model, where people cannot become resistant to the disease, but instead become susceptible again after curing. Influenza is a common example which can be modelled accordingly [7]. These two models form the basis of epidemiological modelling. Although the original SIS model formulation has proven to be successful at modelling diseases like sexually transmittable diseases [6], it fails to accurately model others.

A major aspect which these models fail to address is the local interaction between people. The compartments S, I (and R) are assumed to be mixed perfectly. This is never the case, but for some diseases, more local interactions are required than for others. To solve this issue, agent-based models have been developed, where every individual is represented by a node in a large network of connections. Just as before, every individual is labelled to be susceptible, infected or resistant to the virus. In these networks, susceptible nodes can be infected by infected nodes with a certain probability. Curing can either take place after a fixed time [8] or with a certain probability [9]. Most importantly, people can only infect people whom they are connected to. This allows for a far more local behaviour of disease spreading. In cities, every individual can be modelled separately, allowing to model population groups like children, elderly, working class and others separately. For example, elderly and children are more common to adopt the flu. In this formulation, each member of the community receives a different infection and curing rate. Using this approach, the impact of the disease on specific neighbourhoods can be predicted. The modelling of diseases over contact networks was initialised in the early 2000s and is called *network epidemiology* [10]. In literature, for several contact networks numerous key properties have been derived, such as the point from which an endemic might develop [11], the effectiveness of vaccination [12], quarantining [13] and many others.

Most models considered in network epidemiology consider the underlying contact network to be static or varying autonomously over time. Some diseases, like AIDS and influenza, are known to be modelled accurately using this assumption [13]. Still, other diseases exist for which the interplay between the disease and the network is vitally important, especially due to a quickly evolving network [14]. For these types of diseases, Gross *et al.* (2006) invented a new model where the network adapts to the healthiness of the individual in the network [15]. This model is called an *adaptive network* as the interplay between the individuals and the network is strong. The connections between susceptible and infected people are broken to prevent the further spreading of the disease. This behaviour, also known as social distancing [16], has been observed in modern day life. People tend to avoid infected people in order to prevent

themselves from getting infected. On the other hand, infected people are generally not feeling well and stay at home. This automatically decreases their number of connections. The total number of connections in the network is sometimes kept constant by letting links between susceptible and infected nodes rewire such that the susceptible is linked to another random susceptible [13].

Just recently, Trajanovski *et al.* (2015) have observed that besides the spreading of diseases, the model formulation can be used in a slightly different form for spreading information amongst people [17]. The spreading process is similar; upon contact, people can influence and can get influenced by others. They may also forget the information (comparable to curing). An important difference is that without any connections, people can get information from themselves (decide for themselves to change their mind) which is impossible for disease-spreading. Classic examples of information spreading include gossip in the real world and social media interaction on the Internet. In both scenarios, information is spread over a network of social interactions and the information is released/forgotten after some time. The adaptive network formulation can be relevant to model the influence of news sites and famous people on certain population groups. In particular, information acquired from Facebook was accurately modelled using this framework [17]. In the future, this framework may be used to predict the influence and spreading of disinformation (more commonly known as fake news), online manipulation, rumours [18], radicalisation (both offline and online) and many other processes where information spreading is involved.

Information spreading and disease modelling are just two examples of the possible fields of application of adaptive networks. In all models, a local rule between two connected agents gives rise to a global change in the behaviour of the process running over the network. It is expected that many other phenomena can be modelled using similar models. A recent study utilises adaptive networks to model large-scale interactions in the human brain [19]. These interactions, which are structural connections in the brain, may be active or inactive at any moment. Therefore these interactions can be modelled as adaptive links in the brain network. Examples of application areas include Alzheimer's disease, Parkinson's disease, epilepsy, brain tumors and multiple sclerosis.

Since it is to be expected that more physical properties can be modelled in the same model formulation, it is necessary to explore the framework of spreading over a network, where the links in the network change depending on the state of the end nodes of a link. One of the main topics of interest is the existence of steady states. A steady state is a state of the system which does not change over time. Another relevant aspect is the point where the disease or information spread changes from a local rumour or small number of infected people to a large topic of discussion or a world-wide epidemic. This bifurcation point, often defined by parameters in the model, allows researchers to predict in early stages how large the final outbreak will be.

In this thesis, spreading theory over adaptive networks is investigated. The main research question is:

> Can the bifurcation point where the spreading develops into an endemic be predicted accurately for Markovian, adaptive spreading models?

The first chapter is devoted to a thorough explanation of the stochastic disease-spreading model. It includes a derivation of the relevant differential equations for the model as well as definitions for key concepts of the model. Chapter 2 shows numerical results for the spreading of epidemics. The models introduced in Chapter 1 are tested for robustness, accuracy, and correctness. Then, in Chapter 3, a more general stochastic framework is introduced. This framework models many types of information spreading, ranging from epidemics to information to brain models. Several results are derived by doing extensive computations, where the focus is laid on the stability of the model. The chapter includes many examples and contains simulation results for each of these examples. Then the obtained results are discussed. The thesis ends with a conclusion.

This master thesis is written as a part of the master Applied Mathematics at Delft, University of Technology, The Netherlands.

1 Theory epidemics

The modelling of epidemics on adaptive networks will be the main subject of this chapter. At first, the Markov process corresponding to the spreading of diseases over the adaptive network is explained in section 1.1. Thereafter, differential equations will be derived from the Markov process. In section 1.3 rescaling of the differential equations takes place. Then, in 1.4, the derived equations are discussed and alternative models are presented. In 1.5 the steady states of the models are analysed and compared. This allows us to introduce the metastable state in section 1.6. The results are summarised in the final section.

1.1 The Markov process

Consider a population of N individuals. Each individual is represented by a node v. Every individual has connections to other individuals, which are modelled as links. The nodes and links form a network $\mathcal{G} = (\mathcal{N}, \mathcal{L})$ where $\mathcal{N}$ is the set of nodes and $\mathcal{L}$ the set of links. The network $\mathcal{G}$ can be written in terms of an adjacency matrix A as follows. When a connection between node i and j exists, then $a_{ij} = 1$ and zero otherwise. Then the network can be rewritten in terms of its adjacency matrix A, which contains the links of all interactions between the nodes. In this model, the connection between i and j is equal to the connection between j and i, hence the adjacency matrix A is symmetric. Also, we assume i and j have at most one connection, and i cannot have a connection with itself ($a_{ii} = 0, \forall i$). In network theory, this means the network is simple and contains no self-loops.

The processes governing the dynamics on the network and the dynamics of the network will be considered Markovian. This means the decision to cure, infect, break links and create links only depends on the current state of the nodes and the network but not on the past.

Every individual is either infected or healthy. Therefore each individual is modelled as a Bernoulli random variable. If $X_i(t) = 1$ node i is infected at time t, and if $X_i(t) = 0$, the node is healthy. When an individual is infected, it can be cured spontaneously with rate δ of a Poisson process. We recall the Poisson distribution with parameter λ as

$$\mathbb{P}(X = k) = e^{-\lambda}\frac{\lambda^k}{k!}, \tag{1.1}$$

where λ is the parameter of the Poisson distribution. We want to model the probability of making one transition, i.e. $k = 1$, in a small time step Δt. Since λ is proportional to Δt, Eq. (1.1) can be expanded

$$\mathbb{P}(X = 1) = \lambda e^{-\lambda} = \lambda + \mathcal{O}(\lambda^2). \tag{1.2}$$

The probability of making two transitions can be computed, and is assumed to be of order $\mathcal{O}(\lambda^2)$, so the probability of making no transition is assumed to be $1-\lambda+\mathcal{O}(\lambda^2)$. This simplification immediately gives some constraints on λ, namely $\lambda \ll 1$. During numerical simulations, it is necessary that this condition is satisfied to guarantee meaningful results.

When an individual is healthy, it can be infected by its infected neighbours. We assume the infection to be a Poisson process with rate β. The curing and infection processes are independent processes. Schematically, the following two changes on X_i can take place

$$X_i : \begin{cases} 0 \to 1 & \text{infection by } j \text{ when } X_j = 1, a_{ij} = 1, X_i = 0 \text{ with rate } \beta, \\ 1 \to 0 & \text{curing when } X_i = 1 \text{ with rate } \delta. \end{cases}$$

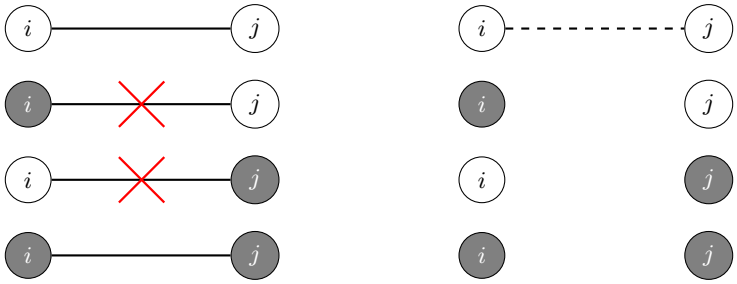

Figure 1.1: Schematic view of two connected nodes. Infected nodes are grey, healthy nodes are white. The link between i and j is broken (left) when X_i is not equal to X_j. The link is recreated (right) when $X_i = X_j = 0$.

Written in terms of transition probabilities, it can be represented as a Markov process;

$$\begin{aligned} \mathbb{P}(X_i(t+\Delta t) = 1 \,|\, X_i(t) = 0, a_{ij}(t) = 1, X_j(t) = 1) = \beta \Delta t \qquad &\text{infection,} \\ \mathbb{P}(X_i(t+\Delta t) = 0 \,|\, X_i(t) = 1) = \delta \Delta t \qquad &\text{curing.} \end{aligned} \tag{1.3}$$

This Markov chain is used to model the infection spread over the network. The model considered here is adaptive, and will therefore change structure based on the well-being of the people. It is highly important to note that no links will be created other than initially existing links. A link between person i and j can be broken when person i is infected and j is healthy or vice-versa. The link-breaking process is modelled as a Poisson process with rate ζ. Naturally, it is also required that $a_{ij}(t) = 1$ and $a_{ij}(0) = 1$. When person i and j are healthy, the link can be restored (created). The link-creation process is a Poisson process with rate ξ, which applies when $X_i(t) = X_j(t) = 0$. When both individuals are infected, i.e. $X_i(t) = X_j(t) = 1$, the link is left unchanged.

The link-breaking and link-creation process can be justified intuitively. The last rule, where it is assumed that the link is preserved when $X_i(t) = X_j(t) = 1$, is most controversial. Another relevant model (in which the link between two infected nodes is removed) is discussed in more detail in Chapter 3.

The link-breaking and link-creation processes can be summarised as

$$a_{ij} : \begin{cases} 1 \to 0 & \text{link breaking when } X_i \neq X_j, a_{ij} = 1, a_{ij}(0) = 1 \text{ with rate } \zeta, \\ 0 \to 1 & \text{link creation when } X_i = X_j = 0, a_{ij} = 0, a_{ij}(0) = 1 \text{ with rate } \xi. \end{cases}$$

A visualisation is given in Figure 1.1. In terms of transition probabilities,

$$\begin{aligned} \mathbb{P}(a_{ij}(t+\Delta t) = 0 \,|\, X_i(t) \neq X_j(t), a_{ij}(t) = 1, a_{ij}(0) = 1) = \zeta \Delta t \qquad &\text{link breaking,} \\ \mathbb{P}(a_{ij}(t+\Delta t) = 1 \,|\, X_i(t) = X_j(t) = 0, a_{ij}(t) = 0, a_{ij}(0) = 1) = \xi \Delta t \qquad &\text{link creation.} \end{aligned} \tag{1.4}$$

The equations (1.3) and (1.4) with initial conditions for X_i and a_{ij} form a Markov chain. This model is called the adaptive-SIS model in literature, or ASIS for short [11]. Generally, random initial conditions can be taken for X_i and an initial structure for a_{ij} needs to be supplied. Throughout this thesis, the initial network is taken to be a complete network. This means that each node is connected to all other nodes in the network.

It is important to note that the Markov chain contains all possible states the system can be in. Hence, every link l in the initial network $A(0)$ and every node v has two possible values: zero and one. This brings us to 2^{N+L} possible Markov states, where N is the number of nodes and L the number of links. In general, time is taken to be continuous throughout this thesis. This means we have a continuous-time discrete-state-space Markov process, commonly abbreviated as CTMC. Simulations will however be performed using a discrete-time Markov process, which is called a Markov chain.

As shown in the next section, the Markov states are hard to enumerate. In literature, a more convenient way of enumerating all Markov states is known [20]. This construction is however based on many variables with sub- and superscripts. Since this thesis does not require this enumeration, this approach is not used.

Although the Markov process is a valid representation of the stochastic process, it is sometimes inconvenient to use. For example, it is hard to perform calculations to show there exist states which are

approximately constant over time. Therefore we will derive the master equation for the Markov process, and subsequently find differential equations for the evolution of the average of the random variables.

1.2 Derivation of the master equation

The master equation of a Markov process is the change in probability of being in a specific state of the Markov process. The master equation will first be derived for 2 nodes, whereafter the general case is examined.

1.2.1 2 connected nodes

We consider two initially connected nodes, i.e. $a_{12}(0) = 1$. This Markov process has three random variables X_1, X_2 and a_{12}. Each of them is Bernoulli distributed, thus is allowed to be zero or one. Hence there are $2^3 = 8$ possible states. Using the notation (X_1, X_2, a_{12}), these are: $(0,0,0), (0,0,1), (0,1,0)$, $(0,1,1)$, $(1,0,0), (1,0,1)$, $(1,1,0), (1,1,1)$.

Each of the states makes transitions to other states defined by Eqs. (1.3) and (1.4). For example, consider the $(1,1,1)$ state. We will allow, over a time of Δt, the system to make only one transition. There are three options: (I) the system remains in the $(1,1,1)$ state, (II) X_1 is infected by X_2 or (III) X_2 is infected by X_1. So, for a time $t + \Delta t$, we have the following;

$$\begin{aligned}\mathbb{P}((1,1,1)(t+\Delta t)) = \mathbb{P}((1,1,1)(t))\mathbb{P}(\text{stay in } (1,1,1)) + \\ \mathbb{P}((0,1,1)(t))\mathbb{P}(\text{jump to } (1,1,1)) + \mathbb{P}((1,0,1)(t))\mathbb{P}(\text{jump to } (1,1,1)).\end{aligned}$$

Since we have a Markov process, the probability of jumping to another state is independent of the current time. Moreover, this probability is given in Eqs. (1.3) and (1.4), such that

$$\mathbb{P}((1,1,1)(t+\Delta t)) = \mathbb{P}((1,1,1)(t))(1-2\delta\Delta t) + \mathbb{P}((0,1,1)(t))\beta\Delta t + \mathbb{P}((1,0,1)(t))\beta\Delta t + \mathcal{O}(\Delta t^2). \quad (1.5)$$

The term $\mathcal{O}(\Delta t^2)$ corresponds to states making multiple transitions over the time span Δt. Their probability will be small, as we will take $\lim_{\Delta t \to 0}$. Therefore these transitions are considered of higher order and are collected in this term.

This procedure can be repeated for all states, leading to a set of linear difference equations of the form

$$y^{t+\Delta t} = P y^t,$$

where P is the *transition matrix* defining all probabilities of making a transition from one state to another. The following transition matrix is obtained;

$$\begin{array}{c} \begin{array}{cccccccc} (0,0,0) & (0,0,1) & (0,1,0) & (0,1,1) & (1,0,0) & (1,0,1) & (1,1,0) & (1,1,1) \end{array} \\ \begin{pmatrix} 1-\xi\Delta t & \xi\Delta t & & & & & & \\ & 1 & & & & & & \\ \delta\Delta t & & 1-\delta\Delta t & & & & & \\ & \delta\Delta t & \zeta\Delta t & 1-(\delta+\beta+\zeta)\Delta t & & & & \beta\Delta t \\ \delta\Delta t & & & & 1-\delta\Delta t & & & \\ & \delta\Delta t & & & \zeta\Delta t & 1-(\delta+\beta+\zeta)\Delta t & & \beta\Delta t \\ & & \delta\Delta t & & \delta\Delta t & & 1-2\delta\Delta t & \\ & & & \delta\Delta t & & \delta\Delta t & & 1-2\delta\Delta t \end{pmatrix} \end{array}$$

All zeros in the matrix have been omitted for readability. The matrix P is a stochastic matrix; every row adds up to one as every state needs to make a transition to another state.

We can rearrange Eq. (1.5) such that

$$\frac{\mathbb{P}((1,1,1)(t+\Delta t)) - \mathbb{P}((1,1,1)(t))}{\Delta t} = -2\delta\mathbb{P}((1,1,1)(t)) + \beta\mathbb{P}((0,1,1)(t)) + \beta\mathbb{P}((1,0,1)(t)) + \mathcal{O}(\Delta t).$$

To find a differential equation for $\mathbb{P}(1,1,1)$, the limit $\lim_{\Delta t \to 0}$ is taken;

$$\frac{d\mathbb{P}(1,1,1)}{dt} = -2\delta\mathbb{P}(1,1,1) + \beta\mathbb{P}(0,1,1) + \beta\mathbb{P}(1,0,1).$$

This procedure can be repeated for every state. These equations are called the *master equations* of the Markov process and govern the complete behaviour of the Markov process [21]. This Markov process is finite, i.e. it contains a finite number of states. This allows for the calculation of the matrix P. In practice, we will see the computation is infeasible for a network with more than 10 nodes.

By rewriting the system in continuous time, the transition matrix P changes as well. The continuous-time version of P, denoted by $\tilde{P}$, can be computed for every state;

$$\tilde{P} = \begin{pmatrix} -\xi & \xi & & & & & & & \\ & 0 & & & & & & & \\ \delta & & -\delta & & & & & & \\ & \delta & \zeta & -\delta-\beta-\zeta & & & & & \beta \\ \delta & & & & -\delta & & & & \\ & \delta & & & \zeta & -\delta-\beta-\zeta & & & \beta \\ & & \delta & & \delta & & -2\delta & & \\ & & & \delta & & \delta & & -2\delta & \end{pmatrix}. \tag{1.6}$$

Although the master equation has been derived, more can be done. For example, we may exploit an important property of Bernoulli random variables: $\mathbb{P}(X = 1) = \mathbb{E}(X)$. This allows us to write the master equation in a different way. We will first introduce some notation to denote marginal probabilities. The following notation is used to denote the probability of being in the state $X_1 = 1$, $X_2 = 1$;

$$\mathbb{P}(1, 1, -) = \mathbb{P}(X_1 = 1, X_2 = 1) = \sum_{k\in\{0,1\}} \mathbb{P}(X_1 = 1, X_2 = 1, a_{12} = k),$$

where the dash in $\mathbb{P}(1, 1, -)$ indicates that we have summed over this variable, which is a_{12} in this case. Using the stochastic matrix $\tilde{P}$ from Eq. (1.6), we find

$$\begin{aligned} \frac{d\mathbb{P}(1,1,-)}{dt} &= \sum_{k\in\{0,1\}} \frac{d\mathbb{P}(1,1,k)}{dt} \\ &= \beta\mathbb{P}(0,1,1) + \beta\mathbb{P}(1,0,1) - 2\delta\mathbb{P}(1,1,0) - 2\delta\mathbb{P}(1,1,1). \end{aligned}$$

The same can be done for $\mathbb{P}(1, 0, -)$;

$$\frac{d\mathbb{P}(1,0,-)}{dt} = -\delta\mathbb{P}(1,0,0) + (-\delta-\beta)\mathbb{P}(1,0,1) + \delta\mathbb{P}(1,1,0) + \delta\mathbb{P}(1,1,1).$$

The procedure can be repeated up to the higher level. For example, for $\mathbb{P}(1, -, -)$, we find

$$\begin{aligned} \frac{d\mathbb{P}(1,-,-)}{dt} &= \sum_{k\in\{0,1\}} \frac{d\mathbb{P}(1,k,-)}{dt} \\ &= \beta\mathbb{P}(0,1,1) - \delta\mathbb{P}(1,0,0) - \delta\mathbb{P}(1,0,1) - \delta\mathbb{P}(1,1,0) - \delta\mathbb{P}(1,1,1). \end{aligned}$$

The left hand side (LHS) is equal to $\mathbb{P}(1, -, -) = \mathbb{P}(X_1 = 1) = \mathbb{E}(X_1)$ where we have used the Bernoulli property and the right hand side (RHS) can also be written in terms of expectation values.[1] So

$$\begin{aligned} \frac{d\mathbb{E}(X_1)}{dt} = \beta\mathbb{E}((1-X_1)X_2a_{12}) - \delta\mathbb{E}(X_1(1-X_2)(1-a_{12})) - \delta\mathbb{E}(X_1(1-X_2)a_{12}) \\ - \delta\mathbb{E}(X_1X_2(1-a_{12})) - \delta\mathbb{E}(X_1X_2a_{12}). \end{aligned}$$

This can be rearranged to

$$\frac{d\mathbb{E}(X_1)}{dt} = -\delta\mathbb{E}(X_1) + \beta\mathbb{E}(a_{12}(1-X_1)X_2). \tag{1.7}$$

[1] For example, $\mathbb{P}(1,1,1) = \mathbb{P}(X_1 = 1, X_2 = 1, a_{12} = 1) = \mathbb{P}(X_1 = X_2 = a_{12} = 1) = \mathbb{P}(X_1X_2a_{12} = 1) = \mathbb{E}(X_1X_2a_{12})$.

Since individuals are interchangeable, we find the same equation for X_2 (where of course every X_1 is interchanged for X_2 and vice versa). Lastly, we wish to construct the same equations for the network structure.

$$\begin{aligned}\frac{d\mathbb{E}(a_{12})}{dt} &= \frac{d\mathbb{P}(a_{12}=1)}{dt} = \frac{d\mathbb{P}(-,-,1)}{dt} \\ &= \sum_{k\in\{0,1\}}\sum_{l\in\{0,1\}} \frac{d\mathbb{P}(k,l,1)}{dt} \\ &= \xi\mathbb{P}(0,0,0) - \zeta\mathbb{P}(0,1,1) - \zeta\mathbb{P}(1,0,1) \\ &= \xi\mathbb{E}((1-a_{12})(1-X_1)(1-X_2)) - \zeta\mathbb{E}((1-X_1)X_2a_{12}) - \zeta\mathbb{E}((X_1)(1-X_2)a_{12}).\end{aligned}$$

The latter can be reshaped into

$$\frac{d\mathbb{E}(a_{12})}{dt} = \mathbb{E}(-\zeta a_{12}(X_1-X_2)^2 + \xi(1-a_{12})(1-X_1)(1-X_2)). \tag{1.8}$$

This completes the derivation of the first-order expectation-differential equations. It is however possible to compute higher orders as well. This might be useful, as the correlation between X_1 and X_2, i.e. $\mathbb{E}(X_1X_2)$ is still undefined. The evolution of the correlation term $\mathbb{E}(X_1X_2)$ can be derived from the Markov process using the same procedure as before. This leads to

$$\begin{aligned}\frac{d\mathbb{E}(X_1X_2)}{dt} &= \frac{d\mathbb{P}(X_1X_2=1)}{dt} = \frac{d\mathbb{P}(X_1=1,X_2=1)}{dt} \\ &= \frac{d\mathbb{P}(1,1,-)}{dt} = \sum_{k\in\{0,1\}} \frac{d\mathbb{P}(1,1,k)}{dt} \\ &= \beta\mathbb{P}(0,1,1) + \beta\mathbb{P}(1,0,1) - 2\delta\mathbb{P}(1,1,0) - 2\delta\mathbb{P}(1,1,1) \\ &= \beta\mathbb{E}((1-X_1)X_2a_{12}) + \beta\mathbb{E}(X_1(1-X_2)a_{12}) - 2\delta\mathbb{E}(X_1X_2(1-a_{12})) - 2\delta\mathbb{E}(X_1X_2a_{12}) \\ &= -2\delta\mathbb{E}(X_1X_2) + \beta\mathbb{E}(a_{12}(X_1+X_2-2X_1X_2)).\end{aligned}$$

The reason for the computation of correlation terms is follows. The expectation-differential equations can be used to derive analytical properties of the given Markov process. It might be interesting to investigate to which extent the expectation-differential equations exhibit the same (stochastic) behaviour as the Markov process. It is also necessary to investigate whether their steady states and their stability are equivalent. When regarding only the first order expectation-differential equations, it is not possible to view these equations as a genuine set of equations, but only as a first step. Information is omitted, such as the evolution of $\mathbb{E}(X_1X_2)$ over time. Deriving explicit differential equations for the correlations solves this problem in a few steps, as the maximum order for correlation terms is 3 (for $\mathbb{E}(X_1X_2a_{12})$) due to the Bernoulli property. Therefore we finish the computation of the other correlation terms;

$$\begin{aligned}\frac{d\mathbb{E}(X_1a_{12})}{dt} &= \frac{d\mathbb{P}(X_1a_{12}=1)}{dt} = \frac{d\mathbb{P}(X_1=1,a_{12}=1)}{dt} \\ &= \frac{d\mathbb{P}(1,-,1)}{dt} = \sum_{k\in\{0,1\}} \frac{d\mathbb{P}(1,k,1)}{dt} \\ &= \beta\mathbb{P}(0,1,1) - (\delta+\zeta)\mathbb{P}(1,0,1) - 2\delta\mathbb{P}(1,1,0) - \delta\mathbb{P}(1,1,1) \\ &= \beta\mathbb{E}((1-X_1)X_2a_{12}) - (\delta+\zeta)\mathbb{E}(X_1(1-X_2)a_{12}) - 2\delta\mathbb{E}(X_1X_2(1-a_{12})) - \delta\mathbb{E}(X_1X_2a_{12}) \\ &= (\zeta-\beta)\mathbb{E}(X_1X_2a_{12}) - (\delta+\zeta)\mathbb{E}(X_1a_{12}) + \beta\mathbb{E}(X_2a_{12}).\end{aligned}$$

Due to symmetry, the equation for $\mathbb{E}(X_2a_{12})$ can be computed analogously. The final equation is;

$$\begin{aligned}\frac{d\mathbb{E}(X_1X_2a_{12})}{dt} &= \frac{d\mathbb{P}(X_1X_2a_{12}=1)}{dt} = \frac{d\mathbb{P}(X_1=1,X_2=1,a_{12}=1)}{dt} = \frac{d\mathbb{P}(1,1,1)}{dt} = \\ &= \beta\mathbb{P}(0,1,1) + \beta\mathbb{P}(1,0,1) - 2\delta\mathbb{P}(1,1,1) \\ &= \beta\mathbb{E}((1-X_1)X_2a_{12}) + \beta\mathbb{E}(X_1(1-X_2)a_{12}) - 2\delta\mathbb{E}(X_1X_2a_{12}) \\ &= -2(\delta+\beta)\mathbb{E}(X_1X_2a_{12}) + \beta\mathbb{E}((X_1+X_2)a_{12}).\end{aligned}$$

The differential equations form a set of seven linear differential equations with seven variables. This simple example can be solved analytically, however, for a general number of nodes this is infeasible. The next section will investigate a general network of N nodes.

1.2.2 General network

The derivation in the previous section involved only two individuals. This section generalises the result to a general number of individuals, as the Markov process is valid for any number of individuals. Consider an individual i of the population N. Although not every node has the same connections (these depend on the initial network structure) we will see it is irrelevant in the derivation. The initial connections of node i are denoted by $a_{ij}(0)$. The total number of initial connections for the network is denoted by L_0. The following result was obtained.

Theorem 1.1. *For N nodes, the resulting differential equations are*

$$\frac{d\mathbb{E}(X_i)}{dt} = -\delta\mathbb{E}(X_i) + \beta \sum_{j=1, j\neq i}^{N} \mathbb{E}((1-X_i)X_j a_{ij}), \tag{1.9}$$

$$\frac{d\mathbb{E}(a_{ij})}{dt} = a_{ij}(0)E\Big[-\zeta a_{ij}(X_i - X_j)^2 + \xi(1-a_{ij})(1-X_i)(1-X_j)\Big]. \tag{1.10}$$

Proof. See Appendix 2. □

We will name Eqs. (1.9) and (1.10) the *expectation differential equations* (or EDE for short). These equations were posed in [11]. During the derivation, two assumptions have been made; from the Markov process to the master equation the focus is shifted from random variables to their probability. From the master equation to the EDEs, the main simplification is the negligence of higher order correlation terms. The latter simplification and its consequences are investigated in more detail in section 1.4.

The term $a_{ij}(0)$ in Eq. (1.10) merely indicates that the differential equation holds for initially existing links (i.e. $a_{ij}(0) = 1$), and that the link cannot be changed when $a_{ij}(0) = 0$. A more correct notation should be used where e.g. the statement 'if $a_{ij}(0) = 1$' is placed after the differential equation. Nevertheless, the current notation is maintained for brevity.

The EDEs give a non-stochastic representation of a purely stochastic model. This simplification needs to be inspected carefully, for example by the investigation of specific properties, like the steady states and their stability. This will be done for the equations derived in this section, but also for other equations which will be derived in section 1.4. This review will take place in section 1.5. Beforehand some general remarks about the EDEs are presented in the next section.

1.3 Model reformulation

In the previous section, the expectation-differential equations (EDEs) have been derived. A common approach is to make equations dimensionless, to possibly reduce the number of parameters and be able to more clearly investigate certain parameters. To that end, introduce a new time variable $\tilde{t} = t\delta$. Define

$$\tilde{\zeta} = \frac{\zeta}{\delta}, \quad \tilde{\xi} = \frac{\xi}{\delta}, \quad \tau = \frac{\beta}{\delta}, \quad \omega = \frac{\zeta}{\xi},$$

where τ is the effective infection rate and ω the effective link-breaking rate. This simplifies the equations (after dropping the tilde) to

$$\frac{d\mathbb{E}(X_i)}{dt} = -\mathbb{E}(X_i) + \tau \sum_{j=1, j\neq i}^{N} \mathbb{E}((1-X_i)X_j a_{ij}), \tag{1.11}$$

$$\frac{d\mathbb{E}(a_{ij})}{dt} = a_{ij}(0)E\Big[-\zeta(X_i - X_j)^2 + \xi(1-a_{ij})(1-X_i)(1-X_j)\Big]. \tag{1.12}$$

Here we observe that the behaviour of the Markov process is independent of the curing rate δ but only depends on ξ, ζ and the ratio $\tau = \frac{\beta}{\delta}$. Therefore, throughout this thesis it is assumed that $\delta = 1$.

1.4 Other models

Although the expectation differential equations are a valid simplification of the ASIS Markov process, it is sometimes insufficient or impractical to use. First it will be shown which problems arise while using the EDEs whereafter several other equations are introduced.

The expectation differential representation is ill-posed due to missing definitions. For the spreading of the epidemic, N equations are available for each node, and L equations are available for the network structure. However, the EDEs have many more variables. These are summarised in Table 1.1.

Table 1.1: The number equations and variables used in the expectation-differential model.

	equations	variables
$\mathbb{E}(X_i)$	N	N
$\mathbb{E}(a_{ij})$	L	L
$\mathbb{E}(X_i X_j)$	–	$\frac{1}{2}N(N-1)$
$\mathbb{E}(X_i a_{ij})$	–	L
$\mathbb{E}(X_i X_j a_{ij})$	–	L

In principle, this is not necessarily a problem. However, if one wants to investigate the behaviour of the EDEs, it is clear the system is underdetermined. A solution is to define new variables of how the system changes over time. These new variables are the so-called *closing relations* of the system. Three possible closing relations are presented below.

1.4.1 Extended EDEs

One could use the Markov process to compute higher order correlations terms to close the sequence. This has been done before for a 2-node network in section 1.2.1. For just two nodes, this is relatively easy, as the interaction between two nodes is not influenced by any others. For a higher number of nodes, this yields a problem. Consider N nodes in a network. The EDEs have correlation terms of at most three elements: X_i, X_j and a_{ij}. In order to compute correlation terms like $\mathbb{E}(X_i X_j)$, the interaction between i and j is important, as well as their interaction on other nodes. This immediately results in higher order correlation terms containing six elements; $X_i, X_j, X_k, a_{ij}, a_{ik}$ and a_{jk}. To compute correlation terms like $\mathbb{E}(X_i X_j a_{ij})$, even higher order correlation terms are required. In order to close this system, one needs to compute even higher order terms, etc. The procedure is stopped when one has computed all correlation terms. The total number of correlation terms is $2^{N+L} - 1$ because all correlation terms may consist of N terms containing X_i terms and L terms including a_{ij}. Each of them can be included or not, finding the given result.[2] This makes the problem equally challenging as it was before since it has the same enormous number of equations. The only simplification is the reduction from a very large stochastic Markov process to a very large set of linear expectation differential equations. We will call these relations the *Extended EDEs*.

1.4.2 Mean-field EDEs

Another possibility to close the sequence is to neglect correlations and apply a mean-field approximation. Hence we assume

$$\mathbb{E}(XY) = \mathbb{E}(X)\mathbb{E}(Y)$$

[2]The '−1' is caused by not having covered the all-zero state by any expectation value. This is no problem, because if all other probabilities are known, one could theoretically calculate it if one would wish to do so.

for every random variable X and Y [20]. This changes the governing equations to

$$\frac{d\mathbb{E}(X_i)}{dt} = -\delta\mathbb{E}(X_i) + \beta \sum_{j=1, j\neq i}^{N} (1 - \mathbb{E}(X_i))\mathbb{E}(X_j)\mathbb{E}(a_{ij}), \tag{1.13}$$

$$\frac{d\mathbb{E}(a_{ij})}{dt} = a_{ij}(0)\Bigg(- \zeta\mathbb{E}(a_{ij})(\mathbb{E}(X_i) + \mathbb{E}(X_j) - 2\mathbb{E}(X_i)\mathbb{E}(X_j)) \tag{1.14}$$

$$+ \xi(1 - \mathbb{E}(a_{ij}))(1 - \mathbb{E}(X_i))(1 - \mathbb{E}(X_j))\Bigg).$$

We will call these the *mean-field EDEs*. Occasionally, in literature, this approximation is named N-intertwined Mean-Field Approximation (NIMFA) [22]. Other closing relations including higher order terms of the form $\mathbb{E}(XYZ)$ are investigated in literature from time to time, but do not seem to give further insight [23, 24] or requires knowledge on the type of correlation in the network [6]. Moreover, higher-order approximations are only valid for perfectly mixed or regular networks [20].

This set of equations is sufficient; the number of equations equals the number of variables. It can therefore be integrated numerically. Also, as $N \to \infty$, by the Central Limit Theorem, the approximation becomes more accurate [25]. By applying a mean-field approximation, the linear (underdetermined) system has been transformed into a non-linear (determined) system. Non-linear models allow for the modelling of more complex behaviour but also opens up possibilities for many more steady states, which may not be physical. It is therefore vital to examine the mean-field EDEs and judge whether this model can be used to accurately model the Markov process. The assumed independence of the random variables is not necessarily a good approximation. This will be investigated in more detail in the next section. Before that, briefly another closing relation is mentioned.

1.4.3 Heterogeneous Mean Field

For static SIS models, a commonly used approximation is the Heterogeneous Mean Field (HMF) approximation, which was first introduced by Pastor-Satorras and Vespignani (2011) [26]. The number of connections of a node is called its *degree*. In this approximation, each node with degree k is collected in one group. Then the differential equations are converted into a new set of differential equations, one for each degree k. Generally, this significantly reduces the number of equations. For adaptive networks, this approach is hard to apply, as the number of degrees of a node is not fixed over time. Moreover, for regular networks, the approximation of HMF is equivalent to NIMFA, and for irregular networks, it generally performs worse [27]. Therefore this approximation is not considered in this thesis.

1.5 Steady states and their stability

Every equation which changes over time could have one or more steady states, in which the solution does not change. Each of these steady states is either stable or unstable. In epidemic modelling, the most common steady state is the state where all individuals are healthy. This will be named the *trivial steady state*. In literature it is occasionally called the disease-free state [9] or the absorbing state [11]. Since the concept of stability is treated differently across the different fields the models originate from, definitions will be supplied first. Thereafter, the steady states are calculated and their stability is derived. In this section, the Markov process will be investigated first and thereafter; the EDEs, the extended EDEs and mean-field EDEs. At the end, the results will be compared.

1.5.1 Markov process

When a system is said to be in a steady state, it means the solution is stationary and will not change at all, not even with a small probability. In a Markov process, these type of states are called *absorbing states*. For the Markov process, there clearly is only one absorbing state. This is the case when every individual is healthy: $X_i = 0$, $\forall\, 1 \leq i \leq N$. We will call this the trivial steady state. The corresponding network structure is not really of interest, but is mentioned here for completeness. For initially existing links, the steady state is $a_{ij} = 1$. Links which did not exist in the initial network cannot be constructed

or removed, so $a_{ij} = 0$. To conclude, the network structure in the steady state is equal to the initial network structure. It is however important to find out how long it takes to arrive at the trivial steady state.

Our approach will be the investigation of the existence of an *ergodic set*. Once such a set is entered, it cannot be left. In our case we define $\bar{X}$ to be the ergodic set which consists of just one state: the trivial state $X_i = 0$ for all i and $a_{ij}(t) = a_{ij}(0)$ for all i, j. In this case, the ergodic set is an absorbing state. We present the following theorem.

Theorem 1.2. *(Kemeny and Snell, Theorem 3.1.1) Let $\mathcal{M} = (X_1, X_2, ...)$ be a finite-sized discrete-time Markov chain and $\bar{X} \in \mathcal{M}$ be an absorbing state. Then the probability of being in the absorbing state while starting in a random state tends to 1 as time increases to infinity;*

$$\mathbb{P}(X_n \to \bar{X}) = 1, \qquad as\ n \to \infty.$$

Proof. See [28]. □

The ASIS Markov process is a continuous process whereas this theorem uses discrete-time Markov chains. While introducing the Markov process, it was argued that both representations can be used simultaneously. For example, the EDEs are continuous whereas the simulation method utilises the discrete Markov chain. The specific choice of taking discrete- or continuous-time Markov processes is therefore irrelevant, and the result of Theorem 1.2 applies.

When the Markov process is written in matrix form containing the probabilities of making a transition from one state to another, more properties can be derived. This matrix is called the transition matrix P. This matrix can be separated into different parts;

$$P = \begin{pmatrix} Q & R \\ \mathbf{0} & I \end{pmatrix}$$

where Q is a t-by-t matrix containing the transition rates from the non-ergodic states to other non-ergodic states, R is a r-by-t matrix containing the transition probabilities from the non-ergodic states to the ergodic states and I is the probability matrix of transitions from one ergodic state to another. We know that absorbing states cannot be left, so I is the r-by-r identity matrix.

The only matrix of interest is Q. We are interested to find the average time required when starting in a random state to end up in the ergodic set. To this end, it is necessary to compute $I + Q + Q^2 + ...$ It has been shown that [28, Theorem 3.2.1]

$$(I - Q)^{-1} = \sum_{k=0}^{\infty} Q^k.$$

By introducing the fundamental matrix $\tilde{N}$ as

$$\tilde{N} \equiv (I - Q)^{-1},$$

the following result was obtained [28, Theorem 3.3.5]

$$\mathbf{s} = \tilde{N}\mathbf{1}.$$

The vector $\mathbf{s}$ contains the average number of steps required, when starting in a certain initial state, to arrive at the ergodic set. One could average over all these states to find

$$s_{av} = \frac{1}{|\tilde{N}|}\mathbf{1}^T\tilde{N}\mathbf{1}, \tag{1.15}$$

which is used to compute the average number of steps required starting in a random initial state (that is; not the absorbing state) to converge to the absorbing state. Note that it says *steps*, not time. To compute the average time required to converge to the absorbing state, multiply s_{av} by Δt. In case one wants to investigate how long it takes from the all-ones state, one can simply take the last element of $\mathbf{s}$ and multiply it by Δt. An example for 2 nodes is shown below.

Example 1. The convergence of a 2-node network
We will consider 2 connected nodes, i.e. $a_{12}(0) = 1$. Then in total 8 different Markov states are available: $(0,0,0), (0,0,1), (0,1,0), (0,1,1), (1,0,0), (1,0,1), (1,1,0), (1,1,1)$. Each of them has a transition to another state defined by Eqs. (1.3) and (1.4). The transition matrix P has been derived in section 2.2.1, and is repeated here.

$$\begin{array}{c} (0,0,0) \\ (0,0,1) \\ (0,1,0) \\ (0,1,1) \\ (1,0,0) \\ (1,0,1) \\ (1,1,0) \\ (1,1,1) \end{array}
\begin{pmatrix}
1-\xi\Delta t & \xi\Delta t & & & & & & \\
 & 1 & & & & & & \\
\delta\Delta t & & 1-\delta\Delta t & & & & & \\
 & \delta\Delta t & \zeta\Delta t & 1-(\delta+\beta+\zeta)\Delta t & & & & \beta\Delta t \\
\delta\Delta t & & & & 1-\delta\Delta t & & & \\
 & \delta\Delta t & & & \zeta\Delta t & 1-(\delta+\beta+\zeta)\Delta t & & \beta\Delta t \\
 & & \delta\Delta t & & \delta\Delta t & & 1-2\delta\Delta t & \\
 & & & \delta\Delta t & & \delta\Delta t & & 1-2\delta\Delta t
\end{pmatrix}$$

The row and column corresponding to the absorbing state needs to be removed. In our case, this is row/column 2 corresponding to the state $(0,0,1)$. After removal, we have found the matrix Q. Then the fundamental matrix $\tilde{N}$ can be computed. After many steps, the following result was obtained for the average time to end up in the ergodic state:

$$\mathbb{E}(T_{\text{random}}) = \frac{14\delta\zeta + 3\beta\xi + 14\delta\xi + 14\zeta\xi + 8\delta^2}{2\delta\xi(\delta+\zeta)}. \tag{1.16}$$

Compare this result to the case where we start in $(1,1,1)$ (and therefore not in a random non-ergodic state)

$$\mathbb{E}(T_{(1,1,1)}) = \frac{2\delta\zeta + \beta\xi + 3\delta\xi + 3\zeta\xi}{2\delta\xi(\delta+\zeta)}. \tag{1.17}$$

Notice the difference when $\delta \to \infty$:

$$\lim_{\delta\to\infty} \mathbb{E}(T_{random}) = \frac{4}{\xi},$$
$$\lim_{\delta\to\infty} \mathbb{E}(T_{(1,1,1)}) = 0.$$

Starting in a random state, the system might start in $(0,0,0)$ where link restoring still needs to take place. This takes up some finite time. For the latter, the starting state is always the same, thus allowing immediate convergence to the $(0,0,1)$ state without the need to recreate a link.
End of Example 1.

The most important conclusion from Example 1 is that the transition matrix Q is sparse, but not very sparse. It contains approximately N non-zeros per row for an N^2-by-N^2 matrix. This sparsity can be used when calculating the fundamental matrix $\tilde{N}$. Most importantly, the expression

$$\frac{1}{|\tilde{N}|}\mathbf{1}^T(I-Q)^{-1}\mathbf{1}$$

can be calculated by solving $(I-Q)\mathbf{s} = \mathbf{1}$, and then computing

$$s_{av} = \frac{1}{|\tilde{N}|}\mathbf{1}^T\mathbf{s}.$$

The matrix Q is of size $2^{N+L}-1$ where L is the number of links in the initial network. For a complete network of 40 nodes, Q is around 10^{246} in size, making the computation infeasible. The reduction from the Markov process to the expectation-differential equations is necessary to handle networks with more than 10 nodes. With this in mind, the analysis for steady states of the EDEs is presented in the next section.

1.5.2 EDEs

The expectation-differential equations are given by Eqs. (1.9) and (1.10). Naturally, the all-healthy state $\mathbb{E}(X_i) = 0$ for all $1 \leq i \leq N$ is a steady state solution. This trivial steady state is a natural steady state, since a healthy population with no infected people cannot spread the disease. Possibly other steady states exist, however, the current approach does not allow for the computation of these steady states because the number of variables (including higher order correlation terms) is much larger than the number of equations.

1.5.3 Extended EDEs

Since the extended EDEs form a set of many, many differential equations, it is exponentially hard to derive all steady states. Still, we know the equations to be linear by construction. Naturally, $\mathbb{E}(X_i) = 0$ for all i is a steady-state solution. Other solutions might be possible when the corresponding matrix has an eigenvalue $\lambda = 0$. One could use the more structured representation of the Markov process as in [20] to compute the existence of other steady states. The differential equations are linear, so the stability of the steady states (including the trivial one) can be determined. Since the system consists of exponentially many equations, both the theoretical and practical impact of the Extended EDEs is small. Therefore the steady states are not determined for the Extended EDEs.

1.5.4 Mean-field EDEs

For clarity, the mean-field EDEs are

$$\frac{d\mathbb{E}(X_i)}{dt} = -\delta\mathbb{E}(X_i) + \beta \sum_{j=1,j\neq i}^{N} (1 - \mathbb{E}(X_i))\mathbb{E}(X_j)\mathbb{E}(a_{ij}), \tag{1.18}$$

$$\frac{d\mathbb{E}(a_{ij})}{dt} = a_{ij}(0)\Bigg(-\zeta\mathbb{E}(a_{ij})(\mathbb{E}(X_i) + \mathbb{E}(X_j) - 2\mathbb{E}(X_i)\mathbb{E}(X_j)) + \xi(1 - \mathbb{E}(a_{ij}))(1 - \mathbb{E}(X_i))(1 - \mathbb{E}(X_j))\Bigg). \tag{1.19}$$

Analytic computation of all steady states for this non-linear system is difficult. Therefore we will resort ourselves to symmetric steady states of the form $\mathbb{E}(X_i) = \mathbb{E}(X_j) = x_v$ for all i, j. Substituting this value and setting the derivatives to zero;

$$0 = -\delta x_v + \beta \sum_{j=1,j\neq i}^{N} (1 - x_v)x_v\mathbb{E}(a_{ij}),$$

$$0 = a_{ij}(0)\Bigg(-2\zeta\mathbb{E}(a_{ij})x_v(1 - x_v) + \xi(1 - \mathbb{E}(a_{ij}))(1 - x_v)^2\Bigg).$$

Assume $x_v \neq 0$ (otherwise we resort to the trivial steady state) such that

$$1 = (1 - x_v)\tau \sum_{j=1,j\neq i}^{N} \mathbb{E}(a_{ij}),$$

$$2\omega\mathbb{E}(a_{ij})x_v(1 - x_v) = (1 - \mathbb{E}(a_{ij}))(1 - x_v)^2, \qquad \text{if } a_{ij}(0) = 1,$$

where $\tau = \frac{\beta}{\delta}$ is the effective infection rate and $\omega = \frac{\zeta}{\xi}$ the effective lin-breaking rate. By assuming $x_v = 1$, the last equation is satisfied. However, the first yields $1 = 0$ which is impossible. So we assume $x_v \neq 1$ such that

$$1 = (1 - x_v)\tau \sum_{j=1,j\neq i}^{N} \mathbb{E}(a_{ij}), \tag{1.20}$$

$$2\omega\mathbb{E}(a_{ij})x_v = (1 - \mathbb{E}(a_{ij}))(1 - x_v), \qquad \text{if } a_{ij}(0) = 1. \tag{1.21}$$

Eq. (1.21) can be rewritten in terms of $\mathbb{E}(a_{ij})$:

$$\mathbb{E}(a_{ij}) = \frac{1 - x_v}{2\omega x_v + 1 - x_v}, \qquad \text{if } a_{ij}(0) = 1. \tag{1.22}$$

Inserting this result back into Eq. (1.20) and using that $\mathbb{E}(a_{ij}) = 0$ when $a_{ij}(0) = 0$ we find

$$1 = (1 - x_v)\tau d_i(0)\frac{1 - x_v}{2\omega x_v + 1 - x_v}.$$

In order for this to be solvable, we require $d_i(0) = d(0)$. In other words, the network should be d-regular. The equation can be rewritten as

$$2\omega x_v + 1 - x_v = d(0)\tau(1 - x_v)^2.$$

Define $X_v = 1 - x_v$ such that

$$d(0)\tau X_v^2 + (2\omega - 1)X_v - 2\omega = 0,$$

which is a quadratic function in X_v. Solving gives

$$X_v = \frac{1 - 2\omega}{2d(0)\tau} \pm \sqrt{\left(\frac{1 - 2\omega}{2d(0)\tau}\right)^2 + \frac{2\omega}{d(0)\tau}}$$

such that

$$x_v = 1 - \frac{1 - 2\omega}{2d(0)\tau} \pm \sqrt{\left(\frac{1 - 2\omega}{2d(0)\tau}\right)^2 + \frac{2\omega}{d(0)\tau}}. \tag{1.23}$$

Remark that $\frac{2\omega}{d(0)\tau} > 0$. We notice the equation is of the form

$$x_v = 1 - x \pm \sqrt{x^2 + y},$$

where $x = \frac{1-2\omega}{2d(0)\tau}$ and $y = \frac{2\omega}{d(0)\tau}$. Here $x \in \mathbb{R}$ and $y > 0$. Since $y > 0$, we have $\sqrt{x^2 + y} > x$, so

$$x_v = 1 - x + \sqrt{x^2 + y} > 1,$$

which is an infeasible solution. The only solution is

$$x_v = 1 - \frac{1 - 2\omega}{2d(0)\tau} - \sqrt{\left(\frac{1 - 2\omega}{2d(0)\tau}\right)^2 + \frac{2\omega}{d(0)\tau}}. \tag{1.24}$$

As a constraint, we require that $x_v > 0$. This results in

$$1 - \frac{1 - 2\omega}{2d(0)\tau} > \sqrt{\left(\frac{1 - 2\omega}{2d(0)\tau}\right)^2 + \frac{2\omega}{d(0)\tau}}. \tag{1.25}$$

Taking the square on both sides gives

$$1 - \frac{1 - 2\omega}{d(0)\tau} + \left(\frac{1 - 2\omega}{2d(0)\tau}\right)^2 > \left(\frac{1 - 2\omega}{2d(0)\tau}\right)^2 + \frac{2\omega}{d(0)\tau}.$$

Both sides contain equal terms which cancel out, such that we require

$$\tau > \frac{1}{d(0)} \tag{1.26}$$

to have a feasible solution. To sum up, the steady state solution is given by Eq. (1.24) and the corresponding links by Eq. (1.22). This solution is stable for the condition in Eq. (1.26). Its existence depends on τ but not on any other variables. This means the interplay between process and network is

not very strong. The effective link-breaking rate ω mostly influences the height of the steady state and not its existence criterium.

To compute the linear stability of the trivial solution, we require the Jacobian of the mean-field EDEs. We directly substitute $\mathbb{E}(X_i) = 0$ for all i to find

$$J = \begin{pmatrix} J_1 & 0 \\ J_2 & J_3 \end{pmatrix},$$

where

$$\begin{aligned} J_1 &= J_{static}, \\ J_2 &= -a_{ij}(0)\zeta\mathbb{E}(a_{ij})J_{EN} - a_{ij}(0)\xi(1-\mathbb{E}(a_{ij}))J_{EN}, \\ J_3 &= -a_{ij}(0)\xi I_E, \end{aligned}$$

where J_{static} is the Jacobian for the static network which is the same as the one in Eq. (A3.2), J_E is a L-by-L all-ones matrix and I_N is the N-by-N identity matrix. We see J is block lower-triangular, so we only need J_1 and J_3 to find the eigenvalues. The eigenvalues for J_1 have already been calculated in Appendix 3, and are shown to be strictly negative. For J_3, the eigenvalues are on the diagonal, and are either negative or zero (depending on the network structure). This shows the system is marginally stable. The higher order terms need to be considered to determine the stability. It is expected these yield a stable solution.

For static networks, a more thorough analysis can be performed. This is expounded in Appendix 3.

1.5.5 Overview

In this section, we have investigated the steady states and their stability for all models. The Markov process only possesses the trivial steady state in which all nodes are healthy. The non-linear mean-field EDEs have an extra steady state, which exists for large values of the effective infection rate τ. The interpretation of this state will be given in the next section. The EDEs and the Extended EDEs could not provide any further insight, as the system is underdetermined (EDEs) or the number of equations too large (Extended EDEs). From this moment on, the Extended EDEs are not used in thesis any more.

Although the long-term behaviour is equivalent for the Markov process and the EDEs, the behaviour over the semi-long term is equally important, if not more. The average time for the disease to stay active, which was computed for small networks in the first section, is an important parameter to be able to predict how long and how many individuals will be infected throughout a time period. This property of the model is discussed in more detail in the next section.

1.6 Metastable states

Aside from the existence of steady states as discussed in the previous section, the Markov process also exhibits similar but slightly different behaviour. This happens when the system is not truly found to be in a steady state, but it stays in the neighbourhood of a certain solution, and appears not to leave it over a long period of time. This will be called the *metastable state*. Before the definition can be supplied, the prevalence is introduced.

Definition 1.3. *The **prevalence** y is the average portion of the total population which is infected at a certain time* [29]. *Mathematically, we can define it as*

$$y = \frac{1}{N}\sum_{i=1}^{N}\mathbb{E}(X_i). \tag{1.27}$$

The prevalence is an order parameter of the system, implying that it is a variable where a bifurcation occurs [25]. This allows us to define the metastable state.

Definition 1.4. *(Empirically) The* ***metastable state****, also called* ***meta-stable state****,* ***quasi-stationary state****,* ***endemic state*** *or* ***oscillatory state*** *is a non-zero prevalence solution y^* which exists for a period $T = t_2 - t_1$ and varies during this period less than some $\varepsilon > 0$;*

$$|y(t) - y^*| < \varepsilon, \qquad \text{for } t \in [t_1,\ t_2]. \tag{1.28}$$

Naturally, the prevalence is bounded as $0 \leq y^* \leq 1$ and equality is reached for a purely healthy population ($y^* = 0$) and a completely infected population ($y^* = 1$). In the remainder of this thesis, the asterisk is dropped and the prevalence is denoted by y. For practical use, the definition in Eq. (1.28) might be insufficient. For example, when considering the Markov process, the variables take values 0 or 1 and no other. Using this insight, a more practical definition can be applied which was also stated in [16].

Definition 1.5. *(Practically) The* ***metastable state*** *is a solution y which is non-zero for a large period T and can be estimated by*

$$y = \frac{1}{NT} \int_0^T \sum_{i=1}^{N} \mathbb{E}(X_i(t))dt. \tag{1.29}$$

The system can be in the metastable state, but it always collapses to the trivial steady state as $t \to \infty$. The average time over which this happens can theoretically be calculated using the procedure explained in section 1.5.1. This calculation will be verified numerically for 2 nodes, and will be estimated for a higher number of nodes in Chapter 3.

The non-trivial steady state from the mean-field EDEs is nearly equivalent to the metastable state of the Markov process. The relation between the two will be discussed in more detail in Chapter 3.

During simulations, it is occasionally useful to prevent the system to collapse to the trivial steady state. For example, one might want to estimate the prevalence y from Definition 1.3. In Chapter 3, some possible solutions are presented for this issue. Being in the metastable state requires the network to be more or less in the same state. Then other properties of the network, like the number of links, the clustering coefficient, etc. will remain constant over time as well. This will be verified by numerical results as well in the next chapter.

Finally we wish the procedure not to depend on given initial conditions. In every model, an initial network needs to be supplied. Several choices are possible, but we will restrict ourselves to the complete network. In the Markov process, each simulation starts in the all-infected state. Although the genuine outbreak of a disease starts with one infected individual, the analysis of the metastable state can be performed more easily when starting in the all-infected state. For the EDEs, we give every individual a uniformly distributed value between zero and one. By using random initial conditions, it allows us to start in random state, not constraining ourselves by starting in a particular state. Occasionally, other initial conditions will be used. Whenever this is done, this will be mentioned explicitly.

1.7 Overview

This completes our theoretical overview of the Markov process and EDEs for the SIS model on an adaptive network. We have seen the derivation of the EDEs from the original Markov process, which resulted in an underdetermined set of differential equations. To solve this issue, we proposed two solutions: deriving more equations by reinvestigation of the Markov process (Extended EDEs) or by applying a mean-field correction (mean-field EDEs). The Extended EDEs are a too large system of linear equations to be useful. All four models have a trivial steady state, in which all individuals are healthy. The metastable state was defined as the state in which the Markov process tends to stay over a long time. Only the mean-field EDEs have extra steady states, which are nearly equivalent to the metastable state of the Markov process.

2 Numerical results epidemics

After the theoretical study of the ASIS model in the previous chapter, it is time to verify the obtained results. Several model properties, such as the prevalence, are determined numerically. Simulations are performed using 2,000 time units of initialisation time and 40,000 time units of computation time. This number of time units was chosen to have sufficiently accurate results and a feasible computation time. Later in this chapter, this choice will be explained in more detail. In [11], an initialisation time of 40,000 time units was used but we have found no evidence for such slow convergence towards the metastable state.

The first section reviews the SIS model (i.e. a static network structure) and the evolution of the Markov process and the expectation-differential equations. In the previous chapter, it was shown that these are expected to show good agreement with each other. The investigation is continued in section 2.2 for adaptive networks with a complete initial network structure. Finally, the results are summarised in the last section.

2.1 The static SIS network

The static SIS network is a simplification of the ASIS model in which the links are unchangeable. This can be obtained by setting $\zeta = \xi = 0$ in the ASIS model. This simplifies the Markov process to

$$\begin{aligned} \mathbb{P}(X_i(t+\Delta t) = 1 \,|\, X_i(t) = 0, a_{ij}(0) = 1, X_j(t) = 1) &= \beta \Delta t, \qquad \text{infection} \\ \mathbb{P}(X_i(t+\Delta t) = 0 \,|\, X_i(t) = 1) &= \delta \Delta t. \qquad \text{curing} \end{aligned} \tag{2.1}$$

The corresponding EDEs are

$$\frac{d\mathbb{E}(X_i)}{dt} = -\delta \mathbb{E}(X_i) + \beta \sum_{j=1}^{N} a_{ij} \mathbb{E}\left[(1 - X_i) X_j\right]. \tag{2.2}$$

2.1.1 Markov process

Performing a single run of the Markov process is relatively simple, as one only need to perform random draws from Poisson distributions to model the Markov process based on Eq. (2.1). The result of a single run of the Markov process is shown in Figure 2.1.

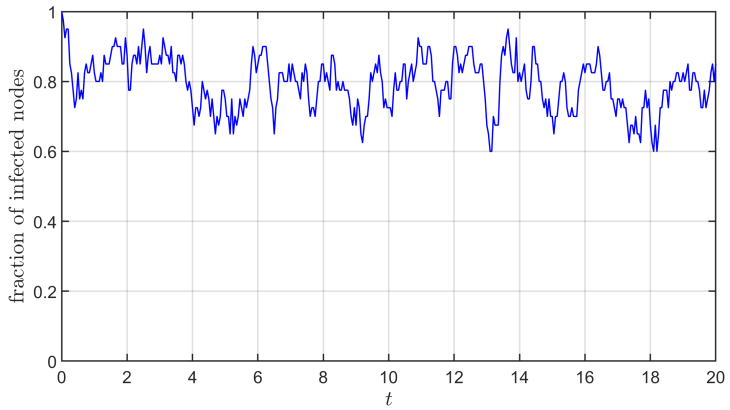

Figure 2.1: A single run of the Markov process for the static network. We have taken $N = 40$, $\delta = 1$, $\beta = 0.125$, $\Delta t = 0.05$ and a complete static network.

The simulation in Figure 2.1 was initialised by taking a completely infected population. This corresponds to $y = 1$. Thereafter, the prevalence y decreases quickly until it has reached $y \approx 0.8$. From there on, the process oscillates around the metastable state. In the metastable state, roughly 80% of the people are sick over time, with limits at 60% and 95%. Exceeding those bounds seems to rarely occur, although

this will happen at a finite time. Unfortunately, it is impossible to estimate the average time of existence of this metastable state based on the absorbing Markov process property. This is caused by the large number of equations, which was discussed in detail in section 1.5.1.

The solution oscillates around the metastable state in Figure 2.1. This process seems stable, however, it has been shown in Chapter 1 that it is unstable. For lower values of the infection rate β, the averaged prevalence converges exponentially to zero over sufficiently large time. However, this already happens for some $\beta > 0$. This bifurcation point is called the epidemic threshold, which is defined more precisely below.

Definition 2.1 (Empirically)**.** *The **epidemic threshold** is the critical number of susceptible hosts required for an epidemic to occur. Above this value, the epidemic persists.*

This is an important parameter in epidemiology, as it indicates the point where the disease changes from a small disease to an endemic [11, 17]. The following definitions will be applied analytically and numerically respectively.

Definition 2.2 (Analytically)**.** *The **epidemic threshold** τ_c is the largest value of the effective infection rate τ for which the prevalence y (average portion of infected individuals) drops to zero over sufficiently large time.*

$$\tau_c = \sup\{\tau \,:\, y(t;\tau,\omega,\xi) = 0 \text{ for sufficiently large time } t\}.$$

Definition 2.3 (Numerically)**.** *The **epidemic threshold** τ_c is the largest value of the effective infection rate τ for which the prevalence (average portion of infected individuals) drops below $\frac{1}{N}$ (i.e. less than one individual having the disease).*

The estimation of the metastable number of infected individuals y is a difficult task. The system can at any time collapse to the trivial steady state. However, this is undesired behaviour, as we wish to determine the value around which the solution oscillates before convergence to the steady state is observed. To prevent this from happening, several approaches are available. One approach is to immediately infect one individual again when the system just collapsed to the trivial steady state [30]. Another approach is the so-called ε-ASIS model, which was introduced by Van Mieghem and Cator (2012) [31]. In this model, a self-infection rate ε is introduced where $\varepsilon < \frac{\delta}{N}$. This means a healthy node can infect itself with a small probability. This removes the trivial steady state, and allows for the investigation of the metastable state. This approach will be used throughout this thesis, as it allows for a more accurate description of the epidemic threshold. The value of ε should be chosen sufficiently small, which is shown in a later section. On the other hand, ε is not a small perturbation parameter. In the limit of $\varepsilon \to 0$, the Markov process always collapses to the trivial steady state over sufficiently long time. Hence a small change in ε significantly changes the location of the epidemic threshold [31]. This is also investigated in more detail in this chapter.

The relation between the effective infection rate τ and the metastable prevalence y is shown in Figure 2.2.

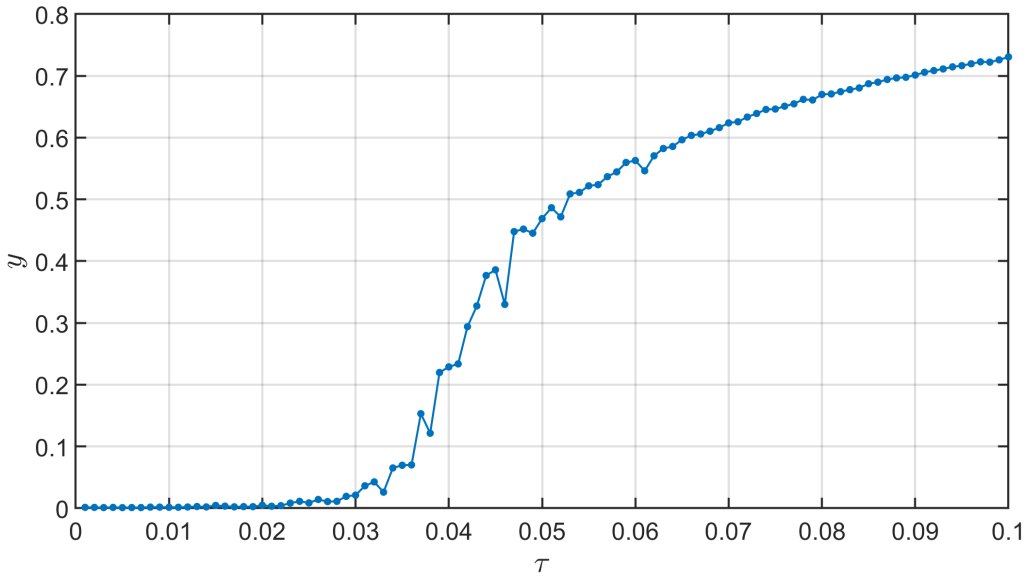

Figure 2.2: The relation between the effective infection rate τ and metastable prevalence y. We have taken $N = 40$, $\delta = 1$, $\varepsilon = 0.001$, $\Delta t = 0.05$ and a complete static network. The epidemic threshold is estimated to be at $\tau_c \approx 0.028$.

The metastable prevalence y in Figure 2.2 increases rather smoothly as τ increases. For a larger number of time units, a smooth curve can be obtained. Due to computational restrictions, only 40,000 time units have been used although at least 1,000,000 time units are required for a smooth bifurcation diagram. The epidemic threshold τ_c can be estimated from Figure 2.2 and is estimated to be located at $\tau_c \approx 0.028$. In a small region of τ-values above the epidemic threshold τ_c, the largest ascent for the prevalence y is observed. This makes the epidemic threshold a relevant parameter in epidemiology. Although Figure 2.2 is only shown for $0 < \tau < 0.1$, the behaviour smoothly extends to $y = 1$ as the effective infection rate τ approaches infinity.

2.1.2 Mean-field EDEs

The mean-field EDEs are an approximation of the Markov process. One of the main topics of this thesis is to investigate to what extent the behaviour of the Markov process can be approximated by a mean-field approximation. It would be preferred to use the EDEs, however, they have shown to be incomplete. The Extended EDEs cannot be utilised either due to their enormous number of equations. Therefore the mean-field EDEs are compared to the Markov process. This is important, because for larger networks, the mean-field EDEs are currently the only way to compute properties of the network.

For clarity we repeat the mean-field EDEs for a static network

$$\frac{d\mathbb{E}(X_i)}{dt} = -\delta\mathbb{E}(X_i) + \beta\sum_{j=1}^{N} a_{ij}\mathbb{E}(X_j)(1-\mathbb{E}(X_i)). \tag{2.3}$$

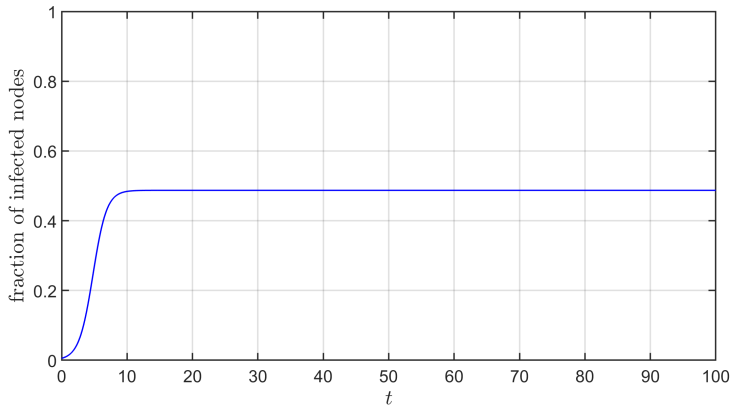

Figure 2.3: A single run of the mean-field EDEs in a static network. We have taken $N = 40$, $\delta = 1$, $\beta = 0.05$, $\Delta t = 0.05$. As initial condition, we have taken $\mathbb{E}(X_i)$ to be a uniform random number between 0 and 0.01.

A single run of the mean-field EDEs is shown in Figure 2.3. The system rapidly converges to the steady state. The value for the infection rate β in Figure 2.3 is low; for larger values of β, convergence happens even faster; in the order of 1 time step. This was also observed in literature [25, Fig 17.2].

During the simulation, all nodes converge to the same value for $\mathbb{E}(X_i) = y$. This is proven in Appendix 3 for any d-regular network. Hence, by using the formulas from Appendix 3 and the bifurcation diagram from Figure A3.1, the mean-field EDEs estimate the bifurcation to occur at $\tau_c^{\mathrm{MF}} = 1/d$, where d is the number of degrees of the nodes. Since the network is complete, $d = N - 1$. This result can be interpreted as follows. Suppose one node is infected and all others are healthy. Since the network is complete, it is connected to all other nodes. In case the probability of spreading the disease to any node (which is approximately $\beta \cdot (N - 1)$) is equal to the curing rate δ, the epidemic persists. For smaller values of β, the epidemic dies out and for larger β, the epidemic develops into an endemic.

For a network of 40 nodes, the mean-field epidemic threshold τ_c^{MF} is

$$\tau_c^{\mathrm{MF}} = \frac{1}{d} = \frac{1}{39} \approx 0.0256. \tag{2.4}$$

The epidemic threshold τ_c from the Markov process can be estimated from Figure 2.2. This is estimated to be at $\tau_c \approx 0.028$, which is slightly above the mean-field approximation. The difference between the approximation and the simulated value is less than 10%, indicating a relatively small difference. The obtained result from Appendix 3 can be combined with the bifurcation diagram of the Markov process (Figure 2.2) to show the close agreement between the two models, which is illustrated in Figure 2.4.

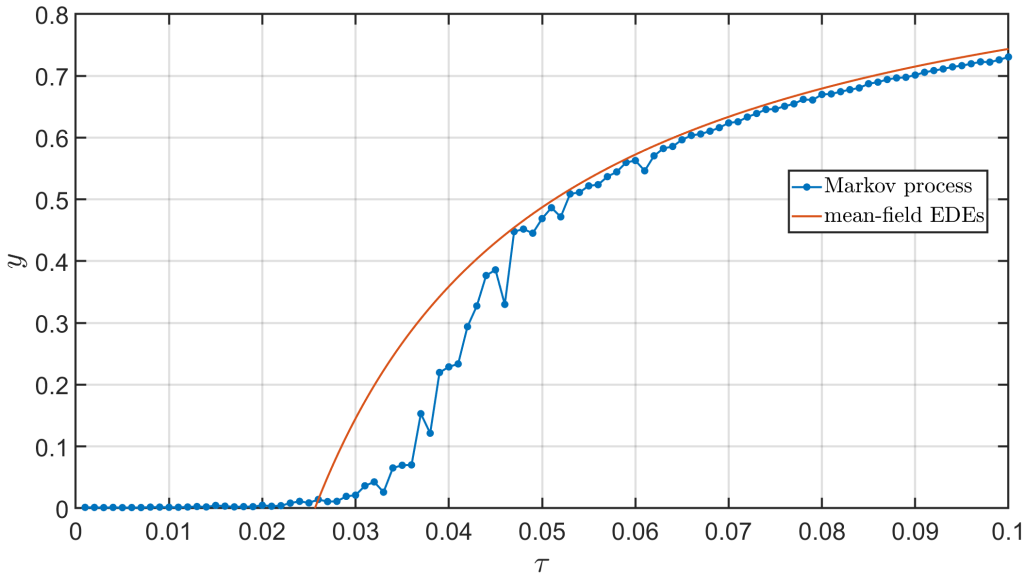

Figure 2.4: The relation between the effective infection rate τ and metastable prevalence y. We have taken $N = 40$, $\delta = 1$, $\varepsilon = 0.001$, $\Delta t = 0.05$ and a complete static network. The blue line shows the Markov process and the red solid line is based on the mean-field EDEs.

The mean-field EDEs seem to overestimate the Markov process. Remember that the mean-field approximation assumed that

$$\mathbb{E}(XY) = \mathbb{E}(X)\mathbb{E}(Y) \tag{2.5}$$

for each random variable X and Y in the model. This assumption of no correlation between the nodes introduces an error. Since it was proven that two adjacent nodes are positively correlated in the SIS model [32], the mean-field approximation serves as an upper bound for the exact solution. This is also observed in Figure 2.4.

This completes the overview of the static SIS model. The next section will discuss the adaptive network, which exhibits similar but occasionally different behaviour.

2.2 Complete adaptive network

After reviewing a static network in the previous section, in this section the network changes over time. The key concept is the coupling between the process spreading on the network and dynamics of the topology of the network. These interact with each other, transforming the SIS model into an adaptive model: the adaptive SIS model. Although the section is titled 'complete', the considered network is not complete; only the initial network is. General initial networks are not examined in this thesis.

2.2.1 Markov process

The Markov process exhibits several properties which will be investigated in this section. First, we start by showing a single run of the ASIS model. Using the ε-ASIS model, which was discussed in the previous section, the metastable fraction of infected nodes y is estimated.

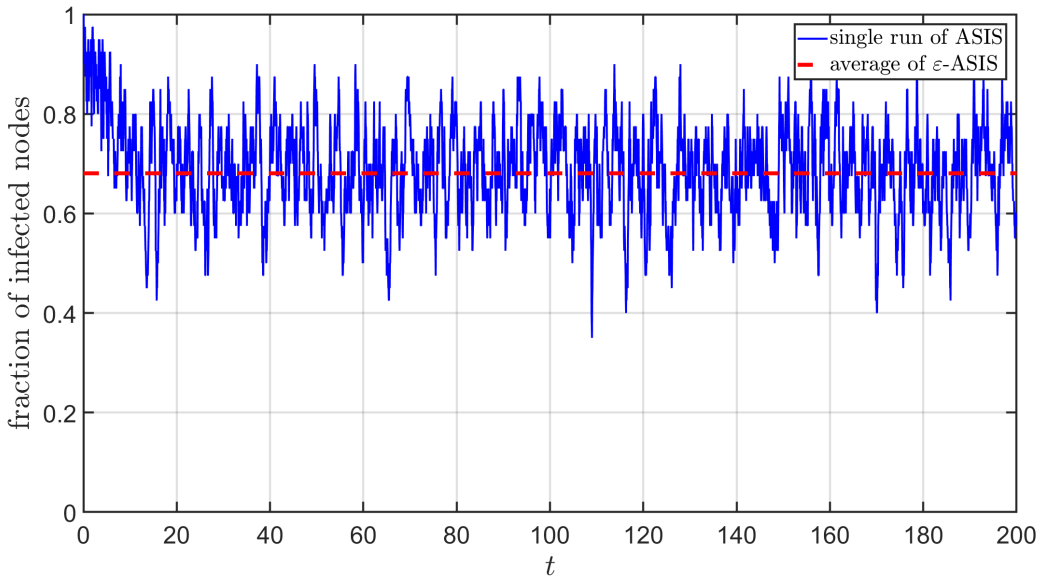

Figure 2.5: A single run of the Markov process for the adaptive network and the averaged value of an ε-ASIS run. We have taken $N = 40$, $\delta = 1$, $\beta = 0.5$, $\zeta = 1$, $\xi = 1$, $\varepsilon = 0.001$, $\Delta t = 0.05$ and a complete initial network. The red dashed line is the average prevalence y obtained using ε-ASIS by averaging over 40,000 time units.

The ε-ASIS model is accurately able to predict the metastable number of nodes as shown in Figure 2.5. This makes the ε-ASIS ultimately useful to predict the average value. Still, the value of ε has some influence on the height of the metastable state, which will be investigated later.

For 2 nodes, an analytic expression for the average absorption time was derived in Eq. (1.17). By performing many independent simulations for the 2-node network, the computed average absorption time and the numerical absorption time are compared.

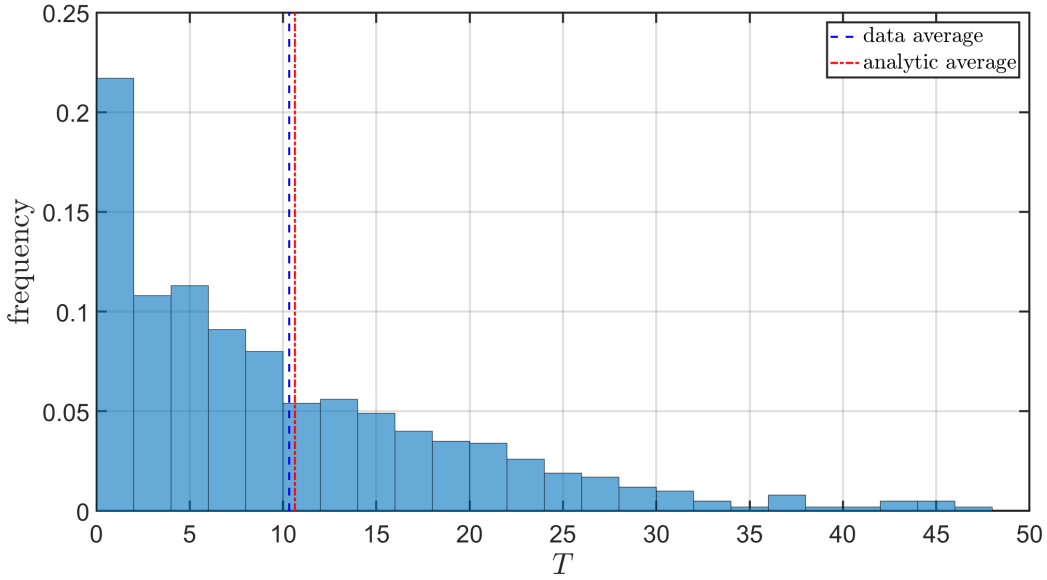

Figure 2.6: The distribution of the absorption time in the Markov process in the adaptive network of 10,000 simulations. We have taken 2 nodes, $\delta = 1$, $\beta = 1$, $\zeta = 10$, $\xi = 0.1$, $\Delta t = 0.5$. The dashed blue line indicates the average of the simulations whereas the red dash-dotted line shows the theoretically predicted average by Eq. (1.17).

The simulation average in Figure 2.6 is not completely in compliance with the analytic average. A possible problem might be the following. In the derivation of the EDEs, we assumed the time step to be sufficiently small to allow only one transition per time step. Since a finite time step was used, a small error was introduced in the simulations. To compare, the simulations are repeated for $\Delta t = 0.125$ which is four times as small in Figure 2.7.

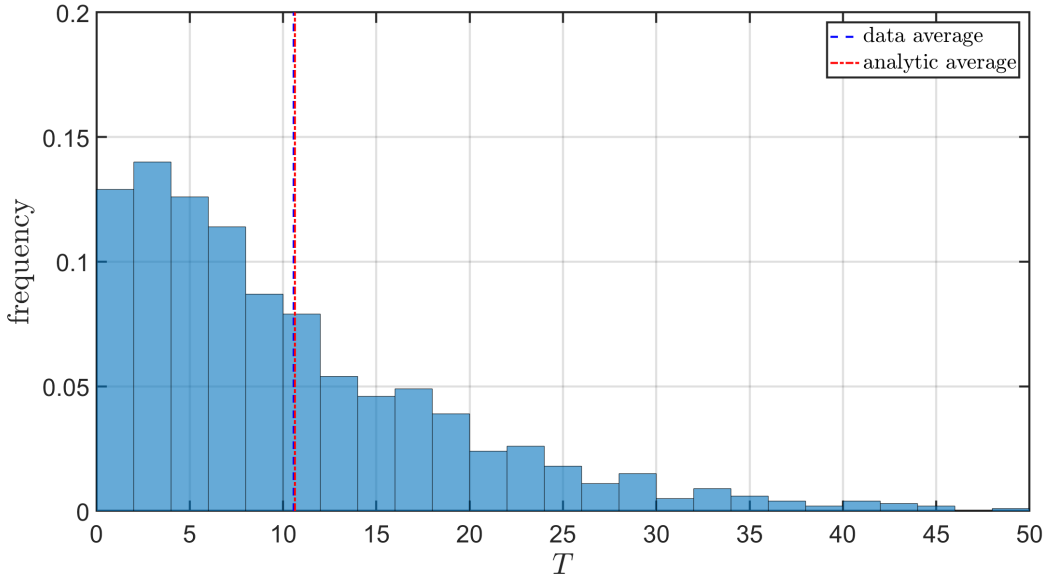

Figure 2.7: Repetition of Figure 2.6 for $\Delta t = 0.125$. The analytic average remains the same, whereas the data average slowly converges towards the analytic average.

The result has been improved, and in the limit of $\Delta t \to 0$ and the number of experiments to infinity, the error converges to zero. However, for any fixed Δt, an error is made to the exact solution. This numerical error only vanishes for $\Delta t \to 0$. Throughout this thesis, $\Delta t = 0.05$ is chosen. This choice ensures the simulations are reasonably accurate and the computation time is not too large.

Throughout this thesis, the same network is used. This network is complete and consists of 40 nodes. As derived in Chapter 1, no analytic absorption time can be calculated any more. The absorption time is simulated in Figure 2.8.

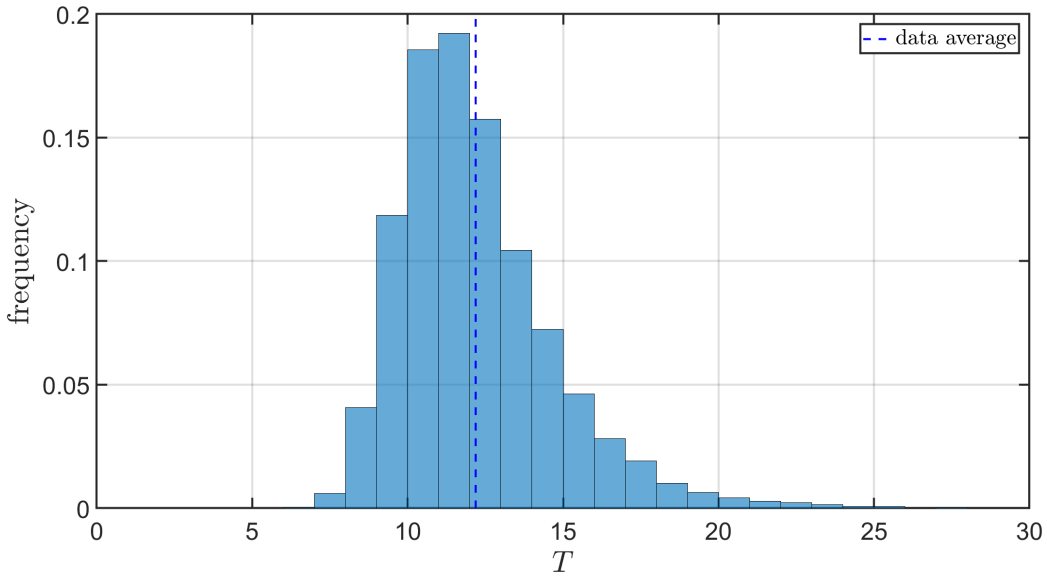

Figure 2.8: The distribution of the absorption time in the Markov process in the adaptive network over 10,000 simulations. We have taken $N = 40$, $\delta = 1$, $\beta = 0.05$, $\zeta = 1$, $\xi = 1$, $\Delta t = 0.05$ and a complete initial network.

The distribution of the absorption time T in Figure 2.8 seems to follow a Poisson distribution. This is reasonable, as the Markov process is governed by Poisson processes. The absorption rate can be estimated by $\frac{1}{\langle T \rangle}$ where $\langle T \rangle$ is the data average in Figure 2.8. For Poisson processes, the uncertainty is relatively large. The 95% confidence interval lies between $T = 8$ and $T = 20$. Therefore, single runs of the model can show entirely different behaviour. Possibly this effect is averaged out for a larger number of nodes, however, this hypothesis has not yet been verified.

Analogous to the static SIS model, a bifurcation diagram can be computed for the adaptive model. The diagram is shown in Figure 2.9. The behaviour of the bifurcation diagram is comparable to the static SIS network which was shown in Figure 2.2. However, the epidemic threshold τ_c is estimated to be at $\tau_c \approx 0.06$ whereas this is $\tau_c \approx 0.028$ for the static network. Around $\tau = \tau_c$, the prevalence seems to have smoothed out; the sudden increase in the prevalence y has become less steep due to the adaptive link-breaking and link-creation processes. The remaining part of the diagram is almost unchanged.

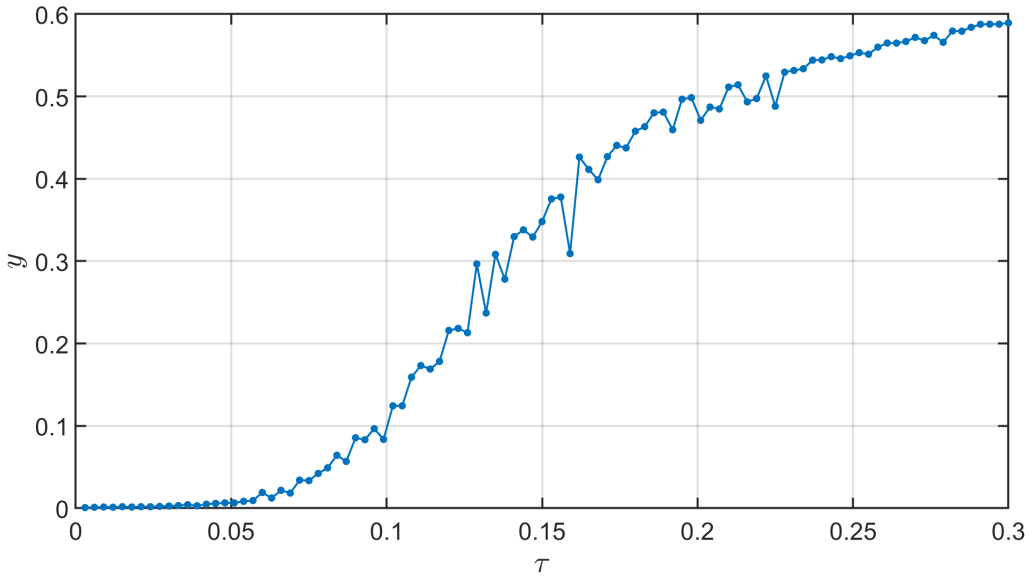

Figure 2.9: The relation between the effective infection rate τ and metastable prevalence y. We have taken $N = 40$, $\delta = \zeta = \xi = 1$, $\varepsilon = 0.001$, $\Delta t = 0.05$ and a complete initial network.

2.2.2 Mean-field EDEs

The mean-field EDEs for the adaptive network have been computed in Eqs. (1.13) and (1.14). A single run is shown in Figure 2.10.

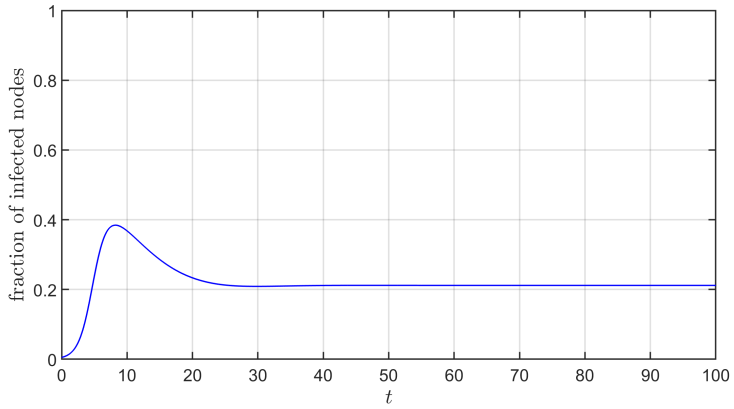

Figure 2.10: A single run of the mean-field EDEs in an adaptive network. We have taken $N = 40$, $\delta = 1$, $\beta = 0.05$, $\zeta = 0.1$, $\xi = 0.1$, $\Delta t = 0.05$. As initial condition, we have taken $\mathbb{E}(X_i)$ to be a uniform random number between 0 and 0.01.

Comparing the behaviour of the static SIS model (Figure 2.3) and the adaptive SIS model (Figure 2.10), the observed behaviour is different. However, both figures show a fast convergence towards the steady state. The height of the steady state has changed in the ASIS model as well. Nevertheless, the most relevat aspect is the stability of the steady state. An analytical expression for the steady state of the mean-field EDEs was derived in section 1.5.4. Using that result, the bifurcation diagram from Figure 2.9 is depicted including the mean-field approximation in Figure 2.11.

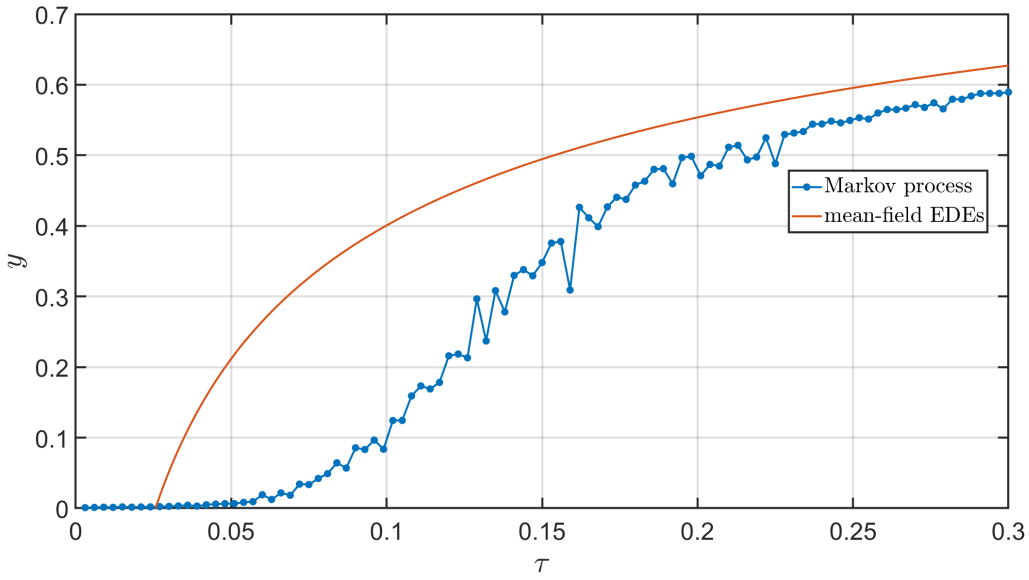

Figure 2.11: The relation between the effective infection rate τ and metastable prevalence y. We have taken $N = 40$, $\delta = \zeta = \xi = 1$, $\varepsilon = 0.001$, $\Delta t = 0.05$ and a complete initial network.

The difference between the Markov process and the mean-field EDEs is larger than in the static network. The mean-field EDEs predict an epidemic threshold of $\tau_c^{\text{MF}} = 0.025$ whereas the Markov process has an epidemic threshold of $\tau_c \approx 0.06$. So the epidemic threshold fails to be predicted accurately by the mean-field EDEs, which is in contrast to the static case, where the difference between the two was smaller. Also, when comparing the bifurcation diagrams for the static case (Figure 2.4) and the adaptive case (Figure 2.11), the metastable prevalence y has shifted to the right and to the bottom. This is caused by the adaptive part of the network, which removes links to slow down the spreading of the disease. For high values of τ, the infection rate is so high that the adaptive process has barely any influence, as most nodes will be infected before the link-breaking process can occur. Therefore the difference between the static and adaptive version is small for high τ values. For small τ values, the adaptive effect is much stronger. Breaking the link between susceptible and infected individuals causes the spread of the disease to slow down. This reduces the prevalence y. When the link-breaking rate ζ is large, other effects might occur. In section 3.6 more research is conducted on the relation between the epidemic threshold τ_c and the effective link-breaking rate ω.

The epidemic threshold can be estimated using higher order correlation terms of the Markov process. A possible method is described by Ogura and Preciado (2016) where the system of EDEs is rewritten in terms of $\mathbb{E}(X_i)$ and $\mathbb{E}(a_{ij}X_i)$ [16]. The obtained system is separated into a linear and a non-linear part. Using linear stability analysis, a lower bound for the epidemic threshold τ_c is obtained. This will be derived for a general framework of models in Chapter 3. The ASIS model is included in this framework, and the lower bound is given by

$$\tau_c \geq \frac{1 + \omega\xi}{\rho} \tag{2.6}$$

where ρ is the spectral radius of the initial network. This implies the epidemic threshold scales at least linearly in effective link-breaking rate ω. This is in contrast to the static model, where the epidemic threshold was larger than some constant determined by the initial network. The result from Figure 2.11 is in accordance with Eq. (2.6). In Chapter 3, the relation between the epidemic threshold τ_c and effective link-breaking ω is examined in more detail.

The final subject to be discussed regarding the epidemic threshold in the Markov process is the dependence on the self-infection rate ε.

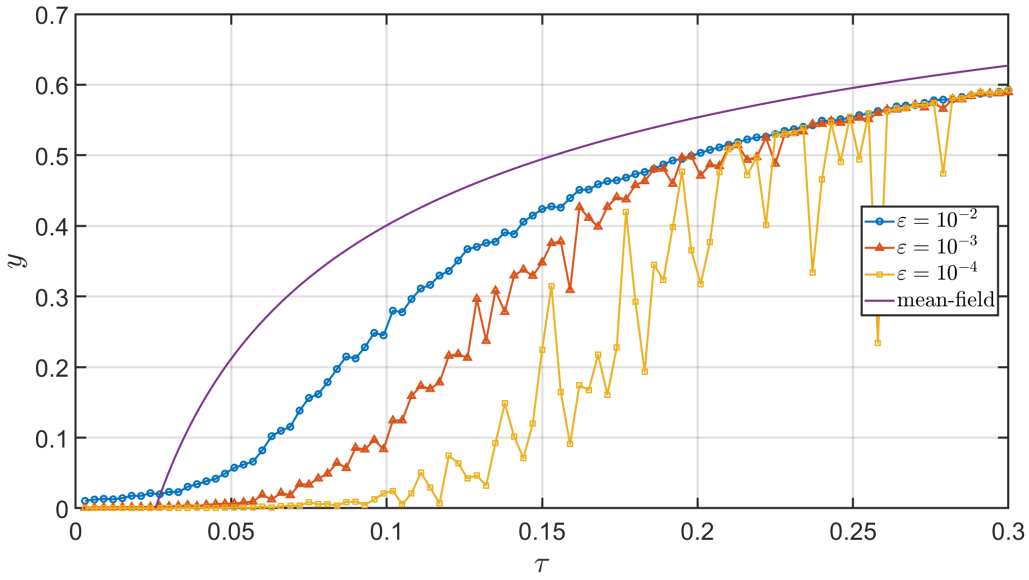

Figure 2.12: The relation between the effective infection rate τ and metastable prevalence y for various values of the self-infection rate ε. The mean-field approximation is included for reference. We have taken $N = 40$, $\delta = \zeta = \xi = 1$, $\Delta t = 0.05$ and a complete initial network.

Although the value of the self-infection rate ε is small, its impact is large [25, Figure 17.7]. In Figure 2.12 the bifurcation diagram is shown for various values of the self-infection rate ε. As ε decreases, the bifurcation lines are shifted towards the right. For $\tau > 0.28$ all lines overlap, indicating the value of ε is no longer relevant. The epidemic threshold seems to follow a logarithmic relationship in ε of the form

$$\tau_c \sim \log\left(\frac{1}{\varepsilon}\right). \tag{2.7}$$

Following the empirical relationship from Eq. (2.7), the epidemic threshold increases to infinity for $\varepsilon \to 0$. Intuitively, this should not be the case, as the self-infection rate ε was merely introduced as a mathematical tool to study the epidemic threshold of the model; its final impact on the bifurcation curve should be as small as possible. On the other hand, the Markov process has a stable, trivial, steady state where every individual is healthy. So the probability of finding the system to be in the trivial steady state increases to one as time approach infinity. Although the self-infection rate ε was introduced a small parameter, its influence is large. Nevertheless the ε-ASIS is the most promising method to investigate the metastable state.

Another relevant aspect to discuss is the uncertainty in Figure 2.12. For $\varepsilon = 10^{-2}$, a smooth curve is obtained for all τ values. By the central limit theorem, the curve becomes smooth for the number of time steps going to infinity. Moreover, it is conjectured that, based on the central limit theorem, it is sufficient to use

$$\text{time steps} \sim \frac{1}{\varepsilon^2}, \tag{2.8}$$

to find a smooth bifurcation curve. Around the epidemic threshold, a positive self-infection rate ε is used to subsequently find small time periods where the epidemic exists after which it collapses to the trivial state. When ε is too low, self-infection rarely happens, significantly increasing the risk of 'accidentality' infecting more often than average. When averaging takes place over a time period which is too small, this results in fluctuations in the bifurcation diagram, which is particularly visible for $\varepsilon = 10^{-4}$ in Figure 2.12. Based on this observation, we suggest to investigate another method to compute the epidemic threshold. Instead of applying a self-infection rate on a random individual, a random individual should be self-infected after a fixed amount of time. This ensures self-infection happens regularly and not stochastically, potentially improving the quality of the simulations. This proposal has not been verified in this thesis, and its utility is left for future research.

2.2.3 Network properties

Until now, the focus is laid on the prevalence in the ASIS model. In this section, the corresponding network structure is also reviewed. Unfortunately, most network properties cannot be determined using the mean-field EDEs. The mean-field EDEs allow $\mathbb{E}(X_i)$ and $\mathbb{E}(a_{ij})$ to have any value between 0 and 1, whereas most network properties require a link to exist ($a_{ij} = 1$) or not ($a_{ij} = 0$). These properties can therefore not be predicted using the mean-field EDEs and need to be analysed using extensive simulations of the Markov process.

A single run for the number of links in the network is shown in Figure 2.13. At the start of the simulation, the network is fully connected and has 780 links. Over a short period of time, a rapid decrease of the number of links is observed. Thereafter the system is found to be in the metastable state. The metastable number of links can be estimated by the ε-ASIS model as before.

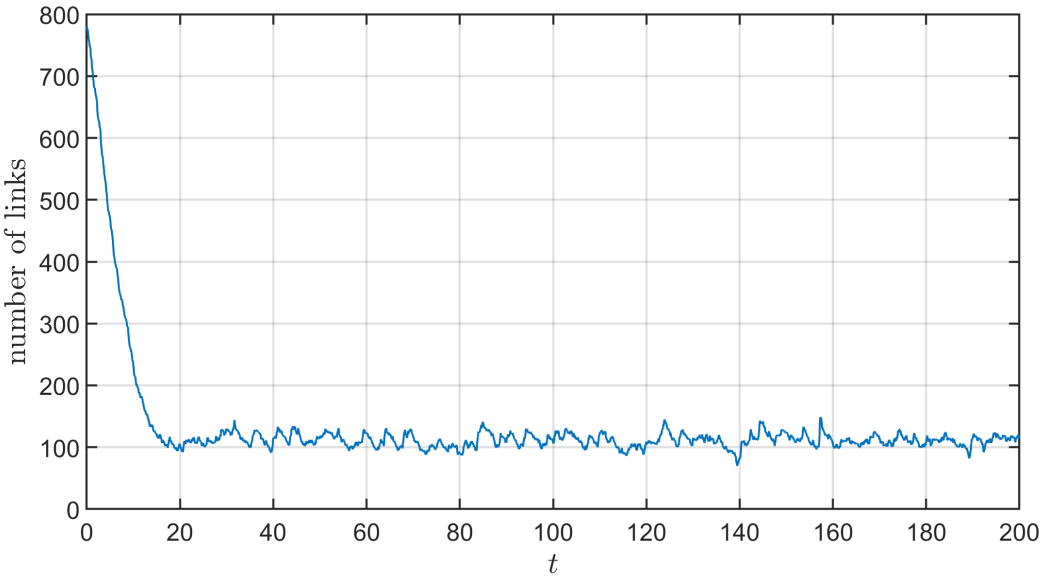

Figure 2.13: The number of links of a single run of the Markov process for the adaptive network. We have taken $N = 40$, $\delta = \beta = \zeta = \xi = 1$, $\varepsilon = 0.001$, $\Delta t = 0.05$ and a complete initial network.

Equivalently to the bifurcation diagram for the prevalence y in Figure 2.11, one may construct a bifurcation diagram for the number of links. Before that, define

$$\bar{L} = \frac{L}{L_0}$$

where L is the number of active links and L_0 the number of links in the initial network. Then $\bar{L}$ can be interpreted as the fraction of currently active links. The bifurcation diagram for $\bar{L}$, including the mean-field approximation, is shown in Figure 2.14.

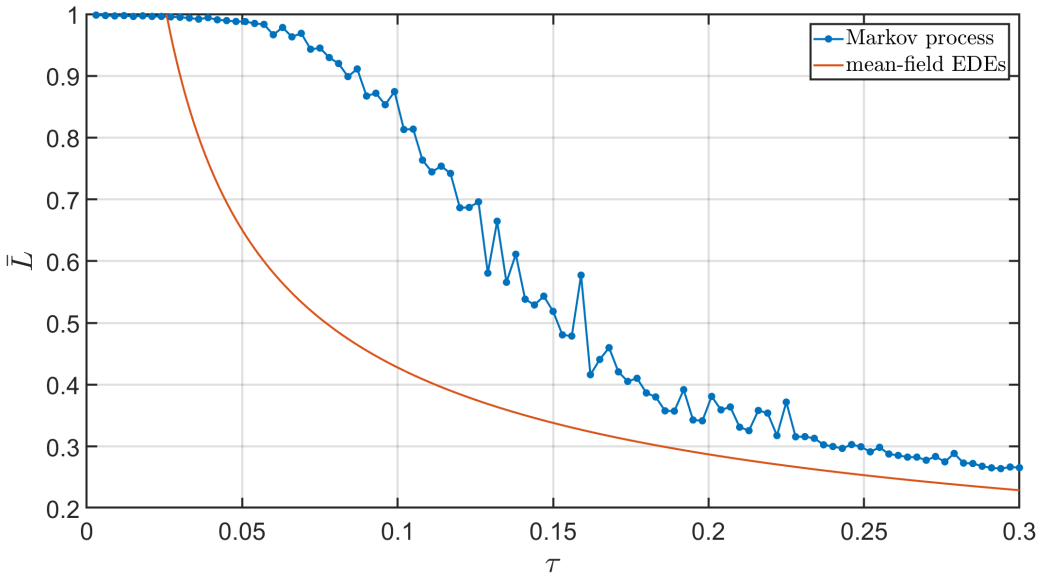

Figure 2.14: The relation between the effective infection rate τ and metastable fraction of active links $\bar{L}$. We have taken $N = 40$, $\delta = \zeta = \xi = 1$, $\varepsilon = 0.001$, $\Delta t = 0.05$ and a complete initial network.

Similarly to Figure 2.11 for the prevalence y, the mean-field approximation for the fraction of active links $\bar{L}$ in Figure 2.14 is decent for large values of τ but fails to address its behaviour near the epidemic threshold. The assumed independence of nodes appears to hold for large τ but is definitely incorrect around the epidemic threshold. Others methods need to be developed to accurately estimate metastable properties for the Markov process around the epidemic threshold.

The remainder of this section will be devoted to particular network properties. Two of them will be considered: the clustering coefficient and the modularity. The network is likely to exhibit a clustered network due to nodes infecting neighbouring nodes. The *clustering coefficient* C is the average fraction of neighbours of a node that are also neighbours of each other [33]. Define for each node i

$$C_i = \frac{2z}{d_i(d_i - 1)}, \tag{2.9}$$

where z is the number of links connecting the d_i neighbours of node i. Then the clustering coefficient is defined as the average over all nodes;

$$C = \frac{1}{N} \sum_{i=1}^{N} C_i. \tag{2.10}$$

Intuitively, one could see this as a measure of the number of triangles in the network. It is however unclear whether the number of triangles is a good measure for being clustered in the ASIS model, as the clustering does not necessarily result in a large number of triangles. The mean-field EDEs cannot be used for comparison since the mean-field EDEs allow variables to have any value between 0 and 1. The mean-field computation of the clustering coefficient is therefore meaningless. Hence extensive numerical simulations are required to gain inside into the clustering of the network. The bifurcation diagram for the clustering coefficient C is shown in Figure 2.15.

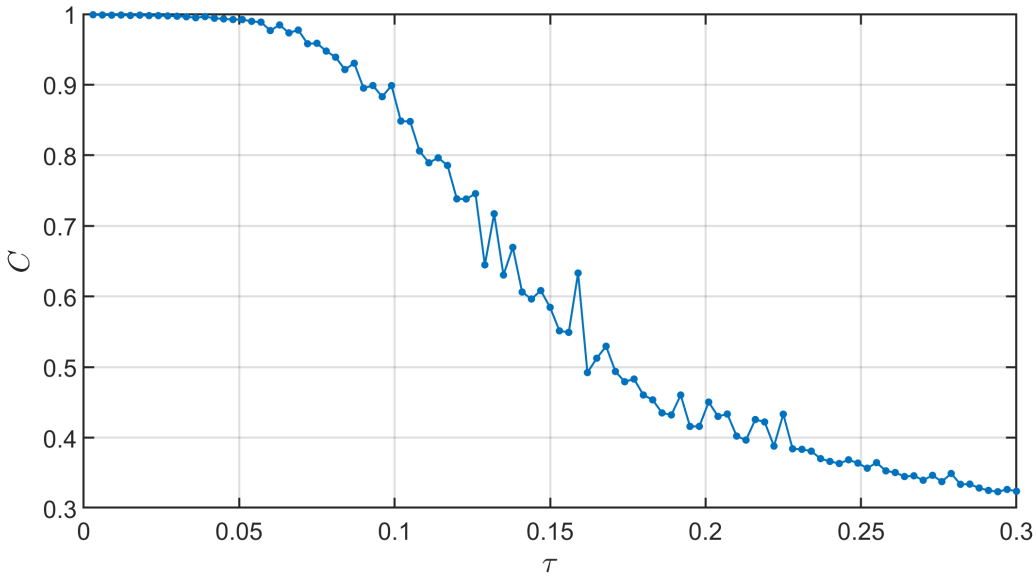

Figure 2.15: The relation between the effective infection rate τ and the metastable clustering coefficient C. We have taken $N = 40$, $\delta = \zeta = \xi = 1$, $\varepsilon = 0.001$, $\Delta t = 0.05$ and a complete initial network.

The bifurcation diagram for the fraction of active links $\bar{L}$ in Figure 2.14 and the clustering coefficient C in Figure 2.15 are similar. For $\tau \approx 0$, the clustering coefficient and the fraction of active links are one because the complete network is still intact and everyone is healthy. As τ grows above the epidemic threshold τ_c (which is around $\tau \approx 0.028$) the clustering and the fraction of active links decrease due to an enlarged possibility of link-breaking between susceptible and infected nodes. As τ increases to 0.2, the clustering and the fraction of active links are nearly constant as a function of τ. For $\tau > 0.2$, the number of links is low due to link-creation only occurring between two susceptible nodes and few nodes are actually susceptible. Link-breaking, which occurs between susceptible and infected nodes, happens at a relatively large scale.

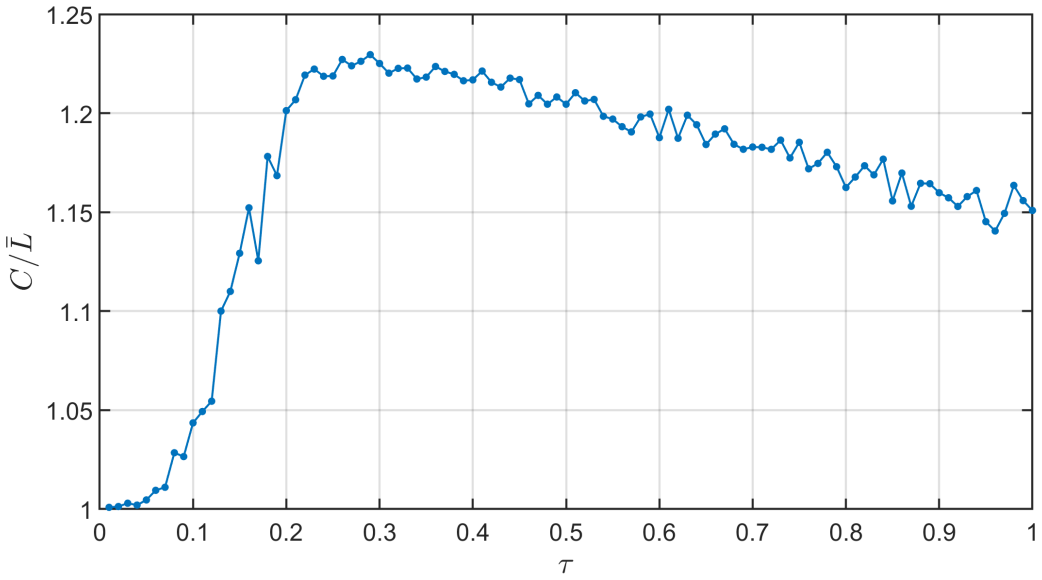

Figure 2.16: The relation between the effective infection rate τ and the ratio $C/\bar{L}$. We have taken $N = 40$, $\delta = \zeta = \xi = 1$, $\varepsilon = 0.001$, $\Delta t = 0.05$ and a complete initial network.

It is conjectured that the ratio between the clustering coefficient C and the fraction of active links $\bar{L}$ is more or less constant. In order to test this hypothesis, the ratio $C/\bar{L}$ is shown in Figure 2.16. For $\tau = 0$, the network stays intact and the ratio $C/\bar{L}$ is one. As τ increases, nodes start to infect their neighbours. Infected neighbours again infect theirs, which increases the opportunity to find triangles in the network. The majority of the nodes is still healthy for $\tau < 0.1$, leaving the complete network untouched. For τ approaching 0.2, infection takes place on a large scale. There is no further distinguishing between neighbours and other nodes. Therefore the relative clustering is no longer increased. Since link-breaking occurs easier than link-creation (the latter requires two healthy nodes which are rarely found) the number of links of the network slowly decreases, and the relative clustering decreases to zero as well.

The modularity is another possibly relevant network characteristic for the ASIS model. Generally, real-world networks can be divided into different communities. In each community, all individuals are closely connected, but are hardly connected to members of other communities. This gives rise to the *modularity* of a network. The susceptible nodes and infected nodes are separated in two groups. When the modularity is high, these two groups are well-separated. The modularity is defined as [34, 35]

$$M = \frac{1}{2L} \sum_{i=1}^{N} \sum_{j=1}^{N} \left(a_{ij} - \frac{d_i d_j}{2L} \right) 1_{(\text{if } i \text{ and } j \text{ belong to the same community})}. \tag{2.11}$$

The modularity is ranged between $[-1, 1]$. Alternative definitions are available, but can be rewritten in terms of Eq. (2.11). Mostly, the modularity serves as a measure to compare two networks. The absolute number cannot be used to derive many properties, although $M > 0.3$ usually implies a highly modular network [36]. An example of a high modular graph is shown in Figure 2.17.

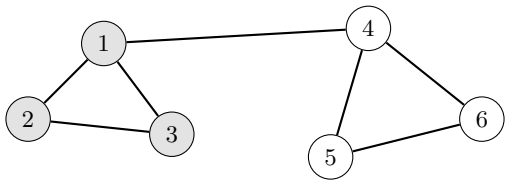

Figure 2.17: An example network of high modularity. The grey nodes and the white nodes form two modular groups.

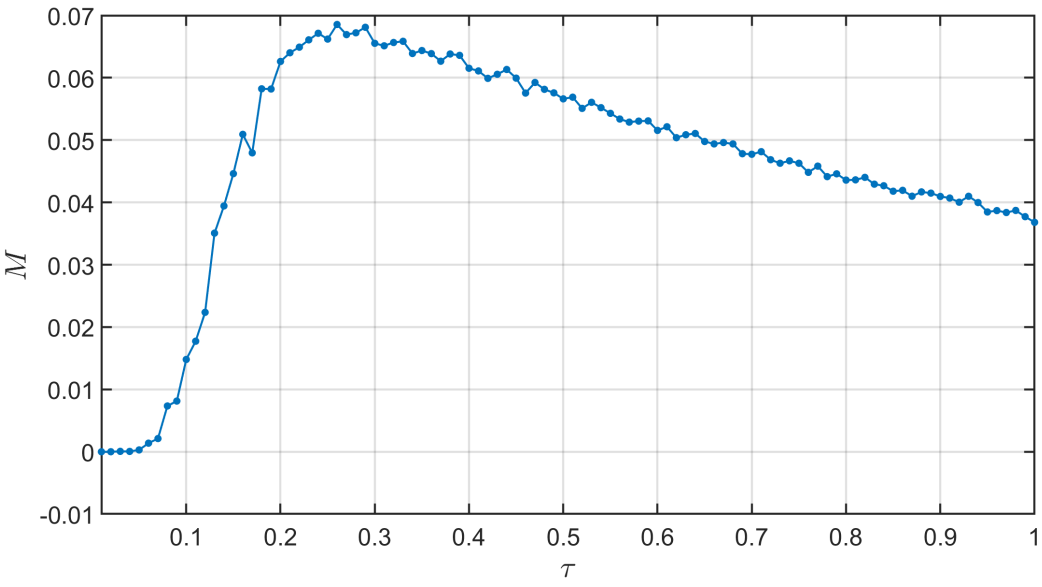

Figure 2.18: The relation between the effective infection rate τ and the metastable modularity M. We have taken $N = 40$, $\varepsilon = 0.001$, $\delta = \zeta = \xi = 1$, $\Delta t = 0.05$ and a complete initial network.

In the ASIS model, the nodes are separated into two groups: the susceptible nodes and the infected nodes. The modularity is a measure of the separation between susceptible and infected nodes. Despite nodes constantly switching groups, it is conjectured that the modularity is positive for any infection rate τ. The relation between the effective infection rate τ and the modularity M is shown in Figure 2.18. For $\tau \approx 0$, the modularity is zero as almost all nodes are susceptible and the network is complete. For τ increasing to 0.25, the modularity increases. The number of infected nodes increases, and the link-breaking mechanism removes many links between susceptible and infected nodes. This increases the modularity. As τ increases further, the majority of the nodes is infected. Then the modularity mainly decreases due to nodes changing from the susceptible group to the infected group. When the distribution of the nodes over the two groups becomes more skewed, the modularity almost inevitably decreases. The continuous decline of the modularity continues until $M = 0$ as $\tau \to \infty$. Namely, then the number of healthy people is zero, and therefore the modularity is zero.

2.3 Overview

In this chapter, the ASIS model has been analysed numerically in terms of its Markov process and the corresponding mean-field EDEs. For a complete static network, the epidemic threshold τ_c in the SIS model was located slightly above $\tau_c^{\mathrm{MF}} = \frac{1}{N-1}$ where τ_c^{MF} is the mean-field epidemic threshold. This result was supported by simulations and mean-field calculations. It was concluded that the mean-field approximation slightly overestimates the true epidemic threshold.

In the adaptive network, the epidemic threshold τ_c has been investigated as well. It was observed (and computed) that the epidemic threshold τ_c increases compared to the static network. This is caused by the adaptive process, which breaks links to reduce the spreading of the disease. The prevalence, however, is barely changed. The simulations of the Markov process have been compared to the mean-field EDEs. For large τ-values, the mean-field EDEs accurately predict the prevalence y, but fail to address the behaviour around the epidemic threshold. The simulations throughout this chapter have also shown considerable uncertainty. The averaged metastable values have been obtained using a too low number of time units. We have shown that the number of time units must be inversely proportional of the square of the self-infection rate ε to obtain smooth phase diagrams.

The expected time before collapsing to the trivial steady state was computed analytically for 2 nodes and verified numerically using simulations. Also the collapse time for 40 nodes was simulated, which showed a Poisson-like distribution. Since hitting times are in generally Poisson distributed, this result is in accordance with theory.

Finally the clustering of the metastable network was investigated. Two concepts were investigated: the ratio between the clustering coefficient and the fraction of active links and the modularity. When the effective infection rate is zero, both properties are zero. For $\tau > 0$ below the epidemic threshold, both properties increase. Above the epidemic threshold, the properties slowly decline to zero as the infection rate τ increase to infinity. Since links are almost never created when $\tau \to \infty$, the network becomes empty and the properties are both zero. This indicates that the clustering coefficient and modularity behave similarly in the ASIS model. Both show that the network is more clustered around and above the epidemic threshold.

3 Generalised Adaptive SIS Networks

In the previous chapters, a specific Markov process has been investigated: the Adaptive SIS model. In this model the adaptive rewiring of the links between nodes causes the spreading to slow down. Susceptible individuals remove connections with their infected neighbours with Poisson rate ζ. However, for the dynamics of the network structure, other possibilities are available. These possibilities can be assembled in a general Markov process, which we will call Generalised Adaptive SIS (G-ASIS) models. This framework can be used to model processes ranging from epidemics to information transfer among humans, computers, brain cells and more. For each of the adaptive networks in G-ASIS, the condition for existence and stability of the metastable state will be derived. Afterwards, the epidemic threshold is investigated and shown to be either linear in the effective link-breaking rate ω or constant.

In the first section, the G-ASIS framework is introduced. Section 3.2 elaborates on a lower bound for the epidemic threshold. Thereafter, an important theorem is proven. The result of this theorem is used in section 3.4 to find constraints for non-existing metastable states. In section 3.5, we show some examples and simulations for various models in G-ASIS. The sixth section will derive a relation for the epidemic threshold and will show the epidemic threshold to be bounded by a linear function in ω. Section 3.7 summarises the results and presents them in tabular format. The final section investigates another potential bound on the epidemic threshold.

3.1 The framework

We consider the spreading of a contagious process over a network. This includes processes ranging from epidemics to gossip, fake news and brain packets. Throughout this chapter, the wording of epidemic processes is used for simplicity. Every node is an individual which may spread the disease to its neighbours. The initial network $\mathcal{G}$ contains N nodes and is connected. As before, an individual i is infected if $X_i = 1$ and is healthy if $X_i = 0$. Every infected node which is connected to a susceptible node infects it with Poisson rate β. An infected node cures independently with Poisson rate δ. The corresponding EDEs have been derived in Chapter 2, which are

$$\frac{d\mathbb{E}(X_i)}{dt} = -\delta\mathbb{E}(X_i) + \beta \sum_{j=1, j\neq i}^{N} \mathbb{E}((1 - X_i)X_j a_{ij}). \tag{3.1}$$

The network a_{ij} is considered adaptive, i.e. it adapts itself based on the dynamical state of the nodes X_i and X_j in the network. A link in the network is modelled as a Bernoulli random variable, where $a_{ij}(t) = 1$ means the link exists at time t, and $a_{ij}(t) = 0$ means the link does not exist. The rules for the adaption of the network dynamics can be chosen in many ways. Here we present the Generalised Adaptive SIS framework (G-ASIS for short) which includes various models. Within the G-ASIS framework, some assumptions have to be made to reduce the number of models. First of all, it is assumed the network topology only changes when a link was available in the initial network. The links represent real-life connections, and not all nodes are connected to all. This concept was discussed in e.g. [37, Section 3], which is devoted to opinion spreading. Secondly, the network only changes based on two independent processes. One is a link-creation process with Poisson rate ξ (the corresponding rule will be called f_2) and the second is a link-breaking process with Poisson rate ζ (with rule f_1). Third, the network is undirected, implying $a_{ij} = a_{ji}$. Fourth, a link changes based on local information. Hence a link is created or removed based on the state of the end nodes of the link.

Using these assumptions, the EDE for the link a_{ij} is given by

$$\frac{d\mathbb{E}(a_{ij})}{dt} = a_{ij}(0)\mathbb{E}\Big[-\zeta a_{ij} f_1(X_i, X_j) + \xi(1 - a_{ij}) f_2(X_i, X_j)\Big], \tag{3.2}$$

where f_1 is the link-breaking rule and f_2 the link-creation rule. These functions depend on the state of the nodes X_i and X_j but not on a_{ij} or explicitly on time. In the G-ASIS framework, the functions f_1 for link-breaking and f_2 for link-creation are bound to the same set of rules. For convenience, a rule is notated as f. The function f has X_i and X_j as input, and can therefore be represented as

$$f : \{0, 1\}^2 \to \{0, 1\}.$$

The domain of the function f follows from X_i and X_j being Bernoulli random variables. The range of f is chosen such that the link-creation and link-breaking can be switched on or off for different possibilities of X_i and X_j.

We classify the rules according to the number of possible inputs that give $f(X_i, X_j) = 1$. Consider for example $f = X_i X_j$. Then $f = 1$ only for $X_i = X_j = 1$. Any other inputs for X_i and X_j yield $f = 0$. This rule is visualised in Figure 3.1. In the same way, three other rules can be derived where $f = 1$ for one combination of X_i and X_j. The number of permutations of this type can be computed as follows. There are four possible inputs (combinations of X_i and X_j) and one positive outcome: $\binom{4}{1} = 4$. All complying rules are:

$$X_i X_j, \qquad (1 - X_i)X_j, \qquad X_i(1 - X_j), \qquad (1 - X_i)(1 - X_j).$$

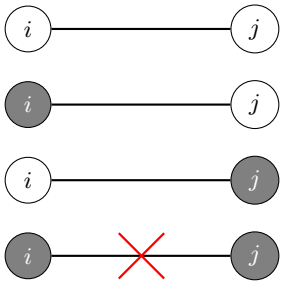

Figure 3.1: Schematic overview of two connected nodes. Grey nodes are infected nodes, white nodes are healthy nodes. The decision to break or recreate the link between node i and j depends solely on its end nodes: X_i and X_j. In this example, the link is broken when $X_i = X_j = 1$ and is otherwise left untouched which corresponds to link-breaking rule $f = X_i X_j$.

There are rules for which two combinations of X_i and X_j yield $f = 1$. As an example, consider $f = (X_i - X_j)^2$. Then $f = 1$ if X_i is not equal to X_j. There are six rules of this type, as there are four inputs and two combinations; $\binom{4}{2} = 6$. These rules are

$$\begin{array}{lll} (X_i - X_j)^2, & X_i, & X_j, \\ 1 - (X_i - X_j)^2, & (1 - X_i), & (1 - X_j). \end{array}$$

Thirdly, there are rules for which three combinations of X_i and X_j yield $f = 1$. For example, consider $f = 1 - X_i X_j$. The function's result is one if $X_i = 0$ or $X_j = 0$. The only situation to find $f = 0$ occurs for $X_i = X_j = 1$. All four rules complying to this result are

$$1 - X_i X_j, \qquad 1 - (1 - X_i)X_j, \qquad 1 - X_i(1 - X_j), \qquad 1 - (1 - X_i)(1 - X_j).$$

Two trivial rules have not yet been specified. These rules ($f = 1$ and $f = 0$) are independent of the state of the nodes X_i and X_j. These rules complete the set of rules for the function f.

All 16 possibilities for the function f have been derived. Each of them can be rewritten in the following standard form

$$f(X_i, X_j) = a + bX_i + \tilde{b}X_j + cX_i X_j, \tag{3.3}$$

where $a, b, \tilde{b}, c \in \mathbb{Z}$. Since the assumed network is undirected, the function f is symmetric in X_i and X_j. Hence, in Eq. (3.3), $\tilde{b} = b$. This removes eight asymmetric rules from the original derivation. Additionally, the trivial rules $f = 0$ and $f = 1$ are removed, since these are independent of X_i and X_j.

By the removal of the non-adaptive and non-symmetric rules, only six rules remain for the function f. Therefore the adaptive link-breaking process f_1 and link-creation processes f_2 each have six possible rules in the G-ASIS framework. Since the link-breaking rule f_1 and the link-creation rule f_2 can be chosen independently, and for each of them six rules are available, in total 36 Markov processes are contained in the G-ASIS framework. Each of these processes contain two rules; a link-breaking rule f_1 and a link-creation rule f_2. Each of these rules are of the form

$$f(X_i, X_j) = a + b(X_i + X_j) + cX_i X_j, \tag{3.4}$$

where $a, b, c \in \mathbb{Z}$. The link-breaking rule is notated as f_1 and its parameters by a_1, b_1 and c_1. The link-creation rule is denoted by f_2 and its coefficients by a_2, b_2 and c_2. An overview of the rules for the link-breaking and link-creation process is presented in Table 3.1.

Table 3.1: All rules for the link-breaking process and the link-creation process in the G-ASIS framework.

rule f	a	b	c
X_iX_j	0	0	1
$1 - X_iX_j$	1	0	-1
$(1 - X_i)(1 - X_j)$	1	-1	1
$1 - (1 - X_i)(1 - X_j)$	0	1	-1
$(X_i - X_j)^2$	0	1	-2
$1 - (X_i - X_j)^2$	1	-1	2

The rules for the link-breaking and link-creation processes are structured. For example, the inverse of any rule f is $1 - f$. Also, the multiplication of any rule f with itself is equal to itself ($f \circ f = f$). This indicates that the G-ASIS framework has much structure, however, the name of this structure was not found.

This chapter will usually focus on complete initial networks since these are computationally easier. Some results are however valid for general initial networks. If the results are valid for general initial networks, this is mentioned explicitly. Otherwise the focus is laid on the complete initial network.

3.2 Lower bound on the epidemic threshold

Analogous to the definition of the epidemic threshold in the adaptive SIS model, the epidemic threshold can be defined for the G-ASIS framework in a similar way. The epidemic threshold τ_c is defined as the largest value of the effective infection rate τ for which the prevalence y exponentially decays to zero over sufficiently large time. In order to find a bound for τ_c in the G-ASIS framework, we follow the approach by Ogura and Preciado (2016) [16] in which a general initial network is assumed. This methodology was also used for the static SIS model by Van Mieghem (2014) [25, Theorem 17.3.1]. In the derivation, the evolution of $\mathbb{E}(a_{ij}X_i)$ over time is used. Using techniques explained in Chapter 1, it was found that $\mathbb{E}(a_{ij}X_i)$ changes as follows

$$\begin{aligned}\frac{d\mathbb{E}(a_{ij}X_i)}{dt} = a_{ij}(0)\Bigg\{&(a_2+b_2)\xi\mathbb{E}(X_i) - (a_1\zeta + a_2\xi + b_1\zeta + b_2\xi + \delta)\mathbb{E}(a_{ij}X_i) \\ &+ (b_2+c_2)\xi\mathbb{E}((1-a_{ij})X_iX_j) - (b_1+c_1)\zeta\mathbb{E}(a_{ij}X_iX_j) + \beta\mathbb{E}\left[(1-X_i)a_{ij}\sum_{k=1}^{N}a_{ik}X_k\right]\Bigg\}.\end{aligned} \tag{3.5}$$

In this derivation, the evolution of $\mathbb{E}(X_i)$ and $\mathbb{E}(a_{ij}X_i)$ are used. The equations will be rewritten in terms of a linear and a non-linear part. Higher order terms around $\mathbb{E}(X_i) = \mathbb{E}(X_j) = 0$ and $\mathbb{E}(a_{ij}) = 1$ are denoted by W.

It is necessary that all terms are assembled in the linear part or are higher order correlation terms. The infection term (with coefficient β) can be rewritten as

$$\beta\mathbb{E}\left[(1-X_i)a_{ij}\sum_{k=1}^{N}a_{ik}X_k\right] = \beta\sum_{k=1}^{N}\mathbb{E}\left(a_{ik}X_k - X_ia_{ik}X_ka_{ij} - (1-a_{ij})a_{ik}X_k\right).$$

All other terms in Eq. (3.5) are linear terms or higher order terms. The equation can be rewritten as

$$\begin{aligned}\frac{d\mathbb{E}(a_{ij}X_i)}{dt} = a_{ij}(0)\Bigg\{&(a_2+b_2)\xi\mathbb{E}(X_i) - (a_1\zeta + b_1\zeta + a_2\xi + b_2\xi + \delta)\mathbb{E}(a_{ij}X_i) \\ &+ \beta\mathbb{E}\left[\sum_{k=1}^{N}a_{ik}X_k\right] - W_A\Bigg\},\end{aligned}$$

where the higher order terms of the network W_A are

$$W_A = -(b_2 + c_2)\xi\mathbb{E}((1 - a_{ij})X_iX_j) - (b_1 + c_1)\zeta\mathbb{E}(a_{ij}X_iX_j) + \beta\sum_{k=1}^{N}\mathbb{E}\left[X_iX_ka_{ik}a_{ij} + (1 - a_{ij})a_{ik}X_k\right].$$

The same can be done for the $\mathbb{E}(X_i)$:

$$\frac{d\mathbb{E}(X_i)}{dt} = -\delta\mathbb{E}(X_i) + \beta\sum_{k=1}^{N}\mathbb{E}(a_{ik}X_k) - W_X,$$

where the higher order terms for the nodes W_X are

$$W_X = \beta\sum_{k=1}^{N}\mathbb{E}(X_ia_{ik}X_j).$$

The differential equations can be written in matrix notation. This notation is adopted from [16]. Given a sequence of matrices $A_1, \ldots, A_n$. Let $\mathrm{A} = \oplus_{i=1}^{n}A_i$ be the block diagonal matrix having A_i on its block diagonals. A_i does not necessarily have to be square. The matrix A can be visualised as

$$A = \begin{pmatrix} A_1 & 0 & 0 & \ldots \\ 0 & A_2 & 0 & \ldots \\ \vdots & \ddots & \ddots & \ddots \\ \ldots & 0 & 0 & A_n \end{pmatrix}.$$

Define the matrices $q_i = \underset{j\,:\,a_{ij}(0)=1}{\mathrm{col}}\Big(\mathbb{E}(a_{ij}X_i)\Big)$ and $q = \underset{1\le i\le N}{\mathrm{col}}\Big(q_i\Big)$. Moreover, we define T_i as the row vector satisfying

$$T_iq = \sum_{k\,:\,a_{ik}(0)=1}\mathbb{E}(a_{ki}X_k).$$

Here T_i is a boolean row vector containing ones when an initial link is present between node i and node j (where j is the j'th element of T_i) and zero otherwise. The dimension of T_i is therefore $1 \times 2L_0$ where L_0 is the number of links in the initial network. Then define the matrix $T = \underset{1\le i\le N}{\mathrm{col}}\Big(T_i\Big)$. Also define the matrix $J = \oplus_{i=1}^{n}\mathbf{1}_{d_i}$ where d_i is the number of degrees of node i in the initial network. Let $S = \underset{1\le i\le N}{\mathrm{col}}\Big(\mathbf{1}_{d_i} \otimes T_i\Big)$ where $\otimes$ is the Kronecker product. To summarise, the following parameters have been defined;

$$\begin{aligned} q_i &= \underset{j\,:\,a_{ij}(0)=1}{\mathrm{col}}\Big(\mathbb{E}(a_{ij}X_i)\Big), \\ q &= \underset{1\le i\le N}{\mathrm{col}}\Big(q_i\Big), \\ T_iq &= \sum_{k\,:\,a_{ik}(0)=1}\mathbb{E}(a_{ki}X_k), \\ T &= \underset{1\le i\le N}{\mathrm{col}}\Big(T_i\Big), \\ J &= \oplus_{i=1}^{n}\mathbf{1}_{d_i}, \\ S &= \underset{1\le i\le N}{\mathrm{col}}\Big(\mathbf{1}_{d_i} \otimes T_i\Big). \end{aligned}$$

The system of equations can be formulated as

$$\frac{d}{dt}\begin{bmatrix}\mathbb{E}(X_i) \\ \mathbb{E}(a_{ij}X_i)\end{bmatrix} = M\begin{bmatrix}\mathbb{E}(X_i) \\ \mathbb{E}(a_{ij}X_i)\end{bmatrix} + \begin{bmatrix}W_X \\ W_A\end{bmatrix}, \tag{3.6}$$

where

$$M = \begin{pmatrix} -\delta I & \beta T \\ (a_2 + b_2)\xi J & \beta S - (a_1\zeta + b_1\zeta + a_2\xi + b_2\xi + \delta)I \end{pmatrix}. \tag{3.7}$$

In order to compute the stability of the non-linear autonomous system of equations above, it is necessary to regard the following theorem from literature.

Lemma 3.1 (M. Braun, Theorem 2)**.** *Let*

$$\dot{\boldsymbol{x}} = A\boldsymbol{x} + \mathbf{g}(\boldsymbol{x}) \tag{3.8}$$

be an autonomous system of equations. Suppose that $\mathbf{g}(\boldsymbol{x})/\|\boldsymbol{x}\| \equiv \mathbf{g}(\boldsymbol{x})/\max(|x_1|, ..., |x_n|)$ *is a continuous function of* $x_1, \dots x_n$ *which vanishes for* $\boldsymbol{x} = \mathbf{0}$*. Then the equilibrium solution* $\boldsymbol{x}(t) = \mathbf{0}$ *of Eq. (3.8) is asymptotically stable if the equilibrium solution* $\boldsymbol{x}(t) = \mathbf{0}$ *of the linearised equation* $\dot{\boldsymbol{x}} = A\boldsymbol{x}$ *is asymptotically stable. Equivalently, the solution* $\boldsymbol{x}(t) = \mathbf{0}$ *of Eq. (3.8) is asymptotically stable if all eigenvalues of A have negative real part.*

Proof. See [38, p. 386]. □

In case the eigenvalues of the matrix M are smaller than zero, the solution is bounded by an exponentially decaying function. This implies the solution dies out over sufficiently large time. The point where one of the eigenvalues becomes zero, changes the solution from an exponentially decaying function to a growing function. This bifurcation point is commonly known as the epidemic threshold. In order to derive a bound for the epidemic threshold, the eigenvalues of M need to be investigated. Specifically, the largest (real) eigenvalue is of interest. This eigenvalue is determined using Perron-Fröbenius theory.

Theorem 3.2. *Given a positive eigenvector* $\boldsymbol{x}$ *of* M*, its corresponding eigenvalue is the largest eigenvalue of* M*.*

Proof. The initial network was taken to be connected. Since the network is undirected, it is also strongly connected. It is proven by Ogura and Preciado (2016) that the matrix M is irreducible when the initial network is strongly connected [16, Appendix A]. Then, by Perron-Fröbenius theory for irreducible matrices, the statement follows [39, Theorem 8.4.4]. □

Based on Theorem 3.2, our approach is to construct an eigenvector for M which is positive. Using the positive eigenvector, a lower bound for the epidemic threshold can be computed. Afterwards the result is compared with some models known in literature.

Theorem 3.3. *The epidemic threshold for the G-ASIS framework is bounded from below by*

$$\tau_c \geq \frac{1 + \dfrac{\omega(a_1 + b_1)}{a_2 + b_2 + \delta/\xi}}{\rho}. \tag{3.9}$$

where ρ *is the spectral radius of the initial network.*

Proof. First a positive eigenvector is constructed. Since it was assumed that the initial network is strongly connected, there exists a positive eigenvector $\boldsymbol{v}$ corresponding to eigenvalue ρ (the spectral radius) [16]. We define $\boldsymbol{w} = \underset{1 \leq i \leq N}{\text{col}}\left(v_i \mathbf{1}_{d_i}\right)$. Using the definition of T_i, it follows that

$$T_i \boldsymbol{w} = \sum_{k\,:\,a_{ik}(0)=1} w_{ki} = \sum_{k\,:\,a_{ik}(0)=1} v_k = (Av)_i = \rho v_i. \tag{3.10}$$

So $T\boldsymbol{w} = \rho\boldsymbol{v}$. Equivalently, it follows that $S\boldsymbol{w} = \rho\boldsymbol{w}$.

Define the vector $\boldsymbol{x} = \begin{pmatrix} z\boldsymbol{v} \\ \boldsymbol{w} \end{pmatrix}$. Here $z \in \mathbb{R}$. This is an eigenvector of M:

$$\begin{aligned} M\begin{pmatrix} z\boldsymbol{v} \\ \boldsymbol{w} \end{pmatrix} &= \begin{pmatrix} -\delta I & \beta T \\ (a_2+b_2)\xi J & \beta S - (a_1\zeta + b_1\zeta + a_2\xi + b_2\xi + \delta)I \end{pmatrix}\begin{pmatrix} z\boldsymbol{v} \\ \boldsymbol{w} \end{pmatrix} \\ &= \begin{pmatrix} (\beta\rho - z\delta)\boldsymbol{v} \\ ((a_2+b_2)z\xi + \beta\rho - (a_1\zeta + b_1\zeta + a_2\xi + b_2\xi + \delta))\boldsymbol{w} \end{pmatrix} \\ &= \lambda\begin{pmatrix} z\boldsymbol{v} \\ \boldsymbol{w} \end{pmatrix}, \end{aligned}$$

where λ is the corresponding eigenvalue of ξ. Since $\boldsymbol{v}$ and $\boldsymbol{w}$ are positive, the eigenvector ξ is positive if and only if $z > 0$. In order to conclude $z > 0$, a system of equations for z and λ is obtained;

$$\begin{aligned} \beta\rho - z\delta &= z\lambda, \\ z(a_2+b_2)\xi + \beta\rho - (a_1\zeta + b_1\zeta + a_2\xi + b_2\xi + \delta) &= \lambda. \end{aligned} \tag{3.11}$$

Introduce z_1, z_2 as the solutions for z and λ_1, λ_2 the solutions for λ. Define $X = (a_2 + b_2)\xi$ and $Y = -\beta\rho + (a_1 + b_1)\zeta + (a_2 + b_2)\xi + \delta$. Then Eq. (3.11) simplifies to

$$\begin{aligned} \beta\rho &= z(\lambda + \delta), \\ zX + Y &= \lambda. \end{aligned} \tag{3.12}$$

First, the solution for z computed. Inserting the first equation of Eq. (3.12) into the second, we find a quadratic equation in z:

$$Xz^2 + (\delta - Y)z - \beta\rho = 0.$$

Since $X = (a_2 + b_2)\xi = \xi$ (we have $c_2 < 0$) the quadratic solution is

$$z = \frac{Y - \delta \pm \sqrt{(\delta - Y)^2 + 4X\rho\beta}}{2X}.$$

This is of the form

$$z = x \pm \sqrt{x^2 + y},$$

where $y > 0$. Then we find $z_1 < 0$ and $z_2 > 0$. The corresponding values for λ can be obtained using the second equation in Eq. (3.12), which can be rewritten as

$$\lambda = \frac{\beta\rho}{z} - \delta.$$

Since $\beta, \delta, \rho > 0$, we see that if $z_1 < 0$, we have $\lambda_1 < 0$. For $z_2 > 0$, the sign of λ is not determined. However, we require that $z_2 > 0$ to have a positive eigenvector and we require $\lambda_2 < 0$ for stability. From the system in Eq. (3.11), the quadratic equation for λ can be derived as well

$$\lambda^2 + (a_1\zeta + b_1\zeta + a_2\xi + b_2\xi + 2\delta - \beta\rho)\lambda - \underbrace{\beta\rho(a_2\xi + b_2\xi + \delta) + \delta(a_1\zeta + b_1\zeta + a_2\xi + b_2\xi + \delta)}_{\text{constant term}} = 0.$$

We have concluded that $\lambda_1 < 0$. The eigenvalues of M are required to be negative, hence $\lambda_2 < 0$. This can only be the case if the constant term of the quadratic equation is positive. This leads to the condition

$$-\beta\rho(a_2\xi + b_2\xi + \delta) + \delta(a_1\zeta + b_1\zeta + a_2\xi + b_2\xi + \delta) > 0,$$

which can be rewritten as

$$\frac{\beta}{\delta} < \frac{a_1\zeta + b_1\zeta + a_2\xi + b_2\xi + \delta}{\rho(a_2\xi + b_2\xi + \delta)},$$

such that the final form becomes

$$\tau < \frac{1 + \dfrac{\omega(a_1 + b_1)}{a_2 + b_2 + \delta/\xi}}{\rho}.$$

This is a required condition for the system to exponentially decay to zero over sufficiently large time. Therefore the epidemic threshold needs to be larger than those τ-values, which proves the theorem. □

The obtained lower bound for the epidemic threshold τ_c is validated below for two models from literature.

Example: ASIS model
Consider the ASIS model. Substitution of the parameters of this model gives

$$\tau_c \geq \frac{1+\omega\xi}{\rho}.$$

This implies the epidemic threshold of the ASIS model at least scales linearly in the link-breaking rate ω. This will be elaborated upon in one of the future sections.

Example: ASIS† model from Ogura & Preciado (2016)
In [16], another ASIS model was introduced. In this model, the link-breaking rule is equal to $f_1 = X_i + X_j$ and the link-creation rule is $f_2 = 1$. Substituting the parameters, we obtain

$$\tau_c \geq \frac{1+\dfrac{\zeta}{\xi+\delta}}{\rho},$$

which is in compliance with the result obtained in [16]. However, this model is not contained in the G-ASIS framework. The link-breaking rule $f_1 = X_i + X_j$ is not included because the rule has a double contribution for X_i and X_j when $X_i = X_j = 1$. The link-creation rule is a trivial rule, which has been discarded. The obtained lower bound in this section for the epidemic threshold is therefore valid for a larger set of rules than those contained in the G-ASIS framework, and extension of the framework can carried out effortlessly for the result in this section.

3.3 Derivation of the metastable quadratic equation for a complete initial network

The prevalence $y(t)$, which is the number of infected nodes at time t, is an important quantity for each G-ASIS process. Using Eqs. (3.1) and (3.2) a quadratic relation for the prevalence y can be obtained, which is proven in the following theorem.

Theorem 3.4. *The metastable prevalence y for a complete initial network satisfies the quadratic equation*

$$\begin{aligned} &y^2 + \left(\frac{2b_2N\tau - (2b_2+c_2)\tau + c_1\omega + c_2}{c_2N\tau}\right)y \\ &+ \left(\frac{(N-1)a_2}{c_2N} - \frac{a_1\omega + a_2}{c_2N^2}\mathbb{E}\left(\sum_{i=1}^{N} d_i^*\right) + \mathrm{Var}(Z^*)\right. \\ &\left. - \frac{(2b_1+c_1)\omega + 2b_2 + c_2}{c_2N^2}\mathbb{E}\left(\sum_{i=1}^{N} d_i^* X_i^*\right)\right) = 0. \end{aligned} \tag{3.13}$$

Proof. We repeat the derivation as in [11]. Inserting the result from Eq. (3.4) into Eq. (3.2), we find

$$\frac{d\mathbb{E}(a_{ij})}{dt} = a_{ij}(0)\mathbb{E}\Big[-\zeta a_{ij}(a_1 + b_1(X_i+X_j) + c_1X_iX_j) + \xi(1-a_{ij})(a_2 + b_2(X_i+X_j) + c_2X_iX_j)\Big].$$

By using that we have a complete initial network, i.e. $a_{ij}(0) = 1$ for all i, j, we obtain

$$\begin{aligned} \frac{d\mathbb{E}(a_{ij})}{dt} &= a_2\xi + b_2\xi\mathbb{E}(X_i) + b_2\xi\mathbb{E}(X_j) - (a_1\zeta + a_2\xi)\mathbb{E}(a_{ij}) + c_2\xi\mathbb{E}(X_iX_j) \\ &\quad - (b_1\zeta + b_2\xi)\mathbb{E}(a_{ij}X_i) - (b_1\zeta + b_2\xi)\mathbb{E}(a_{ij}X_j) - (c_1\zeta + c_2\xi)\mathbb{E}(a_{ij}X_iX_j). \end{aligned}$$

Taking the sum over all $j \neq i$, and using the degree $d_i = \sum_{j=1, j\neq i}^{N} X_i$ and $a_{ii} = 0$ we obtain

$$\begin{aligned}\frac{d\mathbb{E}(d_i)}{dt} &= a_2\xi(N-1) + b_2\xi(N-1)\mathbb{E}(X_i) + b_2\xi \sum_{j=1, j\neq i}^{N} \mathbb{E}(X_j) - (a_1\zeta + a_2\xi)\mathbb{E}(d_i) \\ &+ c_2\xi\mathbb{E}\left(X_i \sum_{j=1, j\neq i}^{N} X_j\right) - (b_1\zeta + b_2\xi)\mathbb{E}(d_i X_i) - (b_1\zeta + b_2\xi)\mathbb{E}\left(\sum_{j=1}^{N} a_{ij} X_j\right) \\ &- (c_1\zeta + c_2\xi)\mathbb{E}\left(\sum_{j=1}^{N} a_{ij} X_i X_j\right).\end{aligned}$$

Two terms need to be investigated in more detail. The following relations hold

$$\begin{aligned}(N-1)\mathbb{E}(X_i) + \sum_{j=1, j\neq i}^{N} \mathbb{E}(X_j) &= (N-2)\mathbb{E}(X_i) + \sum_{j=1}^{N} \mathbb{E}(X_j), \\ \mathbb{E}\left(X_i \sum_{j=1, j\neq i}^{N} X_j\right) = \mathbb{E}\left(X_i \left(\sum_{j=1}^{N} X_j - X_i\right)\right) &= \mathbb{E}\left(X_i \sum_{j=1}^{N} X_j\right) - \mathbb{E}(X_i),\end{aligned}$$

where in the last equation, for the last equality we used the Bernoulli property. Inserting these back yields

$$\begin{aligned}\frac{d\mathbb{E}(d_i)}{dt} &= a_2\xi(N-1) + \left(b_2\xi(N-2) - c_2\xi\right)\mathbb{E}(X_i) + b_2\xi \sum_{j=1}^{N} \mathbb{E}(X_j) - (a_1\zeta + a_2\xi)\mathbb{E}(d_i) \\ &+ c_2\xi\mathbb{E}\left(X_i \sum_{j=1}^{N} X_j\right) - (b_1\zeta + b_2\xi)\mathbb{E}(d_i X_i) - (b_1\zeta + b_2\xi)\mathbb{E}\left(\sum_{j=1}^{N} a_{ij} X_j\right) \\ &- (c_1\zeta + c_2\xi)\mathbb{E}\left(\sum_{j=1}^{N} a_{ij} X_i X_j\right).\end{aligned}$$

Up to now only the network equations have been used. We use the epidemic equations to get rid of the largest correlation term. Hence we rewrite Eq. (3.1) as

$$\mathbb{E}\left(\sum_{j=1}^{N} a_{ij} X_i X_j\right) = -\frac{1}{\beta}\frac{d\mathbb{E}(X_i)}{dt} - \frac{1}{\tau}\mathbb{E}(X_i) + \mathbb{E}\left(\sum_{j=1}^{N} a_{ij} X_j\right),$$

where $\tau = \beta/\delta$ is the effective infection rate. Inserting this back into the previous result gives

$$\begin{aligned}\frac{d\mathbb{E}(d_i)}{dt} &= a_2\xi(N-1) + \left(b_2\xi(N-2) - c_2\xi\right)\mathbb{E}(X_i) + b_2\xi \sum_{j=1}^{N} \mathbb{E}(X_j) - (a_1\zeta + a_2\xi)\mathbb{E}(d_i) \\ &+ c_2\xi\mathbb{E}\left(X_i \sum_{j=1}^{N} X_j\right) - (b_1\zeta + b_2\xi)\mathbb{E}(d_i X_i) - (b_1\zeta + b_2\xi)\mathbb{E}\left(\sum_{j=1}^{N} a_{ij} X_j\right) \\ &- (c_1\zeta + c_2\xi)\left[-\frac{1}{\beta}\frac{d\mathbb{E}(X_i)}{dt} - \frac{1}{\tau}\mathbb{E}(X_i) + \mathbb{E}\left(\sum_{j=1}^{N} a_{ij} X_j\right)\right].\end{aligned}$$

Taking all time-derivatives to the left, and by dividing every term by ζ, we obtain

$$\begin{aligned}\frac{d}{dt}\mathbb{E}\left(\frac{d_i}{\zeta}-\frac{c_1+c_2\omega^{-1}}{\beta}X_i\right) &= a_2\omega^{-1}(N-1)+\left(b_2\omega^{-1}(N-2)-c_2\omega^{-1}+\frac{c_1+c_2\omega^{-1}}{\tau}\right)\mathbb{E}(X_i)\\ &+ b_2\omega^{-1}\sum_{j=1}^{N}\mathbb{E}(X_j)-(a_1+a_2\omega^{-1})\mathbb{E}(d_i)+c_2\omega^{-1}\mathbb{E}\left(X_i\sum_{j=1}^{N}X_j\right)\\ &- (b_1+b_2\omega^{-1})\mathbb{E}(d_iX_i)-(b_1+b_2\omega^{-1}+c_1+c_2\omega^{-1})\mathbb{E}\left(\sum_{j=1}^{N}a_{ij}X_j\right).\end{aligned}$$

Using $2L=\sum_{i=1}^{N}d_i$ where L is the number of links, we sum over all $1\le i\le N$ to find

$$\begin{aligned}&\frac{d}{dt}\mathbb{E}\left(\frac{2L}{\zeta}-\frac{c_1+c_2\omega^{-1}}{\beta}\sum_{i=1}^{N}X_i\right)\\ &= a_2\omega^{-1}N(N-1)+\left(b_2\omega^{-1}(N-2)-c_2\omega^{-1}+\frac{c_1+c_2\omega^{-1}}{\tau}\right)\sum_{i=1}^{N}\mathbb{E}(X_i)\\ &+ b_2\omega^{-1}N\sum_{j=1}^{N}\mathbb{E}(X_j)-(a_1+a_2\omega^{-1})\mathbb{E}\left(\sum_{i=1}^{N}d_i\right)+c_2\omega^{-1}\mathbb{E}\left(\sum_{i=1}^{N}X_i\sum_{j=1}^{N}X_j\right)\\ &- (b_1+b_2\omega^{-1})\sum_{i=1}^{N}\mathbb{E}(d_iX_i)-(b_1+b_2\omega^{-1}+c_1+c_2\omega^{-1})\mathbb{E}\left(\sum_{j=1}^{N}d_jX_j\right).\end{aligned}$$

Using the fraction of infected nodes $Z=\frac{1}{N}\sum_{i=1}^{N}X_i$, we can simplify this to

$$\begin{aligned}&\frac{d}{dt}\mathbb{E}\left(\frac{2L}{\zeta}-\frac{c_1N+c_2\omega^{-1}N}{\beta}Z\right)\\ &= a_2\omega^{-1}N(N-1)+\left(b_2\omega^{-1}N(N-2)-c_2N\omega^{-1}+\frac{c_1N+c_2\omega^{-1}N}{\tau}\right)\mathbb{E}(Z)\\ &+ b_2\omega^{-1}N^2\mathbb{E}(Z)-(a_1+a_2\omega^{-1})\mathbb{E}\left(\sum_{i=1}^{N}d_i\right)+c_2\omega^{-1}N^2\mathbb{E}(Z^2)\\ &- (b_1+b_2\omega^{-1}+b_1+b_2\omega^{-1}+c_1+c_2\omega^{-1})\mathbb{E}\left(\sum_{j=1}^{N}d_jX_j\right).\end{aligned}$$

When the derivative on the LHS vanishes (in the metastable state which we denote by an asterisk $*$) we have

$$\begin{aligned}&a_2\omega^{-1}N(N-1)+\left(b_2\omega^{-1}N(N-1)-b_2N\omega^{-1}+b_2\omega^{-1}N^2-c_2N\omega^{-1}+\frac{c_1N+c_2\omega^{-1}N}{\tau}\right)\mathbb{E}(Z^*)\\ &- (a_1+a_2\omega^{-1})\mathbb{E}\left(\sum_{i=1}^{N}d_i^*\right)+c_2\omega^{-1}N^2\mathbb{E}((Z^*)^2)\\ &- (2b_1+2b_2\omega^{-1}+c_1+c_2\omega^{-1})\mathbb{E}\left(\sum_{j=1}^{N}d_j^*X_j^*\right)=0.\end{aligned}$$

Using $\mathrm{Var}(Z^*) = \mathbb{E}((Z^*)^2) - \mathbb{E}(Z^*)^2$ and $y = \mathbb{E}(Z^*)$ we finally find

$$c_2\omega^{-1}N^2y^2 + \left(2b_2\omega^{-1}N(N-1) - c_2N\omega^{-1} + \frac{c_1N + c_2\omega^{-1}N}{\tau}\right)y$$
$$+ a_2\omega^{-1}N(N-1) - (a_1 + a_2\omega^{-1})\mathbb{E}\left(\sum_{i=1}^{N} d_i^*\right) + c_2\omega^{-1}N^2\mathrm{Var}(Z^*)$$
$$- (2b_1 + 2b_2\omega^{-1} + c_1 + c_2\omega^{-1})\mathbb{E}\left(\sum_{i=1}^{N} d_i^*X_i^*\right) = 0,$$

which is a quadratic equation in y. Since c_2 is never zero, every term can be multiplied by $\frac{\omega}{c_2N^2}$, which proves the theorem. □

This completes the derivation of the quadratic formula for the metastable prevalence y. To verify the obtained result, two examples from literature are discussed below.

Example 1. ASIS model
Consider the ASIS model. This model has link-breaking rule $f_1 = (X_i - X_j)^2$ and link-creation rule $f_2 = (1 - X_i)(1 - X_j)$. Eq. (3.4) then shows that $(a_1, b_1, c_1) = (0, 1, -2)$ and $(a_2, b_2, c_2) = (1, -1, 1)$ and reduces the metastable prevalence y from Eq. (3.13) to

$$y^2 + \left(-2 + \frac{1}{N} + \frac{1-2\omega}{N\tau}\right)y + \left(1 - \frac{1}{N} + \mathrm{Var}(Z^*) - \frac{1}{N^2}\sum_{i=1}^{N}\mathbb{E}(d_i^*(1 - X_i^*))\right) = 0,$$

which is in accordance with [11].
End of Example 1.

Example 2. AID model
Consider the AID model from [17]. In this model, the link-breaking rule is $f_1 = (1 - X_i)(1 - X_j)$ and link-creation rule is $f_2 = (X_i - X_j)^2$. Eq. (3.4) then shows that $(a_1, b_1, c_1) = (1, -1, 1)$ and $(a_2, b_2, c_2) = (0, 1, -2)$ and reduces the metastable prevalence y from Eq. (3.13) to

$$y^2 + \left(-1 + \frac{2-\omega}{2N\tau}\right)y + \left(\mathrm{Var}(Z^*) + \frac{\omega}{2N^2}\sum_{i=1}^{N}\mathbb{E}(d_i^*(1 - X_i^*))\right) = 0,$$

which is in accordance with [17].
End of Example 2.

3.4 Regions of instability

The quadratic relation for the metastable prevalence y from Theorem 3.4 can be used to find conditions for which the metastable state does not exist. Proving that the metastable state exists is hard, however, the proof that it is non-existent is easier. Hence the latter will be the focus of this section.

The prevalence y is the averaged number of individuals which are infected relative to the total population. Hence $y \in \mathbb{R}$ and $0 \leq y \leq 1$. For the prevalence y to be real, the discriminant of the quadratic formula in Eq. (3.16) should be positive. Let us define

$$V = -\left(\frac{2b_2N\tau - (2b_2 + c_2)\tau + c_1\omega + c_2}{2c_2N\tau}\right), \tag{3.14}$$

$$H = \left(\frac{(N-1)a_2}{c_2N} - \frac{a_1\omega + a_2}{c_2N^2}\mathbb{E}\left(\sum_{i=1}^{N} d_i^*\right) + \mathrm{Var}(Z^*)\right.$$
$$\left. - \frac{(2b_1 + c_1)\omega + 2b_2 + c_2}{c_2N^2}\mathbb{E}\left(\sum_{i=1}^{N} d_i^*X_i^*\right)\right), \tag{3.15}$$

then Eq. (3.13) can be simplified to

$$y^2 - 2Vy + H = 0. \tag{3.16}$$

The two solutions are

$$y = V \pm \sqrt{V^2 - H}. \tag{3.17}$$

In case $V^2 - H < 0$, the solutions to the quadratic equation for the prevalence y are imaginary. This implies the metastable state does not exist. Therefore, it will be investigated for which parameters the relation $V^2 < H$ holds. Substituting the definition of V and H into Eq. (3.17) gives

$$\begin{aligned}\left(\frac{2b_2N\tau - (2b_2 + c_2)\tau + c_1\omega + c_2}{2c_2N\tau}\right)^2 < \Bigg(&\frac{(N-1)a_2}{c_2N} - \frac{a_1\omega + a_2}{c_2N^2}\mathbb{E}\left(\sum_{i=1}^{N} d_i^*\right) + \mathrm{Var}(Z^*) \\ &- \frac{(2b_1 + c_1)\omega + 2b_2 + c_2}{c_2N^2}\mathbb{E}\left(\sum_{i=1}^{N} d_i^* X_i^*\right)\Bigg).\end{aligned} \tag{3.18}$$

3.4.1 Infinitely sized network

The inequality in Eq. (3.18) contains many parameters. Therefore, a network of infinite size is considered first. By taking $\lim_{n\to\infty}$, some simplifications are made which are considered in the next section. The infinite sized network simplifies the inequality to

$$\left(\frac{b_2}{c_2}\right)^2 < \Bigg(\underbrace{\frac{a_2}{c_2}}_{\text{term 1}} \underbrace{- \frac{a_1\omega + a_2}{c_2N^2}\mathbb{E}\left(\sum_{i=1}^{N} d_i^*\right)}_{\text{term 2}} + \underbrace{\mathrm{Var}(Z^*)}_{\text{term 3}} \underbrace{- \frac{(2b_1 + c_1)\omega + 2b_2 + c_2}{c_2N^2}\mathbb{E}\left(\sum_{i=1}^{N} d_i^* X_i^*\right)}_{\text{term 4}}\Bigg). \tag{3.19}$$

It must be verified for which parameters Eq. (3.19) holds. The relation can only hold if the sign of term 3 and terms 2 and 4 are equal (and thus positive). Using Table 3.1, it is found that $a_1, a_2 \in \{0, 1\}$. For term 2 to be positive, it is therefore necessary that $c_2 < 0$. Now we investigate term 4.

- Suppose $a_1 = 0$. Table 3.1 shows that $2b_1 + c_1 \in \{0, 1\}$. In either case, the values in front of the ω-term are zero or positive because $c_2 < 0$.
- Suppose $a_1 = 1$. Then $2b_1 + c_1 \in \{-1, 0\}$. The case where the sum is zero is fine, however, when $2b_1 + c_1 = -1$, the term is negative. However, in this case, term 4 can merged with term 2 as follows
$$-\frac{\omega}{c_2N^2}\mathbb{E}\left(\sum_{i=1}^{N} d_i^*\right) - \frac{-\omega}{c_2N^2}\mathbb{E}\left(\sum_{i=1}^{N} d_i^* X_i^*\right) = -\frac{\omega}{c_2N^2}\mathbb{E}\left(\sum_{i=1}^{N} d_i^*(1 - X_i^*)\right),$$
which is positive as $X_i^* \in \{0, 1\}$ and we have derived that $c_2 < 0$.

The same procedure can be performed for a_2, which goes analogously, with the only exception that fewer states are permitted due to $c_2 < 0$. Still, the result is the same.

Term 1 is negative, as $a_2 \in \{0, 1\}$ and it was determined that $c_2 < 0$. Eq. (3.19) is rewritten such that both sides contain only positive terms:

$$\left(\frac{b_2}{c_2}\right)^2 - \frac{a_2}{c_2} < \left(\mathrm{Var}(Z^*) - \frac{a_1\omega + a_2}{c_2N^2}\mathbb{E}\left(\sum_{i=1}^{N} d_i^*\right) - \frac{(2b_1 + c_1)\omega + 2b_2 + c_2}{c_2N^2}\mathbb{E}\left(\sum_{i=1}^{N} d_i^* X_i^*\right)\right). \tag{3.20}$$

The inequality of Eq. (3.20) is a constraint for which the metastable state does not exist. Then it is certainly non-existent when two positive terms on the RHS are removed;

$$\left(\frac{b_2}{c_2}\right)^2 - \frac{a_2}{c_2} < \mathrm{Var}(Z^*). \tag{3.21}$$

Based on Table 3.1, it can be shown that all combinations for the LHS in Eq. (3.21) are strictly positive. This indicates the $\mathrm{Var}(Z^*)$ is positive as well. Since most nodes are in the same state (zero or one), the variance for the prevalence y is very low. Hence this inequality cannot be satisfied, and the following result is obtained

Non-existent metastable state for infinitely large networks: $c_2 < 0$. (3.22)

3.4.2 Finite-size networks

The results for infinitely sized networks in Eq. (3.22) is not trivially satisfied for networks of finite size. In real-life applications finite networks are used. The assumption of infinitely sized networks removed several terms in Eq. (3.19) to simplify the calculations. It is however necessary to verify whether this approximation was correct, or derive conditions when this approximation is correct in case of finite size networks. By taking $\lim_{N\to\infty}$, the following three approximations were made:

$$\frac{2b_2 + c_2}{2c_2} \ll N, \qquad (A)$$
$$\frac{c_1\omega + c_2}{2c_2\tau} \ll N, \qquad (B)$$
$$-\frac{a_2}{c_2} \ll N. \qquad (C)$$

Using Table 3.1, the following relations can be derived (using $c_2 < 0$ from Eq. (3.22))

$$\frac{2b_2 + c_2}{c_2} \in \left\{-1, -\frac{1}{2}, 0, \frac{1}{2}, 1\right\}, \qquad -\frac{a_2}{c_2} \in \{-1, 0, 1\}.$$

Using these relations, it is clear that (A) and (C) are satisfied. Then the inequality from (B) remains. We have already found that $c_2 < 0$. Now suppose $c_1 < 0$ as well. Then the expression is positive, and a bound for ω or τ appears for fixed N. Suppose we fix ω and N. The constraint for τ becomes

$$\tau \gg \frac{c_1\omega + c_2}{2c_2 N}. \tag{3.23}$$

For general $c_1 < 0, c_2 < 0$, this constraint for τ is not satisfied. Therefore we conclude the G-ASIS model is not necessarily unstable for $c_1 < 0$ and it does not have a non-existent metastable state.

Now consider $c_1 > 0$. We again regard constraint (B). Suppose one chooses $\omega > -\frac{c_2}{c_1}$. Then the LHS of Eq. (3.23) is negative, which satisfies the constraint unconditionally. One could try $\omega < -\frac{c_2}{c_1}$ as well, but it yields another constraint for τ. The constraint will resort to an expression comparable to the case $c_1 < 0$. This case is therefore not contributing anything to the conditions under which the metastable state does not exist.

To sum up, the Generalised Adaptive SIS framework (G-ASIS) is non-existent for

$$\textbf{G-ASIS non-existent for: } c_2 < 0, \quad c_1 > 0, \quad \omega > -\frac{c_2}{c_1}. \tag{3.24}$$

Although the metastable state does not exist when the conditions from Eq. (3.24) are satisfied, it remains unclear what the behaviour of the Markov process is. The next section shows several models of the G-ASIS framework, and simulations are performed to answer this question.

3.5 Examples and simulations

It was proven in Eq. (3.24) that the metastable state does not always exist. However, it remains unclear for which values of the effective infection rate τ this holds and what the behaviour of the process is. Besides the introduction of various models of the G-ASIS framework, this is the main subject of this section.

The simulations are carried out as usual using 2,000 time units of initialisation time and 40,000 time units of computation time. In [11], an initialisation time of 10,000 time units was used but we have found no evidence for a slow convergence towards the metastable state.

Example 1. ASIS model revisited
Before other models are investigated, the ASIS model is reconsidered. The bifurcation diagram was constructed in the previous chapter in Figure 2.11. For clarity, it is repeatedly shown in Figure 3.2.

According to Eq. (3.24), the metastable state is stable. This is observable in Figure 3.2; the line is relatively smooth for all $\tau > \tau_c$.

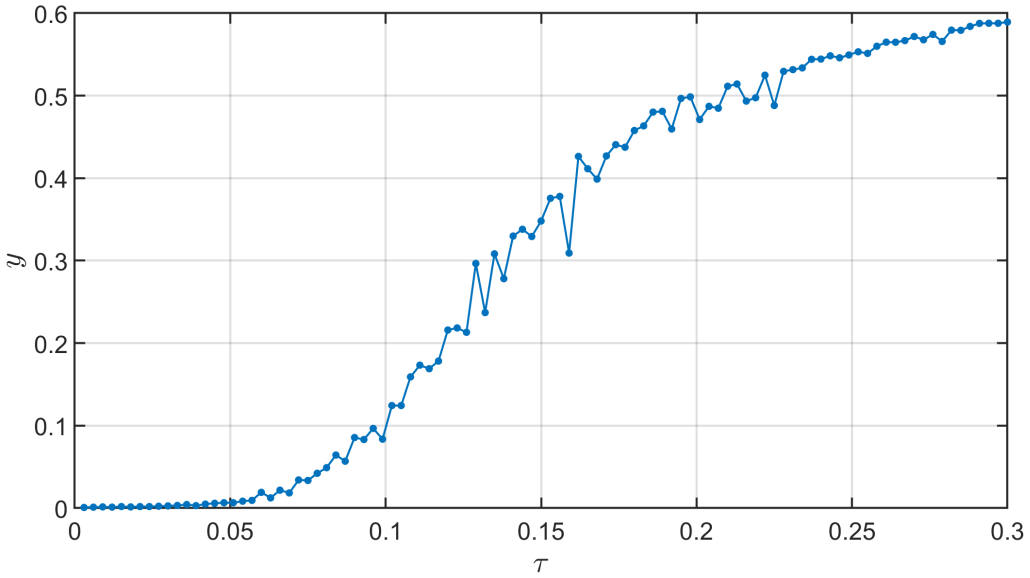

Figure 3.2: (ASIS) The relation between the effective infection rate τ and metastable prevalence y. We have taken $N = 40$, $\Delta t = 0.05$, $\delta = \zeta = \xi = 1$, $\varepsilon = 0.001$ and a complete initial network.

End of Example 1.

Example 2. ASIS* model with different link-breaking rule.
We consider the ASIS model with a slightly modified link-breaking rule. In the original ASIS model, the link between two infected nodes is never broken. In the ASIS* model, the link between two infected nodes can be broken as well, next to the link-breaking between susceptible and infected nodes. The link-creation rule is unchanged: $f_2 = (1-X_i)(1-X_j)$ and the link-breaking rule changes to $f_1 = 1-(1-X_i)(1-X_j)$. This model is based on the following observation. Since infected people are likely to distant themselves from society due to their disease, their contact pattern with infected people is interrupted as well. This causes them to break links with all other people, and not just healthy people. Using the result from Eq. (3.24), it is predicted that this model always has a metastable state.

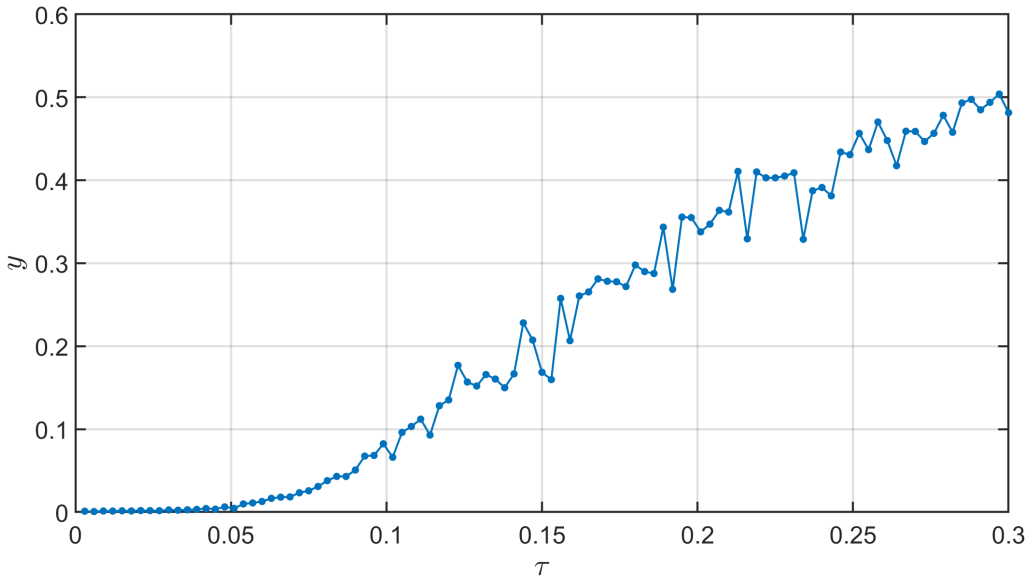

Figure 3.3: (ASIS*) The relation between the effective infection rate τ and metastable prevalence y. We have taken $N = 40$, $\Delta t = 0.05$, $\delta = \zeta = \xi = 1$, $\varepsilon = 0.001$ and a complete initial network.

As expected, the bifurcation diagram for the ASIS* model in Figure 3.3 shows similar behaviour as the ASIS model. The metastable prevalence y is lower than the ASIS model in Figure 3.2. This is caused by the new link-breaking rule, which causes nodes to become isolated more quickly. This decreases the metastable number of infected nodes, as the spread of the infection is slowed down. The location of the epidemic threshold is left unchanged.
End of Example 2.

Example 3. AID model revisited
In section 3.3, the Adaptive Information Diffusion (AID) model has been introduced. In this model, link-breaking occurs between two susceptible nodes who have no interest in each other. Links are created between susceptible and infected nodes to enhance the spreading of information. Based on the result from Eq. (3.24), the metastable state in the AID model does not exist for $\omega > 2$. The bifurcation diagram for $\omega = 5$ is shown in Figure 3.4.

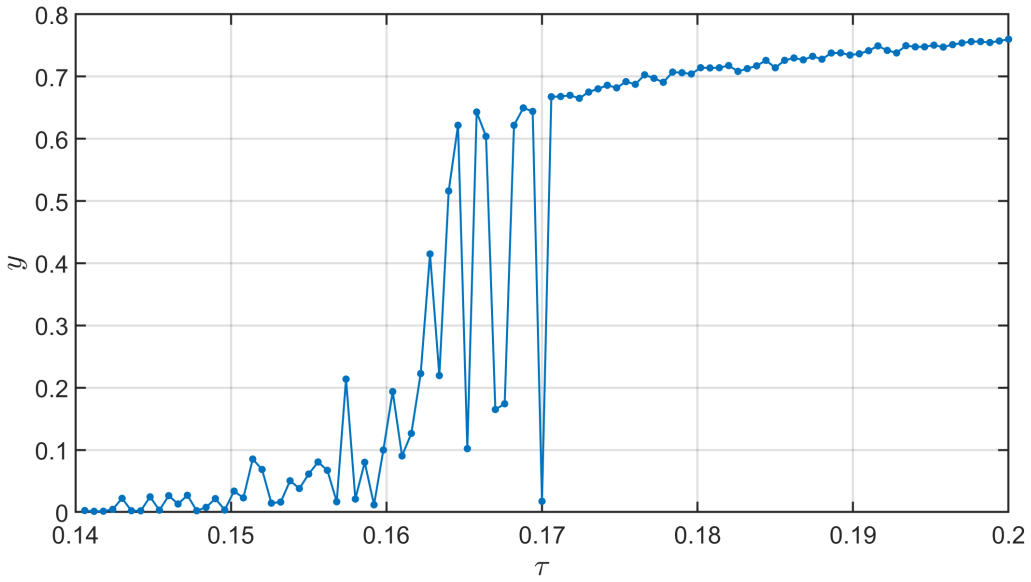

Figure 3.4: (AID) The relation between the effective infection rate τ and metastable prevalence y. We have taken $N = 40$, $\Delta t = 0.05$, $\delta = 1$, $\zeta = 0.5$, $\xi = 0.1$, $\varepsilon = 0.001$ and a complete initial network.

The behaviour for the AID model in Figure 3.4 is different compared to the ASIS model in Figure 3.2. In Figure 3.4, a small region of τ-values is shown corresponding to $\omega = \zeta/\xi = 5$. In this region, the prevalence y rapidly changes from $y = 0$ to $y \approx 0.7$. This change is not smooth as in the ASIS model but shows large fluctuations. It appears the metastable state does not exist for a small range of τ-values, and therein the trivial steady state is unstable as well. This results in unstable, oscillatory behaviour for $0.155 < \tau < 0.17$. In this region, the behaviour of the process can never be predicted accurately due to the instability of the process.
End of Example 3.

Example 4. AID* model with different link-breaking rule.
We consider the AID model with a modified link-breaking rule. In the AID model, the link between two infected nodes is never created. In the AID* model, the link between two infected can be created. This rule is based on the following observation. Two people having the information want to stay in touch, therefore strengthening their relationship. This leaves the link-breaking rule unchanged: $f_1 = (1 - X_i)(1 - X_j)$ and changes the link-creation rule to $f_2 = 1 - (1 - X_i)(1 - X_j)$. Similarly to the AID model, the results from Eq. (3.24) predicts that the metastable state is non-existent for $\omega > 1$. The result for $\omega = 5$ is shown in Figure 3.5.

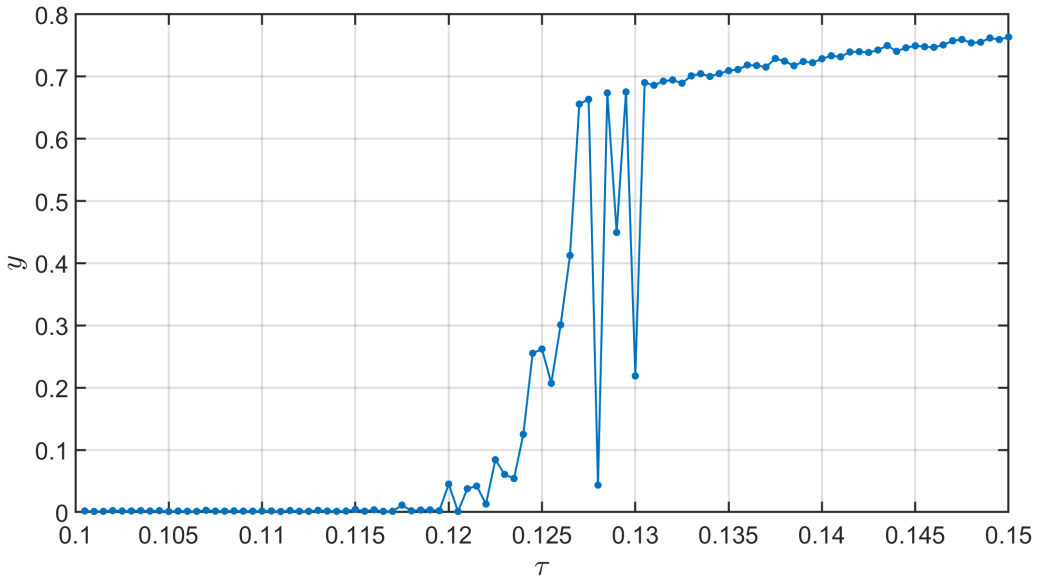

Figure 3.5: (AID*) The relation between the effective infection rate τ and metastable prevalence y. We have taken $N = 40$, $\Delta t = 0.05$, $\delta = 1$, $\zeta = 0.5$, $\xi = 0.1$, $\varepsilon = 0.001$ and a complete initial network.

The bifurcation diagram for the AID* model from Figure 3.5 is comparable to the AID model from Figure 3.4. In both diagrams, the solution increases quickly, but shows large fluctuations. The epidemic threshold τ_c in the AID* model has decreased compared to the AID model. The new link-creation rule enhances the number of links in the network. Therefore spreading can take place at a higher pace, and more people are infected. Moreover, lower infection rates are required for an endemic to develop.
End of Example 4.

Example 5. Adaptive Fake News Diffusion (AFND)
Another relevant spreading phenomenon is the spreading of fake news [40]. We consider a variant of adaptive information diffusion using different link-breaking and link-creation rules. Links between a susceptible and an infected node are broken at rate ζ to model the reluctance of communication between two unlike-minded people. Links can be created between susceptible and infected nodes to demonstrate the effect of being curious to new opinions. Finally, to strengthen the healthy part of the network, links are created between susceptible nodes. To summarise, the link-breaking and link-breaking rule are

$$f_1 = 1 - X_i X_j,$$
$$f_2 = (X_i - X_j)^2.$$

From Eq. (3.24) it is predicted that the metastable state always exists.

One of the most striking differences between the AFND model and the previous ones, is that the link between susceptible and infected nodes can both be broken and created. This introduces competition between both rules. The bifurcation diagram in Figure 3.6 shows more fluctuations than for the ASIS and ASIS* model. Another difference is the epidemic threshold, which is located twice as high as in ASIS at $\tau \approx 0.085$. The conflicting behaviour between susceptible and infected nodes apparently reduces the spreading of fake news compared to similar models like the ASIS and ASIS* model.

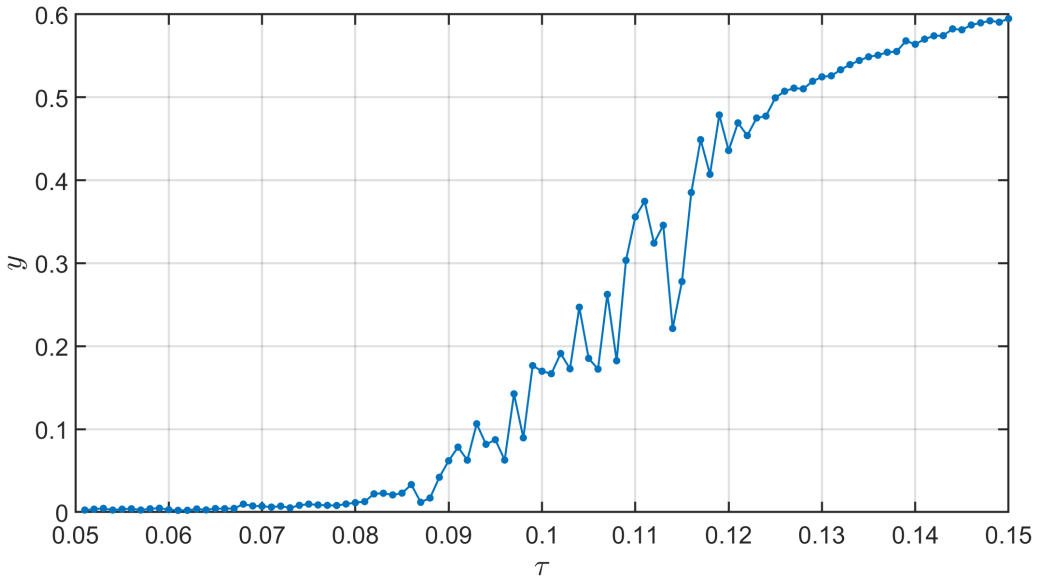

Figure 3.6: (AFND) The relation between the effective infection rate τ and metastable prevalence y. We have taken $N = 40$, $\Delta t = 0.05$, $\delta = \zeta = \xi = 1$, $\varepsilon = 0.001$ and a complete initial network.

End of Example 5.

Example 6. Adaptive Brain Network (ABN)
This model is currently investigated by Stam *et al.* (2019) to model the spreading of information in the human brain [19]. The adaptive network is based on the link-breaking rule $f_1 = X_i X_j$ and on the link-creation rule $f_2 = (1 - X_i)(1 - X_j)$. Eq. (3.24) predicts that the metastable state always exists. The bifurcation diagram is shown below.

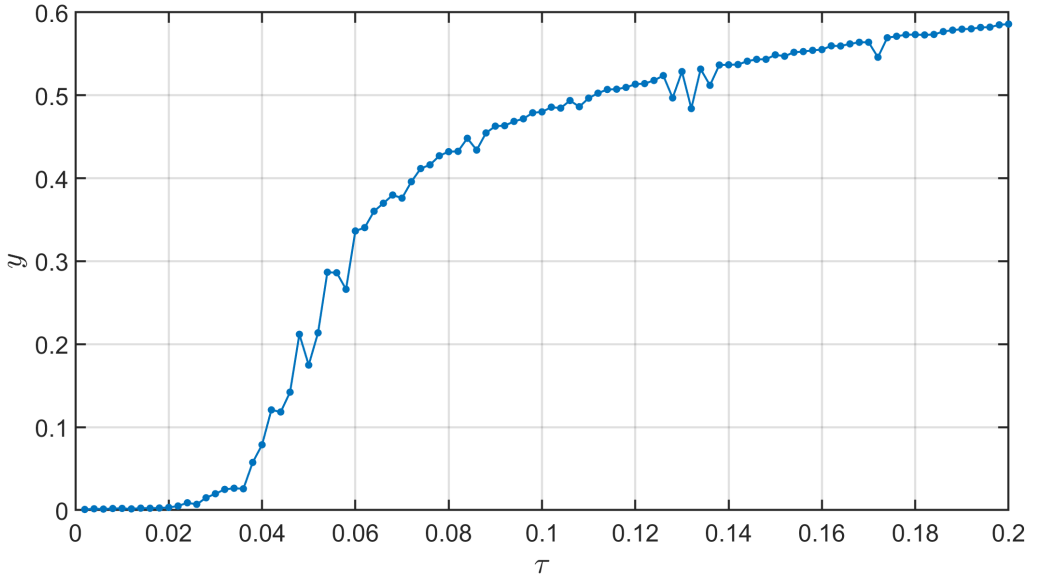

Figure 3.7: (ABN) The relation between the effective infection rate τ and metastable prevalence y. We have taken $N = 40$, $\Delta t = 0.05$, $\delta = \zeta = \xi = 1$, $\varepsilon = 0.001$ and a complete initial network.

The ABN model shows few fluctuations in the bifurcation diagram of Figure 3.7. Moreover, the increase in the prevalence y around the epidemic is very steep. This indicates that the transition from an all-healthy state to an endemic state happens quite sudden. This is probably due to the following. The link between susceptible and infected nodes is preserved in this model, which is in contrast to all previously introduced models. For $\omega < 1$, the link-breaking process has barely any influence, because two infected nodes have no desire to infect one another, and the link-breaking process does not slow down the spreading. For large ω-values, the impact becomes clear; infected nodes can infect their neighbours. When both are infected, the link is broken. After some time one is cured, however, their link remains removed and infection cannot take place. Only when both are susceptible, the link is restored and infection can happen again. To conclude, for small ω-values, this model is comparable to the static SIS as the link-breaking process has barely any effect.
End of Example 6.

Several examples have been introduced in the section. All results comply with the proven statements from the previous sections. From in total 36 models which are available in G-ASIS, 9 are unstable when the effective link-breaking ω is sufficiently high. In practice, this instability implies that the prevalence y above the epidemic threshold τ_c is highly uncertain and exhibits large fluctuations. Simultaneously, two states are available: the trivial steady state where all individuals do not possess the property (are healthy/have no information) and the metastable state which has a non-zero average of the prevalence y. Switching between those states happens constantly for τ-values just above the epidemic threshold τ_c, which implies both states are unstable. This is e.g. observed for the AID model in Figure 3.4.

The epidemic threshold was bounded from below in section 3.2. The next section focusses on the derivation of an upper bound for the epidemic threshold.

3.6 Implicit formula for the epidemic threshold

Aside from the derivation of a lower bound for the epidemic threshold in section 3.4, one can also derive an implicit relationship for the epidemic threshold. Using this relationship, the dependence of the epidemic threshold τ_c on the effective spreading rate ω is investigated in this section.

The quadratic equation for the metastable prevalence y (Eq. 3.16) can be rewritten as

$$V = \frac{1}{2}\left(\frac{H}{y} + y\right), \tag{3.25}$$

where

$$H = \frac{(N-1)a_2}{c_2 N} - \frac{a_1\omega + a_2}{c_2 N^2}\mathbb{E}\left(\sum_{i=1}^{N} d_i^*\right) + \mathrm{Var}(Z^*) - \frac{(2b_1 + c_1)\omega + 2b_2 + c_2}{c_2 N^2}\mathbb{E}\left(\sum_{i=1}^{N} d_i^* X_i^*\right).$$

Using the definition of V from Eq. (3.14), Eq. (3.25) can be rewritten as

$$-\frac{b_2}{c_2} + \frac{(2b_2 + c_2)}{2c_2 N} - \frac{c_1\omega + c_2}{2c_2 N\tau} = \frac{1}{2}\left(\frac{H}{y} + y\right),$$

which can be rearranged to

$$\tau = \frac{c_1\omega + c_2}{2c_2 N\left(-\frac{b_2}{c_2} + \frac{(2b_2+c_2)}{2c_2 N} - \frac{1}{2}\left(\frac{H}{y} + y\right)\right)}.$$

Taking the limit $y \to 0$, we find an implicit formula for the epidemic threshold;

$$\tau_c = \frac{\frac{c_1}{c_2}\omega + 1}{2\frac{b_2}{c_2}(1-N) + 1 - N\lim_{y\downarrow 0}\frac{H}{y}}. \tag{3.26}$$

Since $c_1, c_2 \neq 0$, there always is an explicit dependence of the epidemic threshold τ_c on the effective link-breaking rate ω. As usual, $\delta = 1$ so H is a function on τ, ω and ξ. Since we have taken $\lim_{y\downarrow 0}$,

we have $H(\omega, \tau_c, \xi)$. This makes the relationship from Eq. (3.26) an implicit relation in τ_c. Our main effort will be to show the dependence of τ_c on ω. This will be done by demonstrating the boundedness of $H(\omega, \tau_c, \xi)$. It is therefore irrelevant whether H depends on τ_c, as it will be shown to be bounded for fixed τ_c. In other words, τ_c is treated as a constant in $H(\omega, \tau_c, \xi)$. Due to the continuity of H, we may define

$$\lim_{y \downarrow 0} \frac{H}{y} = h(\omega, \xi),$$

such that the epidemic threshold τ_c becomes

$$\tau_c = \frac{\frac{c_1}{c_2}\omega + 1}{2\frac{b_2}{c_2}(1-N) + 1 - Nh(\omega, \xi)}. \tag{3.27}$$

To derive the dependence of τ_c on ω, the function $h(\omega, \xi)$ must be bounded. In section 3.4, it has been shown that all but the first term of H are positive. The first term is non-negative whenever $\frac{a_2}{c_2} \geq 0$. Therefore two separate cases are required. The first part of the rules is covered by Theorem 3.5.

Theorem 3.5. *Let τ_c be the epidemic threshold from Eq. (3.27) and assume $H \geq 0$. Then τ_c is bounded under a linear function in ω or under a constant.*

Proof. The only models which do not satisfy $H \geq 0$ are models having the link-creation rule $f_2 = 1 - X_i X_j$. These are not included in this theorem, but will be taken care of by the next theorem. This means 30 out of 36 rules are gathered in this theorem. We follow the approach of [17].

Step 1. Exploit that the prevalence y is real.
The solutions of the quadratic equation for the prevalence y need to have a positive discriminant in order to be real solutions. Hence it is required that $H \leq V^2$. Since $H \geq 0$, it is sufficient to show that $\sqrt{H} \leq V$. Inserting the definition of V brings

$$-\sqrt{H} \geq \frac{2b_2 N\tau - (2b_2 + c_2)\tau + c_1\omega + c_2}{2c_2 N\tau},$$

which can be rearranged as

$$\frac{c_1\omega + c_2}{2c_2\tau N} \leq \frac{2\frac{b_2}{c_2} + 1}{2N} - \frac{b_2}{c_2} - \sqrt{H}. \tag{3.28}$$

In the metastable state, the RHS of Eq. (3.28) is positive[3], such that

$$\tau \geq \frac{\frac{c_1}{c_2}\omega + 1}{2\frac{b_2}{c_2}(1-N) + 1 - 2N\sqrt{H}}.$$

This holds for the metastable state, i.e. for all $\tau \geq \tau_c$. Hence

$$\frac{\frac{c_1}{c_2}\omega + 1}{2\frac{b_2}{c_2}(1-N) + 1 - Nh(\omega, \xi)} = \tau_c \geq \tau^* = \frac{\frac{c_1}{c_2}\omega + 1}{2\frac{b_2}{c_2}(1-N) + 1 - 2N\sqrt{H}}. \tag{3.29}$$

We conclude that

$$0 \leq 2\sqrt{H} \leq h(\omega, \xi).$$

Furthermore, since τ_c is bounded for $\frac{c_1}{c_2}\omega + 1 > 0$, the denominator of Eq. (3.27) should be non-zero. In other words,

$$0 \leq 2\sqrt{H} \leq h(\omega, \xi) < \frac{b_2}{c_2}\frac{1-N}{N} + \frac{1}{2N} \qquad \text{for } \frac{c_1}{c_2}\omega + 1 > 0. \tag{3.30}$$

[3]This is not trivial. The argument is based on the non-existence of the metastable state derived in the previous section. For always stable metastable states, this expression is indeed always positive. For models in the G-ASIS framework which have a conditionally non-existent metastable state, this is not true. However, since we take $\lim_{y \downarrow 0}$, the process is assumed to be in the metastable state. This gives an extra constraint on H. Exactly this constraint makes the expression positive.

When the condition of Eq. (3.30) is not satisfied, the function $h(\omega, \xi)$ cannot be bounded using this approach.

Step 2. Bounding $h(\omega, \xi)$ for the other ω values.

Step 2A. Case $\frac{c_1}{c_2} < 0$. (ASIS,AID)
Out of the 30 models considered in this theorem, 15 of them are part of this case.
For the limit of ω approaching $-\frac{c_2}{c_1}$ from below, the value for τ_c should still be non-negative, or at least not suddenly become zero. This can only be assured if the denominator becomes zero as well. This continuity argument shows that equality holds for Eq. (3.30)

$$\lim_{\omega \uparrow -\frac{c_2}{c_1}} h(\omega, \xi) = \frac{b_2}{c_2} \frac{1-N}{N} + \frac{1}{2N}.$$

For τ_c it follows that

$$\lim_{\omega \uparrow -\frac{c_2}{c_1}} \tau_c(\omega, \xi) = -\frac{c_1}{c_2 N \left. \frac{\partial h(\omega, \xi)}{\partial \omega} \right|_{\omega = -\frac{c_2}{c_1}}}.$$

For $\omega > -\frac{c_2}{c_1}$, the epidemic threshold τ_c should be positive as well, so using Eq. (3.29) one finds

$$h(\omega, \xi) > \frac{b_2}{c_2} \frac{1-N}{N} + \frac{1}{2N} \qquad \text{for } \omega > -\frac{c_2}{c_1}.$$

For increasing ω (up to infinity) link-breaking occurs almost immediately. Suppose a node i is infected. The link between node i and its neighbours j will be removed (as ω is high) when the link-breaking rule allows for that. The link can be recreated only when the link-creation rule f_2 has (I) $f_2 = 1$ for either $X_i = 1$ or $X_j = 1$ (these rules are $1 - X_i X_j, 1 - (1 - X_i)(1 - X_j)$ or $(X_i - X_j)^2$) and (II) the link-breaking rule f_1 does not break the link between susceptible and infected nodes (these rules are $(1 - X_i)(1 - X_j)$ or $1 - (X_i - X_j)^2$). Only when (I) and (II) are satisfied, spreading in the network continues despite the link-breaking rate ω increasing to infinity. This allows for a split-up into two classes: Class A and B.

(Class A) (AID) The epidemic threshold remains constant.
The only rules eligible for this class have been listed above. Some of these are still invalid, as they do not obey $H \geq 0$ (the link-breaking rule $f_1 = 1 - X_i X_j$) or do not obey $\frac{c_1}{c_2} \geq 0$ (which is handled in Step 2B). These constraints yield just two rules: $(f_1 = (1 - X_i)(1 - X_j), f_2 = 1 - (1 - X_i)(1 - X_j))$ and $(f_1 = (1 - X_i)(1 - X_j), f_2 = (X_i - X_j)^2)$. These rules have in common that, whilst increasing ω, the epidemic threshold τ_c barely increases. In other words, the limit of $\omega \to \infty$ of τ_c will be finite. So define

$$\lim_{\omega \to \infty} \tau_c(\omega, \xi) = C_1 > 0.$$

We continue to prove that $h(\omega, \xi)$ is linear in ω for large ω. The epidemic threshold can be rewritten in terms of h;

$$h(\omega, \xi) = 2 \frac{b_2}{c_2} \frac{1-N}{N} + \frac{1}{N} - \frac{\frac{c_1}{c_2}\omega + 1}{N \tau_c(\omega, \xi)}. \tag{3.31}$$

Then we may compute the following

$$\frac{1}{NC_1} = \frac{1}{N \lim_{\omega \to \infty} \tau_c(\omega, \xi)} = \lim_{\omega \to \infty} \frac{1}{N \tau_c(\omega, \xi)} \overset{def.}{=} \lim_{\omega \to \infty} \frac{-h(\omega, \xi) + \frac{1}{N} + 2\frac{b_2}{c_2}\frac{1-N}{N}}{\frac{c_1}{c_2}\omega + 1}$$
$$\overset{\text{l'hôpital}}{=} -\frac{c_2}{c_1} \left. \frac{\partial h}{\partial \omega} \right|_{\omega \to \infty} = C_2.$$

Since $C_1 > 0$, we conclude $C_2 > 0$. So $h(\omega, \xi)$ increases linearly in ω for large ω for Class A.

(Class B) (ASIS) The epidemic threshold scales linearly in ω.
The 13 rules not belonging to Class A are part of this class. For each model in this class, the link-breaking rule is dominant in the sense that spreading between susceptible and infected nodes cannot take place (for

$\omega \to \infty$ and fixed τ, ξ) because the link between susceptible and infected nodes is removed immediately. This means that the epidemic threshold must increase along ω to keep spreading the disease (in the limit of $\omega \to \infty$). This proves the epidemic threshold scales linearly in ω.

Step 2B. Case $\dfrac{c_1}{c_2} \geq 0$.
(Class C) (ABN) The remaining 15 rules follow this constraint. For all of these, $\frac{c_1}{c_2} > 0$ according to Table 3.1. This implies the relation in Eq. (3.30) holds for all $\omega \geq 0$. So $h(\omega, \xi)$ is strictly bounded under a constant, also in the limit of $\omega \to \infty$. This implies $h(\omega, \xi)$ is constant in ω. Then the epidemic threshold scales linearly in ω. This proves the theorem. □

All rules have been classified except for the link-creation rule $f_2 = 1 - X_i X_j$. These models are covered by the next theorem.

Theorem 3.6. *Let τ_c be the epidemic threshold from Eq. (3.27) and assume $H < 0$. Then $h(\omega, \xi)$ is bounded under a linear function in ω or under a constant.*

Proof. The only models in the G-ASIS framework satisfying $H < 0$ are models which have link-creation rule $f_2 = 1 - X_i X_j$. Therefore substitute $a_2 = 1, b_2 = 0, c_2 = -1$ to find

$$H = \frac{1}{N} - 1 + \frac{a_1\omega + 1}{N^2}\mathbb{E}\left(\sum_{i=1}^{N} d_i^*\right) + \mathrm{Var}(Z^*) + \frac{(2b_1 + c_1)\omega - 1}{N^2}\mathbb{E}\left(\sum_{i=1}^{N} d_i^* X_i^*\right).$$

Clearly H is negative. We have derived that $y = V \pm \sqrt{V^2 - H}$. Then the prevalence y has two solutions: $y_1 > 0$ and $y_2 < 0$. Our focus lies on the physical solution y_1.

Step 1. Exploit that y_1 is bounded above by 1.
This provides the constraint

$$V + \sqrt{V^2 - H} \leq 1.$$

The sign of V is not determined. The equation above can be rewritten, so

$$V^2 - H \leq 1 - 2V + V^2.$$

Removing V^2 and inserting the definition for V from Eq. (3.14), we find

$$-H \leq 1 - 2\left(\frac{1}{2N} + \frac{c_1\omega - 1}{2N\tau}\right),$$

where the values of a_2, b_2 and c_2 have been substituted already. This can be rewritten as

$$\frac{1 - c_1\omega}{1 - Nh(\omega, \xi)} = \tau_c \geq \tau^* = \frac{1 - c_1\omega}{1 - N - NH}. \tag{3.32}$$

The denominator is positive, so this constraint is confining for $c_1 < 0$ or for $c_1 > 0$ and $\omega < \frac{1}{c_1}$. In the latter case, we may conclude that

$$0 \leq 1 + H \leq h(\omega, \xi) < \frac{1}{N}. \tag{3.33}$$

This means $h(\omega, \xi)$ is always positive.

Step 2. Use a continuity argument. This step is analogous to step 2 from Theorem 3.5.

Step 2A. Case $c_1 > 0$. Since τ_c is positive for $\omega < \frac{1}{c_1}$, by taking $\lim_{\omega \to \frac{1}{c_1}}$, the limit must be finite and non-zero. This implies

$$\lim_{\omega \uparrow \frac{1}{c_1}} h(\omega, \xi) = \frac{1}{N}.$$

Then

$$\lim_{\omega \uparrow \frac{1}{c_1}} \tau_c(\omega, \xi) = \frac{c_1}{N \left. \frac{\partial h}{\partial \omega} \right|_{\omega = \frac{1}{c_1}}}.$$

For the relation in Eq. (3.32) to be meaningful (τ_c should be non-negative) for $\omega > \frac{1}{c_1}$, it is required that

$$h(\omega, \xi) > \frac{1}{N}, \qquad \text{for } \omega > \frac{1}{c_1}.$$

We will now analyse $h(\omega, \xi)$ as ω grows to infinity. For ω increasing and fixed τ, the link-breaking process occurs almost immediately. Nodes will become isolated and cure on their own. There is however a way for this not to happen. The link-creation process is here taken to be $f_2 = 1 - X_i X_j$, which implies a link is created between a susceptible and an infected node. In case the link-breaking process does not include the rule where the link is broken between a susceptible and an infected node, the spreading continues despite $\omega \to \infty$. There are two possibilities.

(Class A) The epidemic threshold remains constant.
The link-creation process is $f_2 = 1 - X_i X_j$ and as link-breaking rule, we need either $f_1 = X_i X_j, f_1 = (1 - X_i)(1 - X_j)$ or $f_1 = 1 - (X_i - X_j)^2$. These rules have in common that, whilst increasing ω, the epidemic threshold barely increases. In other words, the following limit holds;

$$\lim_{\omega \to \infty} \tau_c(\omega, \xi) = C_1 > 0.$$

Then $h(\omega, \xi)$ scales linearly with ω analogous to Theorem 3.6, Step 2A, Class A.

(Class B) The epidemic threshold scales linearly in ω.
No rules belong to this class, as the only eligible do not satisfy $c_1 > 0$.

Step 2B. Case $c_1 < 0$.
(Class C) In this case the relationship from Eq. (3.33) holds for all ω. So $h(\omega, \xi)$ is bounded under a constant for all ω. This implies τ_c scales linearly in ω. This proves the theorem. □

The upper bound for the epidemic threshold has been analysed for 36 models in the G-ASIS framework. Theorems 3.5 and 3.6 have shown that 5 models have an epidemic threshold which is bounded under a constant as $\omega \to \infty$. The remaining 31 rules have an epidemic threshold which is bounded under a linear function in ω.

The obtained result is verified using numerical simulations for the ASIS model and the ABN model. Each simulation was performed using an average over 1,000,000 time units, an accuracy of $\Delta\tau = 0.005$ and $\Delta t = 0.05$. The epidemic threshold was estimated using Definition 2.3 in which the epidemic threshold τ_c is determined where y drops below $\frac{1}{N}$. We have taken $\delta = \xi = 1$ and $\varepsilon = 10^{-3}$ and 40 nodes as before. The relation for the ASIS model is shown in Figure 3.8.

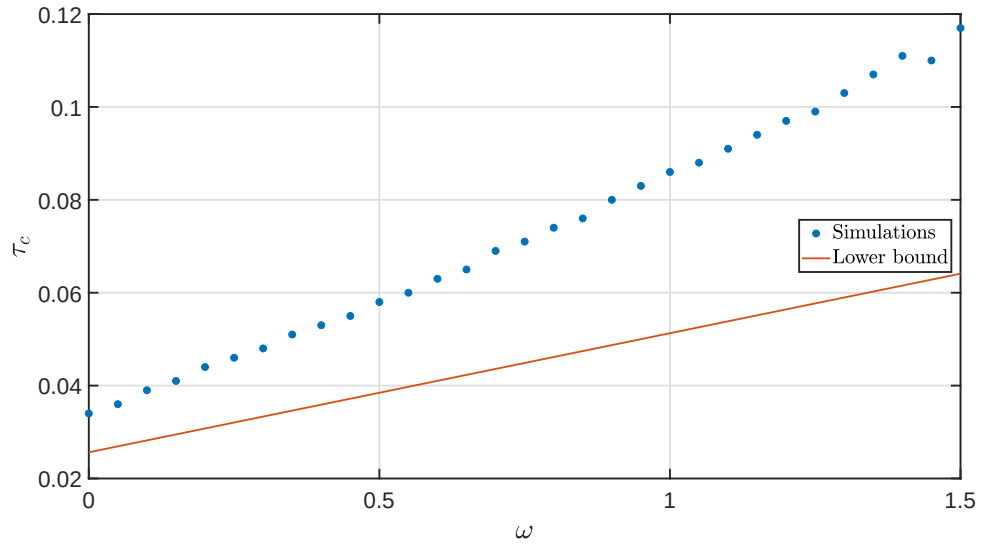

Figure 3.8: (ASIS) The relation between the epidemic threshold τ_c and the effective link-breaking rate ω. The blue dots show the simulation results and the red solid line is the lower bound computed in section 3.2.

In Figure 3.8, the linear relation between the epidemic threshold τ_c and the effective link-breaking rate ω is illustrated. This has been proven in Theorem 3.5 as well. Moreover, the lower bound for the epidemic threshold is depicted in Figure 3.8 and this bound seems to be a loose lower bound. This was expected, as the same was observed in the bifurcation diagram of the ASIS model in Figure 2.11. Also, the lower bound is more strict for $\omega = 0$ which corresponds to a static network.

The relation for the ABN model is shown in Figure 3.9.

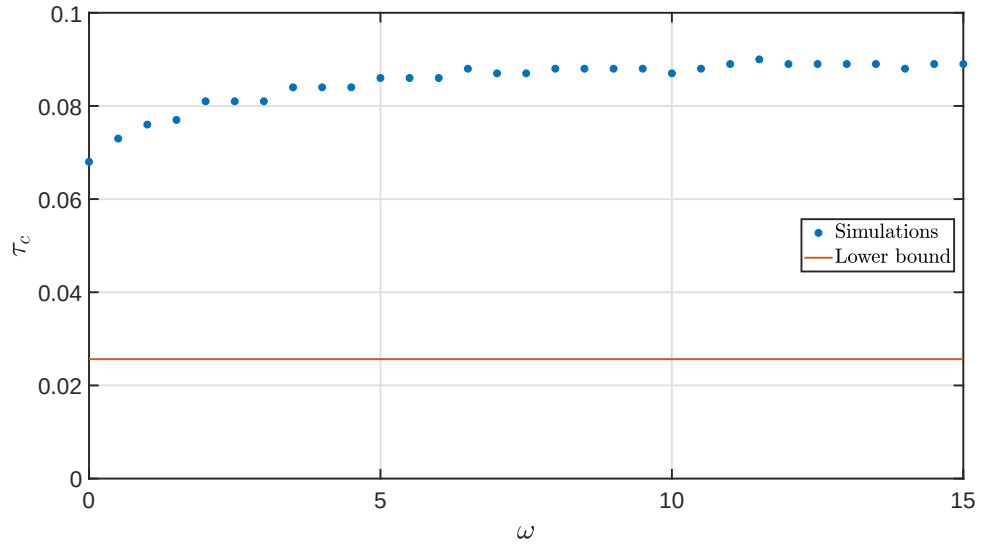

Figure 3.9: (ABN) The relation between the epidemic threshold τ_c and the effective link-breaking rate ω. The blue dots show the simulation results and the red solid line is the lower bound computed in section 3.2.

The lower bound for the ABN model was shown to be constant as a function of the effective link-breaking rate ω. This is represented by the red solid line in Figure 3.9. The upper bound for the epidemic threshold is a function which is linear in ω. Based on Figure 3.9, the lower bound appears to be more strict. Hence the argumentation in Theorem 3.5 is not completely correct. A possible reason for this might be the following. Since the link is preserved between susceptible and infected nodes, the spreading of the disease seems to continue despite $\omega \to \infty$. This is however incorrect, as the link-breaking

process (which happens between two infected nodes) cannot be overcome by the link-creation process (between two healthy nodes). The system is likely to exhibit oscillatory behaviour, where a pair of nodes changes as follows. First the pair is healthy and connected. When one is infected, it infects the other. Then their link is immediately broken (as ω is high). Then both nodes are cured, whereafter their link is recreated. This process repeats itself for every node-node pair in the network. In this way, the epidemic threshold is independent of the effective link-breaking rate ω.

3.7 Overview

In this chapter, the Generalised Adaptive SIS framework has been introduced. The G-ASIS framework contains 36 adaptive models, ranging from epidemics, information diffusion to brain transfers and the spread of fake news. Each model has a different link-breaking rule f_1 and link-creation rule f_2. A lower bound for the epidemic threshold was obtained in section 3.2, which is

$$\tau_c \geq \frac{1 + \dfrac{\omega(a_1 + b_1)}{a_2 + b_2 + \delta/\xi}}{\rho}. \tag{3.34}$$

For a complete initial network, the spectral radius ρ is equal to $N - 1$. Based on Eq. (3.34), for half of the models (18 out of 36) the epidemic threshold scales at least linearly in ω. Additionally, the epidemic threshold has been bounded from above in section 3.6. In 31 rules, the epidemic threshold scales linearly in effective link-breaking rate ω and 5 rules are constant in ω. Therefore we conclude the following:

18 rules:	linear in ω,
5 rules:	constant in ω,
13 rules:	undetermined.

For a complete initial network, the existence of the metastable state was examined. When the following conditions are met, the metastable state does not exist for some τ-values above the epidemic threshold

$$c_2 < 0, \quad c_1 > 0, \quad \omega > -\frac{c_2}{c_1}. \tag{3.35}$$

Hence, in 9 models the metastable state does not always exist. All other 27 models have a metastable state. This view was supported by extensive simulations for various models in section 3.5.

The obtained results for all named rules introduced in this chapter are shown in Table 3.2 and all other rules in the G-ASIS framework are listed in Appendix 4. The main result is based on the relation between the epidemic threshold τ_c and the effective link-breaking rate ω. For the ASIS, ASIS*, AID, AID* and AFND models, we have shown that the lower and upper bound for this relation are equivalent. On the other hand, for the ABN model the relationship between τ_c and ω could not be determined. The relation has only been bounded between a constant and a linear relation. Other methods need to be applied to find the actual relationship between τ_c and ω for the ABN model. Based on the simulations in section 3.6, it is conjectured that the relation is constant. This indicates that the lower bound is more strict for this model. Other models have not been simulated in this thesis.

Table 3.2: All named rules from the G-ASIS framework and their interpretation. YES* does not mean the metastable state is always stable, only that it is not proven it is unstable. This table assumes $\delta = 1$.

Rules (link-breaking) (link-creation)	Model name and appearance in literature	Always metastable	Lower bound on epidemic threshold	Upper bound on epidemic threshold
$(X_i - X_j)^2$ $(1 - X_i)(1 - X_j)$	ASIS model [9, 11, 17, 20]	YES*	$\frac{1+\omega\xi}{\rho}$	Linear
$1-(1-X_i)(1-X_j)$ $(1 - X_i)(1 - X_j)$	ASIS* model [Example 2, p. 46]	YES*	$\frac{1+\omega\xi}{\rho}$	Linear
$(1 - X_i)(1 - X_j)$ $(X_i - X_j)^2$	AID model [17]	NO	$\frac{1}{\rho}$	Constant
$(1 - X_i)(1 - X_j)$ $1-(1-X_i)(1-X_j)$	AID* model [Example 4, p. 48]	NO	$\frac{1}{\rho}$	Constant
X_iX_j $(1 - X_i)(1 - X_j)$	ABN model [19]	YES*	$\frac{1}{\rho}$	Linear
$1 - X_iX_j$ $(X_i - X_j)^2$	AFND model [Example 5, p. 49]	YES*	$\frac{1+\frac{\xi\omega}{\xi+1}}{\rho}$	Linear

In the AID and AID* model, the metastable state does not exist for large link-breaking rate ω. Instead of a smooth phase transition from the all-healthy state to the endemic state, large fluctuations are observed for $\tau > \tau_c$. This behaviour could not be explained.

In Appendix 4, an extensive list of all rules in the G-ASIS framework can be found. These can be classified into the following four categories;

- unstable metastable state, unclear threshold (4x)
- unstable metastable state, constant threshold (5x, including AID, AID*)
- stable metastable state, unclear threshold (9x, including ABN)
- stable metastable state, linear threshold (18x, including ASIS, ASIS*, AFND)

The ASIS, ASIS* and AFND model are models where the adaptive part opposes the spreading over the network. The AID and AID* model can be considered constructive spreading models and finally, the remaining rules, including the ABN model, can exhibit any kind of behaviour. Many other classifications may exist, however, assembling models with similar properties is difficult. Even the suggested categories above are based on just two properties of the processes, and models may exhibit different behaviour whilst being in the same category.

3.8 Potential lower bound: Mean-field EDEs

The mean-field EDEs can be used to approximate or find other bounds for the epidemic threshold. In Appendix 3, the mean-field EDEs have been used successfully to derive a lower bound for the epidemic threshold τ_c in the static SIS model. For the adaptive SIS model, this was successfully done in section 1.5.4. In both cases, the mean-field approximation was a useful estimator for the epidemic threshold. Expansion in the G-ASIS framework seems straightforward, however, some problems arise.

In the static SIS model, it was proven that nodes are positively correlated [32]. Positive nodal correlation is necessary to conclude whether the obtained bound from the mean-field analysis is indeed an overestimation of the real process. As of yet, this has not been proven for any model in the G-ASIS framework.

Although the G-ASIS framework is large, the analysis can be performed analogously to the ASIS model. To memorise, the mean-field EDEs are

$$\frac{d\mathbb{E}(X_i)}{dt} = -\delta\mathbb{E}(X_i) + \beta(1-\mathbb{E}(X_i)) \sum_{j=1,j\neq i}^{N} \mathbb{E}(X_j)\mathbb{E}(a_{ij}), \tag{3.36}$$

$$\begin{aligned}\frac{d\mathbb{E}(a_{ij})}{dt} = a_{ij}(0)\Big[&-\zeta\mathbb{E}(a_{ij})(a_1 + b_1(\mathbb{E}(X_i)+\mathbb{E}(X_j)) + c_1\mathbb{E}(X_i)\mathbb{E}(X_j)) + \\ &\xi(1-\mathbb{E}(a_{ij}))(a_2 + b_2(\mathbb{E}(X_i)+\mathbb{E}(X_j)) + c_2\mathbb{E}(X_i)\mathbb{E}(X_j))\Big].\end{aligned} \tag{3.37}$$

To compute the steady states of the model, we set the derivatives to zero. The equations then reduce to

$$\begin{aligned}0 &= -\delta\mathbb{E}(X_i) + \beta(1-\mathbb{E}(X_i)) \sum_{j=1,j\neq i}^{N} \mathbb{E}(X_j)\mathbb{E}(a_{ij}), \\ 0 &= -\zeta\mathbb{E}(a_{ij})(a_1 + b_1(\mathbb{E}(X_i)+\mathbb{E}(X_j)) + c_1\mathbb{E}(X_i)\mathbb{E}(X_j)) + \\ &\quad \xi(1-\mathbb{E}(a_{ij}))(a_2 + b_2(\mathbb{E}(X_i)+\mathbb{E}(X_j)) + c_2\mathbb{E}(X_i)\mathbb{E}(X_j)) \qquad \text{if } a_{ij}(0) = 1.\end{aligned}$$

A general solution cannot be derived due to the non-linearity of the problem. Therefore non-trivial symmetric steady states are sought, which are of the form $\mathbb{E}(X_i) = \mathbb{E}(X_j) = x_v > 0$. This yields

$$\begin{aligned}\delta x_v &= \beta(1-x_v)x_v \sum_{j=1,j\neq i}^{N} \mathbb{E}(a_{ij}), \\ \zeta\mathbb{E}(a_{ij})(a_1 + 2b_1x_v + c_1x_v^2) &= \xi(1-\mathbb{E}(a_{ij}))(a_2 + 2b_2x_v + c_2x_v^2) \qquad \text{if } a_{ij}(0) = 1.\end{aligned}$$

Since $x_v \neq 0$, the first equation can be simplified. Moreover, introduce $\tau = \beta/\delta$ and $\omega = \zeta/\xi$ as before;

$$1 = \tau(1-x_v) \sum_{j=1,j\neq i}^{N} \mathbb{E}(a_{ij}), \tag{3.38}$$

$$\omega\mathbb{E}(a_{ij})(a_1 + 2b_1x_v + c_1x_v^2) = (1-\mathbb{E}(a_{ij}))(a_2 + 2b_2x_v + c_2x_v^2) \qquad \text{if } a_{ij}(0) = 1. \tag{3.39}$$

Here we conclude that $\mathbb{E}(a_{ij}) \notin \{0,1\}$ (based on Eq. (3.39) and Lemma 3.7) and $x_v \neq 1$ (based on Eq. (3.38)). Then Eq. (3.39) can be rewritten in terms of $\mathbb{E}(a_{ij})$;

$$\mathbb{E}(a_{ij}) = \frac{a_2 + 2b_2x_v + c_2x_v^2}{a_2 + 2b_2x_v + c_2x_v^2 + \omega(a_1 + 2b_1x_v + c_1x_v^2)} \qquad \text{if } a_{ij}(0) = 1. \tag{3.40}$$

Substitution of Eq. (3.40) in Eq. (3.38) gives

$$1 = (1-x_v)\tau d_i \frac{a_2 + 2b_2x_v + c_2x_v^2}{a_2 + 2b_2x_v + c_2x_v^2 + \omega(a_1 + 2b_1x_v + c_1x_v^2)}.$$

where d_i is the number of degrees of node i. Since each nodal value is equal, it is also necessary each node has the same number of links d. Hence we conclude $d_i = d$ for all i. The fractions can be removed using relevant multiplications on both sides

$$(a_2 + 2b_2x_v + c_2x_v^2) + \omega(a_1 + 2b_1x_v + c_1x_v^2) = \tau d(1-x_v)(a_2 + 2b_2x_v + c_2x_v^2). \tag{3.41}$$

In Eq. (3.41) we should make use of the zeros of the functions on the left and right. This is covered by the following lemma.

Lemma 3.7. *The function*

$$g(x_v) = a + bx_v + cx_v^2 \tag{3.42}$$

where a, b, c follow from Table 3.1, is positive.

Proof. There are six rules for the link-creation process f_2 and six for the link-breaking process f_1, which are listed in Table 3.1. Since we have assumed $\mathbb{E}(X_i) = \mathbb{E}(X_j) = x_v$, the following table is obtained.

rule f	a	b	c	quadratic form	zeros
X_iX_j	0	0	1	x_v^2	$x_v = 0$ (2x)
$1 - X_iX_j$	1	0	-1	$(1-x_v)(1+x_v)$	$x_v = 1, x_v = -1$
$(1-X_i)(1-X_j)$	1	-1	1	$(1-x_v)^2$	$x_v = 1$ (2x)
$1-(1-X_i)(1-X_j)$	0	1	-1	$x_v(2-x_v)$	$x_v = 0, x_v = 2$
$(X_i - X_j)^2$	0	1	-2	$2x_v(1-x_v)$	$x_v = 0, x_v = 1$
$1-(X_i - X_j)^2$	1	-1	2	$x_v^2 + (1-x_v)^2$	$x_v \in \mathbb{C}$

Since $0 < x_v < 1$, all functions are strictly positive. □

Another important result is that the zeros of each rule f are different. For the ASIS model, the link-breaking rule f_1 and link-creation rule f_2 have a common zero for $x_v = 1$. In most models, however, the zeros do not coincide. Therefore we assume that the zeros of f_1 and f_2 are different, and continue the derivation. Eq. (3.41) can be rewritten as a third-order equation in x_v. It can in principle be solved analytically, but is not insightful for most cases. This equation is

$$\begin{aligned} G(x_v) = c_2\tau d x_v^3 + (2b_2\tau d - c_2\tau d + c_2 + c_1\omega)\, x_v^2 + \\ (2b_2 + a_2\tau d - 2b_2\tau d + 2b_1\omega)\, x_v + (a_2 + a_1\omega - a_2\tau d) = 0. \end{aligned} \tag{3.43}$$

Example: ASIS model
Consider the ASIS model. Substitution of the model parameters yields

$$\tau d x_v^3 + (1 - 3\tau d - 2\omega)\, x_v^2 + (-2 + 3\tau d + 2\omega)\, x_v + (1 - \tau d) = 0. \tag{3.44}$$

Observe that for any choice of τd and ω a solution is $x_v = 1$. This reduces Eq. (3.44) to a quadratic equation in x_v which greatly simplifies the computation. This was computed in section 1.5.4 and it was found that the steady state exists for $\tau d > 1$ (independent of ω).

Example: AID model
The AID model yields the following relation for x_v

$$-2\tau d x_v^3 + (4\tau d - 2 + \omega)\, x_v^2 + (2 - 2\tau d - 2\omega)\, x_v + \omega = 0.$$

A solution is $x_v = 1$. Then the equation reduces to a quadratic equation

$$2\tau d x_v^2 + (-2\tau d + 2 - \omega) x_v + \omega = 0.$$

Its solutions are

$$x_v = \frac{2\tau d + \omega - 2 \pm \sqrt{(2\tau d + \omega - 2)^2 - 8\tau d\omega}}{4\tau d}. \tag{3.45}$$

In order to verify the obtained result, the mean-field approximation is compared to the Markov process. The mean-field approximation should be real, and in between zero and one. For this model, the latter is always satisfied when the first is. The first can be determined by looking where Eq. (3.45) changes from a real to an imaginary solution. This is found at

$$\tau_c^{\mathrm{MF,AID}} = \frac{\frac{1}{2}(\omega + 2) + \sqrt{2\omega}}{N - 1}. \tag{3.46}$$

This is an approximation of the true epidemic threshold τ_c. It remains unclear whether $\tau_c^{\mathrm{MF,AID}}$ is a lower bound or upper bound for the epidemic threshold τ_c because positive nodal correlation has not been proven. From the earlier derived results for the AID model (the epidemic threshold is constant in ω), it appears this mean-field result is an upper bound for the true epidemic threshold. This has not been proven, but is based on the observations in Figure 3.10, where the mean-field approximation and simulations are shown side by side for several values of the link-breaking rate ω.

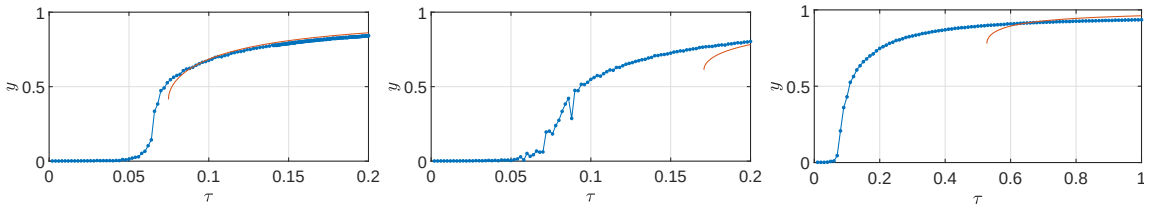

(a) $\omega = 1$ (b) $\omega = 5$ (c) $\omega = 25$

Figure 3.10: (AID) The relation between the effective infection rate τ and prevalence y for different effective link-breaking rates ω. The simulations of the Markov process are shown in blue dotted lines and the mean-field approximations are red solid lines. We have taken $N = 40$, $\Delta t = 0.05$, $\delta = \xi = 1$, $\varepsilon = 0.001$ and a complete initial network.

The mean-field approximation only exists for certain τ-values. The smallest value for which it exists, is the epidemic threshold $\tau_c^{\mathrm{MF,AID}}$. In all cases, the mean-field approximation overestimates the actual epidemic threshold.

Example: ABN model
Substituting of the parameters of the ABN model in Eq. (3.43) yields

$$\tau d x_v^3 + (1 - 3\tau d + \omega)\, x_v^2 + (3\tau d - 2)\, x_v + (1 - \tau d) = 0. \tag{3.47}$$

This equation has three solutions for x_v. These should satisfy three constraints; the solution should be real, larger than zero and smaller than one. It is generally known that a positive discriminant Δ yields three real solutions. A negative discriminant means there is one real solution. The sign of the determinant is therefore important for the solution. In Figure 3.11, in the yellow-green-blue background colours, the values of the discriminant Δ are shown for a (τ, ω)-region.

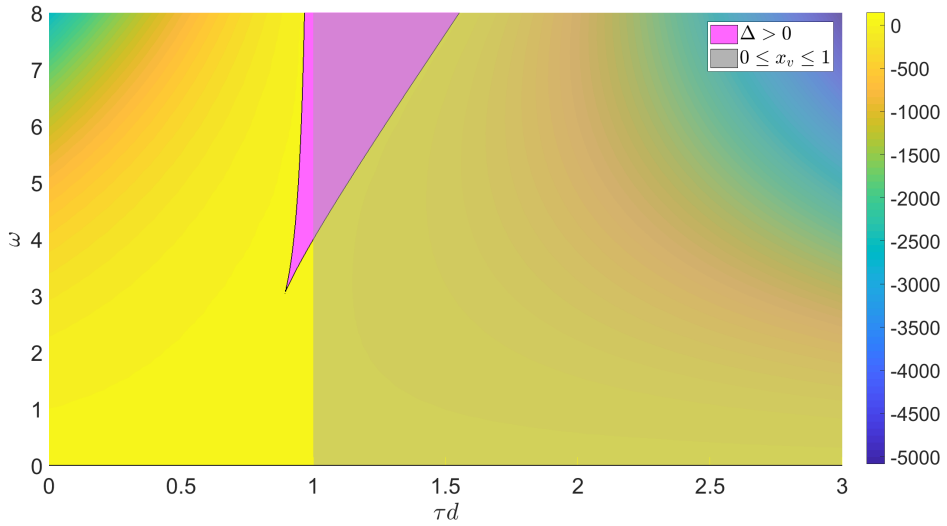

Figure 3.11: The (τ, ω)-plane of the discriminant Δ of Eq. (3.47) for the ABN model. The purple triangle at the top indicates where $\Delta > 0$. The grey-coloured region indicates a physical, real-valued solution for x_v. The horizontal axis for $\tau d > 1$ is grey as well.

Great variations occur for the value of the discriminant Δ. The area where Δ is positive is coloured purple. For larger τ and ω values, Figure 3.11 more or less extends linearly. In the non-purple areas, the only real solution should be bounded between zero and one to be a physical solution. In Figure 3.11, the region where a physical steady state x_v exists is indicated by a light grey overlay. This region corresponds to $\tau d > 1$. In the remaining areas, the (always) real solution is not bounded between zero

and one. In the remaining part of the purple region, the other real solutions are not bounded between zero and one either. These do therefore not contribute to the steady state solution.

The real solution which exists for $\tau d > 1$ is in compliance with the results and simulations from the previous sections. The solution can be computed using Cardano's formula, however, the expression is lengthy and does not give any further insight. Hence, in contrast to the ASIS and AID model, the steady states are not computed in closed form. The result is however in compliance with earlier obtained results.
End of examples

In this section, it has silently been assumed that the steady state exists for each model in the G-ASIS framework. This was however not proven. For some models in the G-ASIS framework, it can be proven that the steady state exists. In Eq. (3.43), we are looking for solutions to $G(x_v) = 0$. At $x_v = 0$, we find $G(0) = a_2(1 - \tau d) + a_1\omega$. At $x_v = 1$, we have $G(1) = (a_2 + 2b_2 + c_2) + \omega(a_1 + 2b_1 + c_1)$. When $G(0) < 0$ and $G(1) > 0$ (and since G is continuous), the Intermediate Value Theorem states that there must be some $x_v \in (0, 1)$ such that $G(x_v) = 0$. This is depicted in Figure 3.12. Unfortunately, for only 12 models this assumption is valid. Other models have coinciding zeros of f_1 and f_2 (see Lemma 3.7) or comply to neither of these criteria. Further research is required to unravel the impact of the mean-field EDEs.

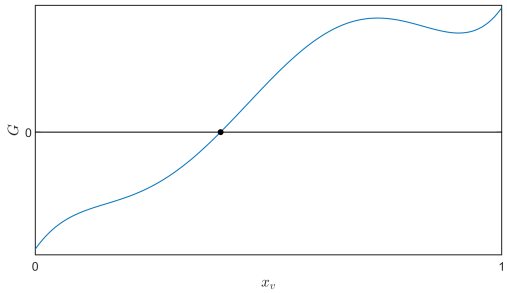

Figure 3.12: An illustration of the Intermediate Value Theorem.

4 Discussion

This chapter considers some topics left undiscussed throughout this thesis and discusses them in more detail. The first section considers the adaptive SIS model. In section 4.2, the General ASIS framework is discussed. Finally some future research directions are outlined.

4.1 ASIS model

The adaptive SIS model was successfully applied in the past for modelling several contagious processes. Most common examples include childhood diseases like measles, whooping cough and mumps and sexually transmittable diseases (STDs) like chlamydia or gonorrhoea [6]. To model these diseases accurately, the development of models like the adaptive SIS model is necessary. Unfortunately, the adaptive network quickly grows in computation time, as the number of links in a complete network grows quadratically with the number of nodes. For any real-world network with thousands of nodes, the adaptive SIS model is infeasible. Therefore mean-field estimates need to be available for the model, and some approaches were outlined in Chapter 1. For the ASIS model, the Markov process and the mean-field approximation showed only a small difference. Only for a growing effective link-breaking rate ω, the results start to deviate significantly. A possible reason might be the changing correlation between two adjacent nodes. For the static network, it was proven that two adjacent nodes have a non-negative correlation [32]. This is not trivial in the adaptive network, where the link-breaking process reduces the correlation between the nodes.

The simulations in Chapter 2 have been performed using a network of 40 nodes. This number of nodes was chosen for two reasons. First, a sufficiently large number of nodes in the network need to remain connected. This is relevant to this model, as the link-breaking process sometimes causes parts of the network to be disconnected. When the components of the disconnected network are too small, finite-size effects take the overhand and each subnetwork will cure exponentially fast. This might be a limiting factor in the accurate measurement of disease spreading. For example, the epidemic threshold might seem lower than it actually is due to the limited number of possible interactions. Second, a larger number of nodes increases computation time. Since many simulations took several hours (especially the simulations for the relation between the epidemic threshold τ_c and the effective link-breaking rate ω in section 3.6), it is undesirable to increase the computation time even further. Both arguments have led to the choice of 40 nodes.

4.2 G-ASIS framework

The Generalised Adaptive SIS framework was introduced in Chapter 3 to model various infection-curing processes. Each research area might require its own (small) modification of some model in the current G-ASIS framework. For example, the Adaptive Brain Network (ABN) introduced in Chapter 3 required exponential weight functions to reduce effects of distant nodes [19]. Table A4.1 includes all rules of the G-ASIS framework. Most of them have not yet been assigned any specific utility. Some possible processes which can be modelled as adaptive processes are available in literature;

- Cell migration in organisms [41]
- Ecological communities, where e.g. invasion or extinction takes place [41]
- Social relationships, conversations, collaborations [41]
- Epidemics of cattle [6]
- Cultural norms [42]
- Viral content on social media [42]
- Automated defence against attacks in power grids [43]

Not all of them have potential in the G-ASIS framework, as the underlying process needs to be a contagion-like process. For example, collaborations cannot be modelled as a contagious process due to their non-competitive nature. Other processes like ecological communities generally have a quick-spreading contagious process and a slow adaptive process. Although an adaptive model is more accurate

in describing the observed phenomena, qualitatively similar results can be obtained using a static or temporal network. Adaptive networks are computationally intensive since the number of equations scales with the number of links. Therefore slowly adaptive processes might not benefit from an adaptive network formulation, and a static or temporal network should be chosen instead.

Many results in Chapter 3 were obtained for the complete initial network. Many real-life networks are known to be scale-free or small-world networks [44]. Although the framework can be extended easily for general initial networks, the results from Chapter 3 are mostly based on all-to-all coupling. Fortunately, in many networks, the local 'environment' of each node is the same. This implies each node is indistinguishable, and the assumption of all-to-all coupling is acceptable. For networks with special structures, the assumption does not hold and the results found in Chapter 3 need to be generalised in order for them to be useful.

The mean-field approximation of the G-ASIS framework, which was discussed in section 3.8, can be computed for all models. The static SIS model and the ASIS model have shown good agreement with their mean-field approximations. However, the analysis of the AID and ABN model in section 3.8 showed that the mean-field approximation may deviate considerably from the Markov process. Although nodes in the static SIS model are positively correlated [25], this is presumably incorrect for all models in the G-ASIS framework. Still, the mean-field approximation may be relevant for a selection of models in the G-ASIS framework. For the remaining processes, other higher order closing relations may be required to accurately approximate the behaviour of the Markov process.

4.3 Future research

Although briefly touched upon in Chapter 3, the Generalised Adaptive SIS framework can be used to model all kinds of phenomena. Examples have been provided in Chapter 3, including the spreading of information, fake news and diseases. The framework might be expanded with other link-breaking and link-creation rules. For example, the rule $f = X_i + X_j$ is currently not included, as this rule contains a double contribution for $X_i = X_j = 1$. The rule considered is a logical one, where both node i and j can separately contribute to the result of f. This rule was introduced by Ogura and Preciado (2016). Most derivations in Chapter 3 cannot be easily extended, because this rule contains no X_iX_j correlation term. By allowing the range of the rule f to include the value 2, many potentially relevant rules can be analysed simultaneously. Some of these can be analysed analogously to the approach in Chapter 3 whereas others need different proofs. In the same fashion, the two trivial rules $f = 0$ and $f = 1$ can be included. The link-breaking rule or the link-creation rule must be a non-trivial rule, otherwise we resort to a static system.

Expanding the adaptive SIS model is also possible in other directions. The AC-SAIS model was introduced by Sahneh *et al.* (2017) where an Alerted group is included in the model [45]. This group is not yet infected, but is cautious to adopt the disease. The G-ASIS framework can be extended to model alerted individuals. On the other hand, one might argue that the link adaptions behave as an alerted group because of the link-breaking between susceptible and infected people. Still, the extension of the G-ASIS framework to include different type of nodal states might be relevant for certain diseases.

The G-ASIS framework can be used to investigate a network's robustness. This is a relevant research area in the human brain. Diseases like Alzheimer and Parkinson's disease are known to affect the ability of the brain to make and repair links. A relevant research question could be: "How does the metastable state change when the link-creation rate of the model decreases due to the disease?" This question was discussed in Chapter 3 in detail by the investigation of the epidemic threshold. Another relevant question might be: "By the removal of most links in the network at some time t_0, is the network able to restore itself?" and "By which probability does this happen and over which time span?" Testing a network's robustness is a common approach in the field of power grids, internet protocols, and more. These research areas could provide relevant tools to analyse the G-ASIS framework's robustness in a meaningful way.

The G-ASIS framework contains 36 different adaptive models. Although this is a large number of models, the processes and parameters have been chosen as simple as possible. Future research for the G-ASIS framework includes but is not limited to: rules based on triangles or subnetworks, directed networks, non-complete initial networks and inhomogeneous infection, curing, link-breaking and link-

creation coefficients. Each of these extensions introduces new analytic challenges, and most will inevitably result in analytically infeasible computations. Therefore the development of models like the mean-field EDEs are important to continue to predict the state of the process.

Different spreading processes can be combined to model more complex phenomena. In 2019, social media are omnipresent in society. Suppose that a network of susceptible and infected nodes in the real-world are coupled in a multilayer network to a social media network. A node from the real world (which can be infected or healthy) can spread information about its health status to others. In this way, $n+1$ networks are required; 1 real-world network and 1 status network for each node in the real-world. Here network i is the information network of the current disease state of node i. In other words, in network i the information is spread whether node i is infected or not. In network i, node i is a source of information and cannot be influenced by others. In the real network, people make decisions to create or break links with other nodes based on the information they receive. Although this formulation is computationally intensive, it may provide further insight in the spreading of contagious diseases in the modern era.

5 Conclusion

In this thesis, the adaptive susceptible-infected-susceptible (ASIS) model has been analysed. It was shown that the model has one steady state, named the trivial steady state, in which all individuals are healthy. When the infection rate is sufficiently high, the process undergoes a phase transition to an endemic state, where most nodes are infected. The state where most nodes are infected, in which the process remains over a long time, was named the metastable state. After this time, the process collapses to the trivial steady state.

Analytically traceable networks were used to study the convergence time required to end up in the trivial steady state. The simulations showed good agreement with the derived theory. Also, the expectation-differential equations have been introduced. By applying a mean-field approximation on these, the Markov process was transferred to a set of non-linear differential equations for the mean of the random variables. This mean-field approximation was accurately able to describe the (averaged) stochastic behaviour for the ASIS model.

Several properties of the metastable network have been analysed. Above the epidemic threshold, the number of links in the network gradually decreases due to the majority of the nodes being infected nodes. Also, the modularity and the ratio of clustering coefficient over the number of links have been analysed. Similar behaviour for these network properties was observed; below the epidemic threshold, a logistic growth is observed. Above the threshold, an exponential decline is shown. This is caused by the infection of neighbouring nodes, thus increasing the clustering between neighbouring nodes (clustering coefficient) and the link-breaking between susceptible and infected nodes increases the modularity.

The ASIS model was extended using different rules for the link-breaking and link-creation processes in the Generalised ASIS framework. In total 36 models have been analysed simultaneously. Out of the 36 models, 9 showed a partially unstable metastable state. This resulted in rapid oscillations of the number of infected number just above the epidemic threshold. The relation between the epidemic threshold and the effective link-breaking rate was also determined. For 5 rules, the epidemic threshold was constant. In 18 cases, the epidemic threshold scales linearly in the link-breaking rate. The remaining 13 cases are bounded between a constant and a linear link-breaking rate, however, its exact dependence remains unclear.

In the G-ASIS framework, it was conjectured that the metastable state of the Markov process can be accurately approximated by the steady state of the mean-field approximation. It was shown this is not true for every model. However in the ASIS model, the mean-field approximation showed close resemblance to the averaged stochastic process results. This may be caused by a positive correlation between the nodes. For the other models, the deviation from the mean field approximation can probably be contributed to the fact that nodes are not positively correlated. Other higher order mean field approximations should be examined to approximate the averaged behaviour of the Markov process.

References

[1] M. Petruzzello. Aqueduct, April 2019. consulted on April 15, 2019, https://www.britannica.com/technology/aqueduct-engineering.

[2] World Health Organisation. Pandemic (H1N1) 2009, Oct 2011. consulted on April 15, 2019, https://www.who.int/csr/disease/swineflu/en/.

[3] K. Dietz and J.A.P. Heesterbeek. Daniel Bernoulli's epidemiological model revisited. *Mathematical Biosciences*, 180(1):1–21, Nov 2002.

[4] F. Brauer, J. Wu, and P. Van den Driessche. *Mathematical Epidemiology*, pages 19 – 22. Springer-Verlag, Berlin Heidelberg, Germany, first edition, 2008.

[5] W.O. Kermack and A.G. McKendrick. Contributions to the mathematical theory of epidemics - ii. the problem of endemicity. *Proc. of the Royal Society*, 138A(1):55–83, 1932.

[6] M. J. Keeling and K. T. D. Eames. Networks and epidemic models. *Journal of The Royal Society Interface*, 2(4):295–307, 2005.

[7] I. Abouelkheir, M. Rachik, O. Zakary, and I. Elmouki. A Multi-regions SIS Discrete Influenza Pandemic Model with a Travel-blocking Vicinity Optimal Control Approach on Cells. *American Journal of Computational and Applied Mathematics 2165-8943*, 7:37–45, 03 2017.

[8] M. E. J. Newman. Spread of epidemic disease on networks. *Phys. Rev. E*, 66:016128, Jul 2002.

[9] I. Tunc, M. S. Shkarayev, and L. B. Shaw. Epidemics in Adaptive Social Networks with Temporary Link Deactivation. *J. Stat. Phys.*, 151:355–366, Apr 2013.

[10] B. Karrer and M. E. J. Newman. Message passing approach for general epidemic models. *Phys. Rev. E*, 82:016101, Jul 2010.

[11] D. Guo, S. Trajanovski, R. van de Bovenkamp, H. Wang, and P. Van Mieghem. Epidemic threshold and topological structure of susceptible-infectious-susceptible epidemics in adaptive networks. *Phys. Rev. E*, 88:042802, Oct 2013.

[12] F.C. Chen. A susceptible-infected epidemic model with voluntary vaccinations. *J. Math. Biol.*, 53:253–272, Aug 2006.

[13] C. Lagorio, M. Dickison, F. Vazquez, L. A. Braunstein, P. A. Macri, M. V. Migueles, S. Havlin, and H. E. Stanley. Quarantine-generated phase transition in epidemic spreading. *Phys. Rev. E*, 83:026102, Feb 2011.

[14] I. B. Schwartz and L. B. Shaw. Rewiring for adaptation. *Physics*, 3, Feb 2010.

[15] T. Gross, C. J. D. D'Lima, and B. Blasius. Epidemic dynamics on an adaptive network. *Phys. Rev. Lett.*, 96:208701, May 2006.

[16] M. Ogura and V. M. Preciado. Epidemic processes over adaptive state-dependent networks. *Phys. Rev. E*, 93:062316, Jun 2016.

[17] S. Trajanovski, D. Guo, and P. Van Mieghem. From epidemics to information propagation: Striking differences in structurally similar adaptive network models. *Phys. Rev. E*, 92:030801, Sep 2015.

[18] M. Nekovee, Y. Moreno, G. Bianconi, and M. Marsili. Theory of rumour spreading in complex social networks. *Physica A: Statistical Mechanics and its Applications*, 374(1):457 – 470, 2007.

[19] C.J. Stam, W. de Haan, P. Tewarie, E. van Dellen, L. Douw, A. Hillebrand, and P. Van Mieghem. A model of adaptive brain networks. 2019. To be published.

[20] P.L. Simon, M. Taylor, and I.Z. Kiss. Exact epidemic models on graphs using graph-automorphism driven lumping. *J. Math. Bio.*, 62:479–508, Apr 2011.

[21] N.G. van Kampen. *Stochastic Processes in Physics and Chemistry*, pages 96 – 99. North Holland, Amsterdam, The Netherlands, third edition, 2007.

[22] P. Van Mieghem. The N-intertwined SIS epidemic network model. *Computing*, 93:147–169, Dec 2011.

[23] M.J. Keeling. The effects of local spatial structure on epidemiological invasions. *Proc. R. Soc. Lond. B*, 266:859–867, Apr 1999.

[24] E. Cator and P. Van Mieghem. Second-order mean-field susceptible-infected-susceptible epidemic threshold. *Phys. Rev. E*, 85:056111, May 2012.

[25] P. Van Mieghem. *Performance Analysis of Complex Networks and Systems*. Cambridge University Press, Cambridge, United Kingdom, 2014.

[26] R. Pastor-Satorras and A. Vespignani. Epidemic dynamics and endemic states in complex networks. *Phys. Rev. E*, 63:066117, May 2001.

[27] C. Li, R. van de Bovenkamp, and P. Van Mieghem. Susceptible-infected-susceptible model: A comparison of N-intertwined and heterogeneous mean-field approximations. *Phys. Rev. E*, 86:026116, Aug 2012.

[28] J. G. Kemeny and J. L. Snell. *Finite Markov Chains*, pages 43–46. Springer-Verlag, Princeton, New Jersey, USA, second edition, 1976.

[29] National Institute of Mental Health. What is prevalence?, November 2017. consulted on March 16, 2019, https://www.nimh.nih.gov/health/statistics/what-is-prevalence.shtml.

[30] E. Cator, R. van de Bovenkamp, and P. Van Mieghem. Susceptible-infected-susceptible epidemics on networks with general infection and cure times. *Phys. Rev. E*, 87:062816, Jun 2013.

[31] P. Van Mieghem and E. Cator. Epidemics in networks with nodal self-infection and the epidemic threshold. *Phys. Rev. E*, 86:016116, Jul 2012.

[32] E. Cator and P. Van Mieghem. Nodal infection in markovian susceptible-infected-susceptible and susceptible-infected-removed epidemics on networks are non-negatively correlated. *Phys. Rev. E*, 89:052802, May 2014.

[33] P. Van Mieghem. *Performance Analysis of Communications Networks and Systems*, pages 319–346. Cambridge University Press, Cambridge, United Kingdom, 2006.

[34] P. Van Mieghem, X. Ge, P. Schumm, S. Trajanovski, and H. Wang. Spectral graph analysis of modularity and assortativity. *Phys. Rev. E*, 82:056113, Nov 2010.

[35] W. Li and D. Schuurmans. Artificial intelligence. In *Modular Community Detection in Networks*, 22, pages 1366–1371, Jul 2011.

[36] M.E.J. Newman. Modularity and community structure in networks. *Proceedings of the National Academy of Sciences*, 103(23):8577–8582, Jun 2006.

[37] G. Deffuant, D. Neau, F. Amblard, and G. Weisbuch. Mixing beliefs among interacting agents. *Advances in Complex Systems*, 03(01n04):87–98, 2000.

[38] M. Braun. *Differential Equations and Their Applications*, page 386. Springer-Verlag New York Inc., New York, USA, fourth edition, 1992.

[39] R. Horn and C. Johnson. *Matrix Analysis*. Cambridge University Press, Cambridge, United Kingdom, second edition, 2012.

[40] S. Vosoughi, D. Roy, and S. Aral. The spread of true and false news online. *Science*, 359(6380):1146–1151, 2018.

[41] H. Sayama, I. Pestov, J. Schmidt, B.J. Bush, C. Wong, J. Yamanoi, and T. Gross. Modeling complex systems with adaptive networks. *Computers and Mathematics with Applications*, 65(10):1645–1664, 2013.

[42] R. Pastor-Satorras, C. Castellano, P. Van Mieghem, and A. Vespignani. Epidemic processes in complex networks. *Rev. Mod. Phys.*, 87:925–979, Aug 2015.

[43] A. Scirè, I. Tuval, and V. M. Eguíluz. Dynamic modeling of the electric transportation network. *Europhysics Letters (EPL)*, 71(2):318–324, jul 2005.

[44] A. Barabási. *Network science*. Cambridge University Press, Cambridge, United Kingdom, Jul 2016.

[45] F. D. Sahneh, A. Vajdi, J. Melander, and C. M. Scoglio. Contact adaption during epidemics: A multilayer network formulation approach. *IEEE Transactions on Network Science and Engineering*, 6(1):16–30, Jan 2019.

[46] S. Gershgorin. Uber die abgrenzung der eigenwerte einer matrix. *Bulletin de l'Academie des Sciences de l'URSS*, 6:749–754, 1931.

[47] S. Noschese, L. Pasquini, and L. Reichel. Tridiagonal toeplitz matrices: properties and novel applications. *Numerical Linear Algebra with Applications*, 20(2):302–326, 2013.

[48] P. Van Mieghem, J. Omic, and R. Kooij. Transactions on networking. In *Virus Spread in Networks*, volume 17, pages 1 – 14. IEEE/ACM, Feb 2009. Lemma 6.

Appendix 1: Bernoulli random variables

A random variable X is a Bernoulli random variable, if it satisfies the following property

$$\mathbb{P}(X = 1) = p, \tag{A1.1}$$
$$\mathbb{P}(X = 0) = 1 - p, \tag{A1.2}$$

where $p \in (0, 1)$. A well-known example is a loaded coin, where the coin lands on heads with probability p and tails with probability $1 - p$. The moments can be computed fairly easily;

$$E(X^n) = \sum_x x^n P(X = x^n) = 0^n \cdot (1 - p) + 1^n \cdot p = p. \tag{A1.3}$$

Hence all moments of a Bernoulli random variable are equal. The variance is

$$\mathrm{Var}(X) = E(X^2) - E(X)^2 = p - p^2 = p(1 - p). \tag{A1.4}$$

This can be generalised in the following theorem.

Theorem A1.1. *(Bernoulli property) Let $\{X_i \,|\, 1 \leq i \leq n\}$ be independent Bernoulli random variables. Also, let $a_i \in \mathbb{N}\ \forall 1 \leq i \leq n$. Then*

$$\mathbb{E}\left(\prod_{i=1}^{n} X_i^{a_i}\right) = \mathbb{E}\left(\prod_{i=1}^{n} X_i\right). \tag{A1.5}$$

Proof. We will use the definition of the expectation;

$$\begin{aligned}
\mathbb{E}\left(\prod_{i=1}^{n} X_i^{a_i}\right) &= \sum_{x \in \{0,1\}} x\mathbb{P}\left(\prod_{i=1}^{n} X_i^{a_i}\right) \\
&= 0 \cdot \mathbb{P}\left(\prod_{i=1}^{n} X_i^{a_i} = 0\right) + 1 \cdot \mathbb{P}\left(\prod_{i=1}^{n} X_i^{a_i} = 1\right) \\
&= \mathbb{P}\left(\prod_{i=1}^{n} X_i^{a_i} = 1\right).
\end{aligned}$$

The X_i's are Bernoulli random variables and their product can only be one if all individuals are one;

$$\mathbb{P}\left(\bigcap_{i=1}^{n} (X_i = 1)\right).$$

This drops out all exponents. So we finish the proof;

$$\mathbb{P}\left(\bigcap_{i=1}^{n} (X_i = 1)\right) = \mathbb{P}\left(\prod_{i=1}^{n} X_i = 1\right) = \mathbb{E}\left(\prod_{i=1}^{n} X_i\right).$$

□

Appendix 2: Proof of Theorem 1.1

Proof of Theorem 1.1 *from section* 1.2.2.

The proof is analogous to the 2-node case from section 1.2.1. Using the law of the total expectation, the evolution of $\mathbb{E}(X_i)$ is given by

$$\begin{aligned}\frac{d\mathbb{E}(X_i)}{dt} &= \frac{d\mathbb{P}(X_i=1)}{dt} \\ &= \underbrace{\sum_{k_{m,n}\in\{0,1\}}}_{\text{for } (m,n)\in\mathcal{L}_0} \quad \underbrace{\sum_{k_j\in\{0,1\}}}_{\text{for } 1\leq j\leq N, j\neq i} \frac{d}{dt}\mathbb{P}(X_1=k_1...,X_i=1,...,X_N=k_N,...,a_{ij}=k_{mn},...).\end{aligned}$$

Note that these sums actually symbolise L_0 and $N-1$ sums respectively. Before one can advance, more concrete properties need to be derived from the original equations. It is important to notice that states of the form $(...,a_{ij}=1,...)$ exist if and only if the initial network allows for it. In order words, the value of a_{ij} can only change when this link is present in the initial network. This means link-creation cannot occur when the link was not available in the initial network. For example, we consider the 2-node case. If those two nodes are not connected, states of the form $(...,...,a_{12}=1)$ cannot exist. Moreover, $\xi=\zeta=\beta=0$ from which follows that

$$\frac{d\mathbb{E}(a_{ij})}{dt}=0 \qquad \text{if } a_{ij}(0)=0.$$

For the moment, assume that every link exists in the initial network. Afterwards the general case will follow naturally. All local interaction takes place between two nodes and their corresponding link. We will therefore use the notation (X_i,X_j,a_{ij}) as before.

Consider $(X_i=1,X_j=0,a_{ij}=0)$. The state is written in concise notation as $(1,0,0)$. The only possible ways the system has ended up in this state over a time step Δt is (we ignore multiple transitions to take place): (I) the link-breaking of a_{ij}, (II) the curing of node j and (III) node i does not cure. Mathematically, this can be formulated as follows;

$$\begin{aligned}&\frac{d\mathbb{P}(1,0,0)}{dt} = \\ &\sum_{j=1,j\neq i}^{N}\zeta\mathbb{P}(-,1(i),-,0(j),-,1(ij)) + \sum_{j=1,j\neq i}^{N}\delta\mathbb{P}(-,1(i),-,1(j),-,0(ij)) - \delta\mathbb{P}(-,1(i),-,0(j),-,0(ij)).\end{aligned}$$

All dashes in the formula above indicate we have summed over all other variables. These all add up to one, which removes them from the equation. The first term is (I) the link-breaking of the $(1,0,1)$ state. This may happen for every link a_{ij}, hence the sum has been taken over all $j\neq i$. Moreover, the second term is (II) the curing of node j of the $(1,1,0)$ state. Each node may cure, therefore we sum over all $j\neq i$. Finally, (III) node i does not cure in the $(1,0,0)$ state. The minus sign appears for the node should not cure.

By using the Bernoulli property again, the equation can be written in terms of expectation values;

$$\frac{d\mathbb{P}(1,0,0)}{dt} = \zeta\sum_{j=1,j\neq i}^{N}\mathbb{E}(X_i(1-X_j)a_{ij}) + \delta\sum_{j=1,j\neq i}^{N}\mathbb{E}(X_iX_j(1-a_{ij})) - \delta\mathbb{E}(X_i(1-X_j)(1-a_{ij}))$$

such that

$$\begin{aligned}\frac{d\mathbb{P}(1,0,0)}{dt} &= -\delta\mathbb{E}(X_i)+\delta\mathbb{E}(X_ia_{ij})+ \\ &\sum_{j=1,j\neq i}^{N}\left(-\zeta\mathbb{E}(X_iX_ja_{ij})+\zeta\mathbb{E}(X_ia_{ij})\right)+\sum_{j=1}^{N}\left(-\delta\mathbb{E}(X_iX_ja_{ij})+\delta\mathbb{E}(X_iX_j)\right).\end{aligned} \tag{A2.1}$$

Now consider $(X_i = 1, X_j = 0, a_{ij} = 1)$. The same method can be used to find

$$\frac{d\mathbb{P}(1,0,1)}{dt} = -\delta\mathbb{P}(-,1(i),-,0(j),-,1(ij)) \\ -(\beta+\zeta)\sum_{j=1,j\neq i}^{N}\mathbb{P}(-,1(i),-,0(j),-,1(ij)) + \delta\sum_{j=1,j\neq i}^{N}\mathbb{P}(-,1(i),-,1(j),-,1(ij)).$$

The first process is staying in $(1,0,1)$ which happens when node i is not cured (first term), the link is not removed (second term) and node j is not infected by node i (also second term). Finally, we could arrive here because node j has cured (third term).

Working this out in terms of expectation values gives

$$\frac{d\mathbb{P}(1,0,1)}{dt} = -\delta\mathbb{E}(X_i(1-X_j)a_{ij}) - (\beta+\zeta)\sum_{j=1,j\neq i}^{N}\mathbb{E}(X_i(1-X_j)a_{ij}) + \delta\sum_{j=1,j\neq i}^{N}\mathbb{E}(X_iX_ja_{ij}). \quad \text{(A2.2)}$$

The same procedure needs to be repeated for $X_i = 1, X_j = 1, a_{ij} = 0$ and $X_i = 1, X_j = 1, a_{ij} = 1$. For $(1,1,0)$, we find

$$\frac{d\mathbb{P}(1,1,0)}{dt} = -\delta\sum_{j=1}^{N}\mathbb{P}(-,1(i),-,1(j),-,0(ij)).$$

Note that we have the sum over all j including i as both i and j can be cured. This can be rewritten as

$$\frac{d\mathbb{P}(1,1,0)}{dt} = -\delta\sum_{j=1}^{N}\mathbb{E}(X_iX_j(1-a_{ij})). \quad \text{(A2.3)}$$

For $(1,1,1)$ it follows that

$$\frac{d\mathbb{P}(1,1,1)}{dt} = \sum_{j=1,j\neq i}^{N}\beta\mathbb{P}(-,0(i),-,1(j),-,1(ij)) \\ +\beta\sum_{j=1,j\neq i}^{N}\mathbb{P}(-,1(i),-,0(j),-,1(ij)) - \delta\sum_{j=1}^{N}\mathbb{P}(-,1(i),-,1(j),-,1(ij)).$$

For the first term, i can be infected by every $j \neq i$. For the second term, i can infect every $j \neq i$. For the last term, everyone should not cure. Using the Bernoulli property,

$$\frac{d\mathbb{P}(1,1,1)}{dt} = \beta\sum_{j=1,j\neq i}^{N}\mathbb{E}((1-X_i)X_ja_{ij}) + \beta\sum_{j=1,j\neq i}^{N}\mathbb{E}(X_i(1-X_j)a_{ij}) - \delta\sum_{j=1}^{N}\mathbb{E}(X_iX_ja_{ij})$$

which can be simplified to

$$\frac{d\mathbb{P}(1,1,1)}{dt} = \sum_{j=1,j\neq i}^{N}(-2\beta\mathbb{E}(X_iX_ja_{ij}) + \beta\mathbb{E}((X_i+X_j)a_{ij})) - \delta\sum_{j=1}^{N}\mathbb{E}(X_iX_ja_{ij}). \quad \text{(A2.4)}$$

Adding Eqs. (A2.1), (A2.2), (A2.3) and (A2.4) we find the equation for $\mathbb{P}(X_i = 1) = \mathbb{E}(X_i)$ using the law of total expectation;

$$\frac{d\mathbb{E}(X_i)}{dt} = \frac{d\mathbb{P}(X_i=1)}{dt} = \frac{d\mathbb{P}(1,-,-)}{dt} \\ = \frac{d\mathbb{P}(1,0,0)}{dt} + \frac{d\mathbb{P}(1,0,1)}{dt} + \frac{d\mathbb{P}(1,1,0)}{dt} + \frac{dP(1,1,1)}{dt} \\ = -\delta\mathbb{E}(X_i) + \beta\sum_{j=1,j\neq i}^{N}\mathbb{E}((1-X_i)X_ja_{ij}).$$

We have not considered the case $a_{ij}(0) = 0$. It is clear that if $a_{ij}(0) = 0$, we have $a_{ij}(t) = 0$ such that the equation for $\mathbb{E}(X_i)$ becomes

$$\frac{d\mathbb{E}(X_i)}{dt} = -\delta\mathbb{E}(X_i) + \beta \sum_{j=1,j\neq i}^{N} a_{ij}(0)\mathbb{E}((1-X_i)X_j a_{ij}).$$

However, the term $a_{ij}(0)$ can be proven to be redundant. Suppose $a_{ij}(0) = 0$, then it is also clear that $a_{ij}(t) = 0$ for all t, and hence the element of the sum is zero. Suppose $a_{ij}(0) = 1$, then the contribution of a_{ij} should be handled in the sum, which is exactly what is happening. For either possibility, we conclude the original equation is correct and $a_{ij}(0)$ may be omitted. This concludes the derivation of the evolution of $\mathbb{E}(X_i)$.

In the same fashion, the network structure can be derived. As before, it is assumed that $a_{ij}(0) = 1$. Consider the state $X_i = 0, X_j = 0, a_{ij} = 1$, $(0, 0, 1)$. The corresponding equation is

$$\frac{d\mathbb{P}(0,0,1)}{dt} =$$
$$\xi \sum_{j=1,j\neq i}^{N} \mathbb{P}(-, 0(i), -, 0(j), -, 0(ij)) + \delta \sum_{j=1,j\neq i}^{N} \mathbb{P}(-, 0(i), -, 1(j), -, 1(ij)) + \delta\mathbb{P}(-, 1(i), -, 0(j), -, 1(ij)).$$

Several possibilities are available to arrive at such a state, which are: link restoring could have happened for any j (first term), curing could have happened for j (second term) or for i (third term). Rewriting in terms of expectations gives

$$\begin{aligned}\frac{d\mathbb{P}(0,0,1)}{dt} = \xi \sum_{j=1,j\neq i}^{N} \mathbb{E}((1-X_i)(1-X_j)(1-a_{ij}) + \\ \delta \sum_{j=1,j\neq i}^{N} \mathbb{E}((1-X_i)X_j a_{ij})) + \delta\mathbb{E}(X_i(1-X_j)a_{ij})\end{aligned}$$

which is, rewritten

$$\begin{aligned}\frac{d\mathbb{P}(0,0,1)}{dt} = \delta\mathbb{E}(X_i a_{ij}) - \delta\mathbb{E}(X_i X_j a_{ij}) + \\ \xi \sum_{j=1,j\neq i}^{N} \mathbb{E}((1-X_i)(1-X_j)(1-a_{ij})) + \delta \sum_{j=1,j\neq i}^{N} \mathbb{E}((1-X_i)X_j a_{ij}).\end{aligned} \tag{A2.5}$$

Regarding $X_i = 0, X_j = 1, a_{ij} = 1$, we find

$$\frac{d\mathbb{P}(0,1,1)}{dt} =$$
$$-(\delta + \beta + \zeta) \sum_{j=1,j\neq i}^{N} \mathbb{P}(-, 0(i), -, 1(j), -, 1(ij)) + \delta\mathbb{P}(-, 1(i), -, 1(j), -, 1(ij)).$$

Here node i should not be infected, node j not be cured and their link not be broken (first term) and node i can be cured (second term). This can be rewritten in terms of expectation values

$$\frac{d\mathbb{P}(0,1,1)}{dt} = -(\delta + \beta + \zeta) \sum_{j=1,j\neq i}^{N} \mathbb{E}((1-X_i)X_j a_{ij}) + \delta\mathbb{E}(X_i X_j a_{ij}). \tag{A2.6}$$

Two cases are still to be considered. The first, $X_i = 1, X_j = 0, a_{ij} = 1$, has been computed in Eq. (A2.2). The second, $X_i = 1, X_j = 1, a_{ij} = 1$, was computed in Eq. (A2.4). This completes all required steps. Using the law of total expectation and the results of Eqs. (A2.2), (A2.4), (A2.5) and (A2.6), the following result is obtained

$$\begin{aligned}\frac{d\mathbb{E}(a_{ij})}{dt} &= -\zeta\mathbb{E}(X_i(1-X_j)a_{ij}) - \zeta\mathbb{E}(X_j(1-X_i)a_{ij}) + \xi\mathbb{E}((1-a_{ij})(1-X_i)(1-X_j)) \\ &= -\zeta\mathbb{E}(a_{ij}(X_i - X_j)^2) + \xi\mathbb{E}((1-a_{ij})(1-X_i)(1-X_j)).\end{aligned}$$

Again we stress this result is only valid for $a_{ij}(0) = 1$. For $a_{ij}(0) = 0$, the solution is constant (and therefore no differential equation is required).

This allows us to incorporate $a_{ij}(0)$ into the differential equation for $\mathbb{E}(a_{ij})$ to finally find the differential equations:

$$\frac{d\mathbb{E}(X_i)}{dt} = -\delta\mathbb{E}(X_i) + \beta \sum_{j=1, j\neq i}^{N} \mathbb{E}((1 - X_i)X_j a_{ij}),$$
$$\frac{d\mathbb{E}(a_{ij})}{dt} = a_{ij}(0)E\Big[- \zeta(X_i - X_j)^2 + \xi(1 - a_{ij})(1 - X_i)(1 - X_j)\Big],$$

which proves the theorem.

□

Appendix 3: Steady states of mean-field EDEs for the SIS network

The computation for all steady states is only possible for a simplified model. Therefore the expectation differential equations are assumed to be mean-field and the network is assumed to be static, such that the governing equations become

$$\frac{d\mathbb{E}(X_i)}{dt} = -\delta\mathbb{E}(X_i) + \beta\sum_{j=1}^{N} a_{ij}\mathbb{E}(X_j)(1-\mathbb{E}(X_i)). \tag{A3.1}$$

These are N coupled non-linear differential equations for given a_{ij}, β and δ. Note that $\mathbb{E}(X_i) = 0$ is always a steady state: this is the trivial steady state. In this appendix, it is investigated whether other steady states exist. Also, their stability will be examined.

The linear stability can be investigated relatively quickly. Define $d_i = -\delta - \beta\sum_{j=1}^{N} a_{ij}\mathbb{E}(X_j)$ and $b_{ij} = \beta a_{ij}(1-\mathbb{E}(X_i))$. Then the Jacobian is

$$J = \begin{pmatrix} d_1 & b_{12} & b_{13} & \cdots & \\ b_{21} & d_2 & b_{23} & & \\ \vdots & \ddots & \ddots & \ddots & \\ & & b_{N-1,N-2} & d_{N-1} & b_{N-1,N} \\ & & & b_{N,N-1} & d_N \end{pmatrix}. \tag{A3.2}$$

Calculating the eigenvalues is not possible, but can be estimated by Gershgorin's circle theorem as [46]

$$|\lambda_i - d_i| \leq \sum_{j=1, j\neq i}^{N} |b_{ij}|.$$

Substituting in J, we find

$$|\lambda_i + \delta + \beta\sum_{j=1}^{N} a_{ij}\mathbb{E}(X_j)| \leq \beta\sum_{j=1, j\neq i}^{N} a_{ij}(1-\mathbb{E}(X_i)). \tag{A3.3}$$

Unfortunately, J is not symmetric so no further steps can be taken.

In section A3.1 three nodes arranged in a triangle are considered. Thereafter all symmetric steady states for N nodes are computed. Finally, three nodes in a line are considered in the last section.

A3.1 Three nodes in a triangle

We will consider three nodes attached to each other in a triangle. This means the network is a complete network and every node is connected to two other nodes. We will use the shorthand notation $\mathbb{E}(X_i) = x_i$ to find the following equations

$$\begin{aligned} \frac{dx_1}{dt} &= -\delta x_1 + \beta(1-x_1)(x_2+x_3), \\ \frac{dx_2}{dt} &= -\delta x_2 + \beta(1-x_2)(x_1+x_3), \\ \frac{dx_3}{dt} &= -\delta x_3 + \beta(1-x_3)(x_1+x_2). \end{aligned}$$

The investigation of the steady states starts by setting all derivatives zero, and after some rewriting using $\tau = \frac{\beta}{\delta}$ we obtain

$$\begin{aligned} \tau(1-x_1)(x_2+x_3) &= x_1, \\ \tau(1-x_2)(x_1+x_3) &= x_2, \\ \tau(1-x_3)(x_1+x_2) &= x_3, \end{aligned}$$

which can be rewritten by expanding the brackets as

$$\tau x_2 + \tau x_3 - \tau x_1 x_2 - \tau x_1 x_3 = x_1, \tag{A3.4}$$

$$\tau x_1 + \tau x_3 - \tau x_1 x_2 - \tau x_2 x_3 = x_2, \tag{A3.5}$$

$$\tau x_1 + \tau x_2 - \tau x_1 x_3 - \tau x_2 x_3 = x_3. \tag{A3.6}$$

Subtracting Eq. (A3.4) from Eq. (A3.5) yields

$$\tau(x_2 - x_1) + \tau(x_2 - x_1)x_3 = -(x_2 - x_1).$$

Hence

$$\text{Case 1: } x_1 = x_2,$$

$$\text{Case 2: } x_3 = -\frac{1+\tau}{\tau}.$$

Case 2 can be ruled out directly, as x_3 should be positive. So we continue with Case 1. The set of equations reduce to two equations (one has become redundant);

$$\tau x_1 + \tau x_3 - \tau x_1^2 - \tau x_1 x_3 = x_1, \tag{A3.7}$$

$$2\tau x_1 - 2\tau x_1 x_3 = x_3. \tag{A3.8}$$

To solve the non-linear equations, take 2· Eq. (A3.7) − Eq. (A3.8):

$$2\tau x_3 - 2\tau x_1^2 = 2x_1 - x_3$$

such that

$$x_3 = \frac{2x_1(1+\tau x_1)}{2\tau + 1}.$$

Inserting back into Eq. (A3.8) we find

$$2\tau x_1 - 2\tau x_1 \frac{2x_1(1+\tau x_1)}{2\tau+1} = \frac{2x_1(1+\tau x_1)}{2\tau+1}.$$

To get rid of fractions, we multiply all elements by $2\tau + 1$ such that

$$2\tau(2\tau+1)x_1 - 4\tau x_1^2(1+\tau x_1) = 2x_1(1+\tau x_1).$$

The solution is either $x_1 = 0$ (which directly implies $x_2 = x_3 = 0$ which is the trivial solution, so not interesting) or satisfies the equation

$$\tau(2\tau+1) - 2\tau x_1(1+\tau x_1) = 1 + \tau x_1.$$

Rearranging;

$$-2\tau^2 x_1^2 - 3\tau x_1 + 2\tau^2 + \tau - 1 = 0.$$

The solution of this quadratic equation is

$$x_1^{\pm} = \frac{1}{4\tau}\left(-3 \pm \sqrt{1 + 8\tau + 16\tau^2}\right).$$

Clearly the negative branch will never yield physical solutions (x_1 needs to be positive) and is therefore uninteresting. The positive branch intersects zero at some point and only increases afterwards. This point is given by $x_1^+ = 0$. Solving this for τ, we find

$$\tau > \frac{1}{2}.$$

We know $\tau > 0$, so this answer is valid and for $\tau > \frac{1}{2}$, the solution grows slowly to 1, and is therefore valid for all $\tau > \frac{1}{2}$. Now we check for x_3;

$$x_3 = \frac{2x_1(1+\tau x_1)}{2\tau+1}.$$

Although it is not clear immediately, after some rewriting, one can show that $x_1 = x_3$. Hence there is only one non-trivial steady state, in which all nodes are equal. We are sure no other steady state exists for this 3-dimensional system.

In the next section, it is verified that the symmetric steady state exists for any network size. Also, the stability of the state is computed.

A3.2 Symmetric steady states for N nodes

We will investigate all symmetric steady states of the form $x_i = x_v$ for all i. We find

$$-\delta x_v + \beta x_v(1 - x_v)\sum_{j=1}^{N} a_{ij} = 0.$$

This equation has two solutions;

$$\begin{aligned} x_v &= 0, \\ x_v &= 1 - \frac{\delta}{\beta d_i} = 1 - \frac{1}{\tau d_i}, \end{aligned}$$

where d_i is the degree of a node and $\tau = \frac{\beta}{\delta}$ the effective infection rate. For this state to exist, it is required that every node has the same degree d, i.e. the network is d-regular. Also, for a physical state to exist, it is necessary that $x_v > 0$. We then require

$$\tau > \frac{1}{d}$$

for the non-trivial steady state to exist.

Now consider the stability. Substituting $\mathbb{E}(X_i) = \mathbb{E}(X_j) = 0$ in Eq. (A3.3), we find

$$|\lambda_i + \delta| \leq \beta \sum_{j=1, j\neq i}^{N} a_{ij}.$$

This assumption makes J symmetric, such that

$$-\delta - \beta d \leq \lambda_i \leq -\delta + \beta d.$$

This stable for all $1 \leq i \leq N$ whenever

$$\tau < \frac{1}{d}.$$

The symmetric steady state is given by $\mathbb{E}(X_i) = \mathbb{E}(X_j) = x_v > 0$, which was found in Eq. (A3.3). Substitution in the stability condition of Eq. (A3.3) yields

$$|\lambda_i + \delta + \beta x_v \sum_{j=1}^{N} a_{ij}| \leq \beta(1 - x_v) \sum_{j=1, j\neq i}^{N} a_{ij}.$$

This assumption makes the matrix J symmetric, hence

$$-\delta - \beta d \leq \lambda_i \leq -\delta + \beta(1 - 2x_v)d.$$

This stable whenever

$$(1 - 2x_v) < \frac{1}{\tau d}.$$

For $x_v > \frac{1}{2}$, this is satisfied automatically. Thus stability is assured for $x_v \geq \frac{1}{2}$ or (when inserting x_v)

$$-1 + \frac{2}{\tau d} < \frac{1}{\tau d}.$$

So it is stable whenever

$$\tau d > 1.$$

To summarize, we have the following:

$$\begin{aligned} \boldsymbol{x} = 0 : &\quad \text{always exists, stable for } \tau d < 1, \\ \boldsymbol{x} = x_v : &\quad \text{exists for } \tau d > 1, \text{stable for } \tau d > 1. \end{aligned}$$

This result can be used to construct a bifurcation diagram of the situation.

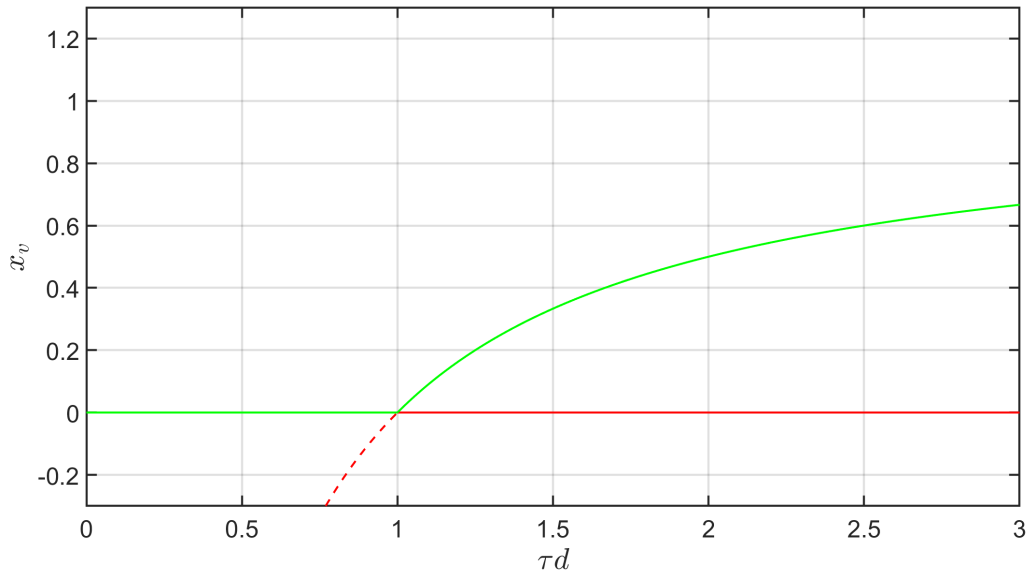

Figure A3.1: The bifurcation diagram for a d-regular network. The bifurcation type is a transcritical. The dashed line implies the results found are non-physical and do therefore not exist.

Although the symmetric steady state has been computed, it remains unclear whether other steady states exist. Since the mean-field EDEs are non-linear, it is infeasible to compute these by hand. The thorough computation of the three-node test case reveals that it is unlikely, however, it remains possible. Moreover, the case where nodes do not have the same degree has not yet been examined. The next section considers a simple non-symmetric network.

A3.3 Three nodes in a line

Here we take, as an example of a non-symmetric network, three nodes in a line. This means one link is removed from the complete network. The resulting network is a tree, where node 2 is connected to both node 1 and 3. The symmetric solution derived in the previous section cannot exist, so the investigation has to take place again.

The equations to solve are

$$\begin{aligned}\tau(1-x_1)x_2 &= x_1,\\ \tau(1-x_2)(x_1+x_3) &= x_2,\\ \tau(1-x_3)x_2 &= x_3,\end{aligned}$$

which can be rewritten by expanding the brackets as

$$\tau x_2 - \tau x_1 x_2 = x_1, \tag{A3.9}$$

$$\tau x_1 + \tau x_3 - \tau x_1 x_2 - \tau x_2 x_3 = x_2, \tag{A3.10}$$

$$\tau x_1 - \tau x_2 x_3 = x_3. \tag{A3.11}$$

From the first and last equation, we find

$$x_1 = x_3 = \frac{\tau x_2}{1+\tau x_2}.$$

Substituting both in Eq. (A3.10), we obtain

$$2\tau\frac{\tau x_2}{1+\tau x_2} - 2\tau x_2\frac{\tau x_2}{1+\tau x_2} = x_2.$$

To remove the fractions, multiply every term by $1 + \tau x_2$ such that

$$2\tau^2 x_2 - 2\tau^2 x_2^2 = x_2(1 + \tau x_2).$$

The solution is $x_2 = 0$ (which results in $x_1 = x_3 = 0$, which is the uninteresting trivial solution) or

$$x_2 = \frac{2\tau^2 - 1}{2\tau^2 + \tau}.$$

Clearly, the solution increases to 1 as τ approaches infinity, and it is zero when $2\tau^2 - 1 = 0$, so it is necessary that

$$\tau > \frac{1}{\sqrt{2}}.$$

Using the result for x_2, we find for $x_1 = x_3$ that

$$x_1 = \frac{\tau \frac{2\tau^2-1}{2\tau^2+\tau}}{1 + \tau \frac{2\tau^2-1}{2\tau^2+\tau}} = \frac{\frac{2\tau^2-1}{2\tau+1}}{\frac{2\tau+1+2\tau^2-1}{2\tau+1}} = \frac{2\tau^2 - 1}{2\tau^2 + 2\tau}.$$

To sum up, the non-trivial steady state solution is

$$x_2 = \frac{2\tau^2 - 1}{2\tau^2 + \tau},$$
$$x_1 = x_3 = \frac{2\tau^2 - 1}{2\tau^2 + 2\tau},$$

which only exists for $\tau > \frac{1}{\sqrt{2}}$. Substituting the results in Eq. (A3.3) to compute its stability brings;

$$-\delta - \beta(1 - \mathbb{E}(X_1) + \mathbb{E}(X_2)) \leq \lambda_1 \leq -\delta + \beta(1 - \mathbb{E}(X_1) - \mathbb{E}(X_2)),$$
$$-\delta - \beta(2 - 2\mathbb{E}(X_2) + \mathbb{E}(X_1) + \mathbb{E}(X_3)) \leq \lambda_2 \leq -\delta + \beta(2 - 2\mathbb{E}(X_2) - \mathbb{E}(X_1) - \mathbb{E}(X_3)).$$

Since $\mathbb{E}(X_1) = \mathbb{E}(X_3)$ the equation for $\mathbb{E}(X_3)$ is omitted for brevity. Using the Jacobian from Eq. (A3.3) the condition for stability is

$$-\delta + \beta(1 - \mathbb{E}(X_1) - \mathbb{E}(X_2)) < 0,$$
$$-\delta + \beta(2 - 2\mathbb{E}(X_2) - 2\mathbb{E}(X_1)) < 0.$$

Both equations are nearly equal. Let $c = \{1, 2\}$. Then we have stability if

$$-\delta + \beta c(1 - \mathbb{E}(X_1) - \mathbb{E}(X_2)) < 0, \qquad c \in \{1, 2\},$$

which can be rewritten as

$$\tau(1 - \mathbb{E}(X_1) - \mathbb{E}(X_2)) < \frac{1}{c}.$$

Clearly, when it satisfies $c = 2$, it also satisfies $c = 1$. So we need to verify when the following inequality holds;

$$\tau(1 - \mathbb{E}(X_1) - \mathbb{E}(X_2)) < \frac{1}{2}.$$

So we compute

$$\begin{aligned}
1 - \mathbb{E}(X_1) - \mathbb{E}(X_2) &= 1 - \frac{2\tau^2 - 1}{2\tau^2 + 2\tau} - \frac{2\tau^2 - 1}{2\tau^2 + \tau} \\
&= \frac{(2\tau^2 + 2\tau)(2\tau^2 + \tau)}{(2\tau^2 + 2\tau)(2\tau^2 + \tau)} - \frac{(2\tau^2 - 1)(2\tau^2 + \tau)}{(2\tau^2 + 2\tau)(2\tau^2 + \tau)} - \frac{(2\tau^2 - 1)(2\tau^2 + 2\tau)}{(2\tau^2 + 2\tau)(2\tau^2 + \tau)} \\
&= \frac{4\tau^4 + 6\tau^3 + 2\tau^2 - (4\tau^4 + 2\tau^3 - 2\tau^2 - \tau) - (4\tau^4 + 4\tau^3 - 2\tau^2 - 2\tau)}{(2\tau^2 + 2\tau)(2\tau^2 + \tau)} \\
&= \frac{-4\tau^4 + 6\tau^2 + 3\tau}{(2\tau^2 + 2\tau)(2\tau^2 + \tau)} \\
&= \frac{-4\tau^3 + 6\tau + 3}{4\tau^3 + 6\tau^2 + 2\tau},
\end{aligned}$$

which yields

$$\frac{-4\tau^3 + 6\tau + 3}{4\tau^2 + 6\tau + 2} < \frac{1}{2}$$

such that

$$-4\tau^3 + 6\tau + 3 < 2\tau^2 + 3\tau + 1,$$

which simplifies to

$$-4\tau^3 - 2\tau^2 + 3\tau + 2 < 0.$$

This holds whenever $\tau > 0.91$. We could calculate the τ values analytically using the ABCD formula, but it would not be of any further use.

Now consider the trivial steady state. We again need to check Eq. (A3.3):

$$\tau(1 - \mathbb{E}(X_1) - \mathbb{E}(X_2)) < \frac{1}{2}.$$

Since $\mathbb{E}(X_1) = \mathbb{E}(X_2) = 0$, we find;

$$\tau < \frac{1}{2}$$

for stability. To summarize, we have the following:

$$\begin{aligned} \boldsymbol{x} = 0: &\quad \text{always exists, stable for } \tau d < \frac{1}{2}, \\ \boldsymbol{x} \neq 0: &\quad \text{exists for } \tau d > \frac{1}{\sqrt{2}}, \text{ stable for } \tau d > 0.91. \end{aligned}$$

This leads to the following bifurcation diagram.

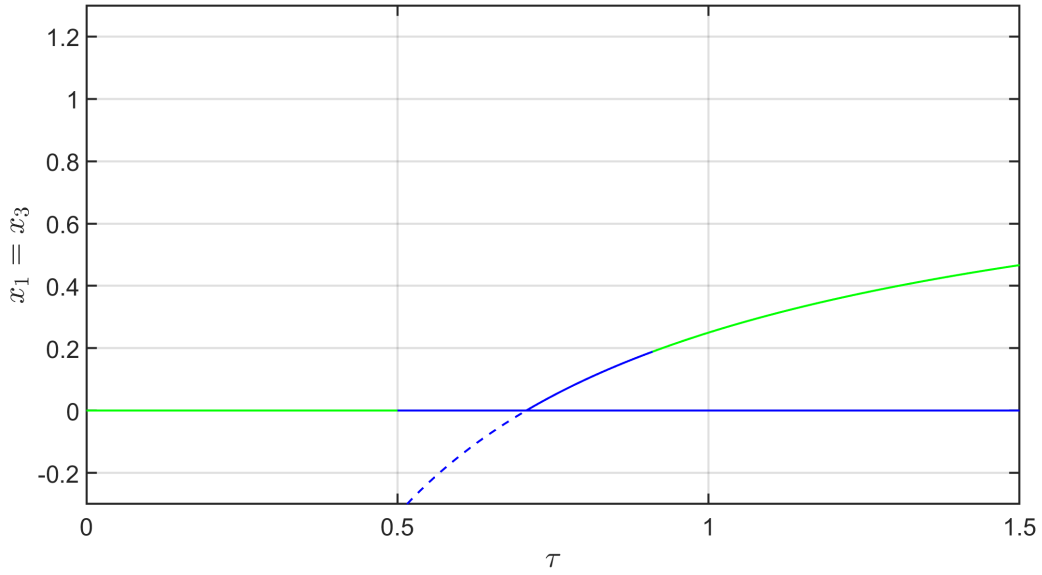

Figure A3.2: The bifurcation diagram for a 3-line network. Stable branches are indicated in green, unstable branches in red and uncertain branches in blue. Dashed lines imply the results found are non-physical and do therefore not exist.

All stable lines have been indicated, but blue lines have been used instead to show the uncertainty of the methodology used. It appears not to be sufficient to use Gershgorin to derive bounds; more steps are required. This is visible by the sudden intermediate region we have found between $\tau = \frac{1}{2}$ and $\tau \approx 0.91$. Therefore we need to investigate the actual eigenvalues. For this small network, this is possible.

The Jacobian for this network is

$$J = \begin{pmatrix} -\delta - \beta\mathbb{E}(X_2) & \beta(1-\mathbb{E}(X_1)) & 0 \\ \beta(1-\mathbb{E}(X_2)) & -\delta - \beta\mathbb{E}(X_1+X_3) & \beta(1-\mathbb{E}(X_2)) \\ 0 & \beta(1-\mathbb{E}(X_3)) & -\delta - \beta\mathbb{E}(X_2) \end{pmatrix}. \tag{A3.12}$$

For $\boldsymbol{x} = 0$, this is

$$J(0) = \begin{pmatrix} -\delta & \beta & 0 \\ \beta & -\delta & \beta \\ 0 & \beta & -\delta \end{pmatrix}. \tag{A3.13}$$

We recognize this as a tridiagonal Toeplitz matrix, which is of the form

$$A = \begin{pmatrix} a & b & 0 & \cdots & \\ c & a & b & \cdots & \\ 0 & \ddots & \ddots & \ddots & \\ & 0 & c & a & b \\ & & 0 & c & a \end{pmatrix}.$$

Its eigenvalues are known [47]

$$\lambda_k = a + 2\sqrt{bc}\cos\left(\frac{k\pi}{n+1}\right), \qquad k = 1, \ldots, n.$$

So we find

$$\begin{aligned} \lambda_1 &= -\delta + \sqrt{2}\beta, \\ \lambda_2 &= -\delta, \\ \lambda_3 &= -\delta - \sqrt{2}\beta. \end{aligned}$$

For stability, we require the eigenvalues to be negative, so

$$\tau < \frac{1}{\sqrt{2}}.$$

The same can be done for the non-symmetric state. The Jacobian is

$$J = \delta \begin{pmatrix} -2\frac{\tau^2+\tau}{2\tau+1} & \frac{2\tau+1}{2\tau+2} & 0 \\ \frac{\tau+1}{2\tau+1} & \frac{-2\tau^2-\tau}{\tau+1} & \frac{\tau+1}{2\tau+1} \\ 0 & \frac{2\tau+1}{2\tau+2} & -2\frac{\tau^2+\tau}{2\tau+1} \end{pmatrix} \tag{A3.14}$$

where δ has been taken out. This matrix is awful, which makes it difficult to investigate its behaviour. The result however, is that $\tau > \frac{1}{\sqrt{2}}$ gives a stable branch. This completes our bifurcation diagram, which is shown below.

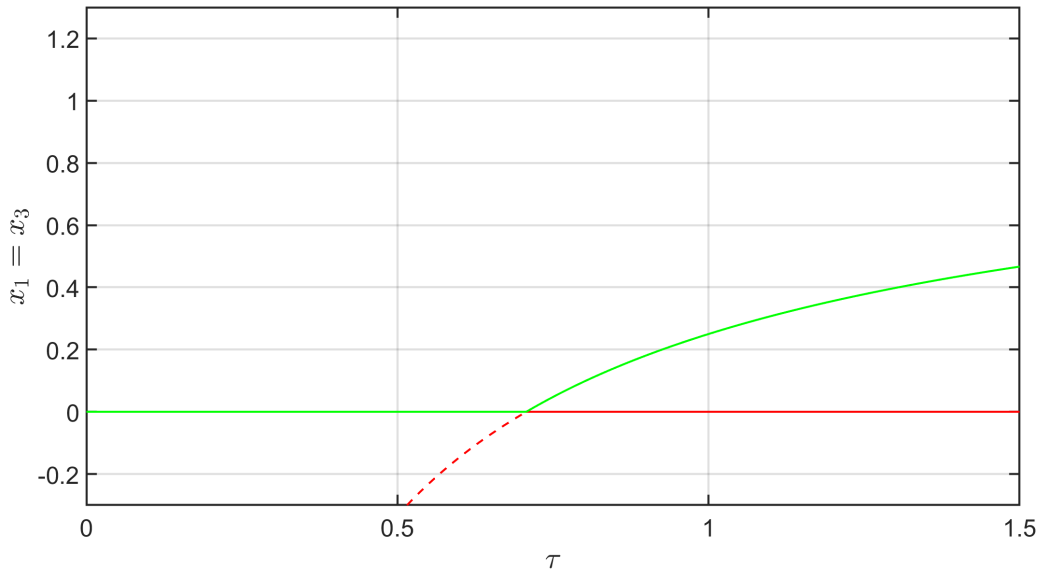

Figure A3.3: The bifurcation diagram for a 3-line network. Stable branches are indicated in green and unstable branches in red. Dashed lines imply the results found are non-physical and do therefore not exist.

The vertical axis of the bifurcation diagram only shows that $x_1 = x_3$ value. Since the solution only exists over a line in the (x_1, x_2) plane, a 3D bifurcation diagram would not yield any further insight. Also, the (τ, x_2)-diagram is nearly equivalent.

To conclude, we have seen that, despite the network being irregular, a non-trivial steady state exists which is stable for $\tau > \frac{1}{d_{\min}}$. From literature, a lower bound for the epidemic threshold is known [48]

$$\tau_c \geq \frac{1}{\rho}. \tag{A3.15}$$

This is a generalisation of the result from this appendix and uses advanced network analysis tools to prove it. All obtained results comply with the lower bound from literature.

Appendix 4: All rules in the G-ASIS framework

The results from Chapter 3 are summarised in the following table, which contains all 36 processes contained in the G-ASIS framework.

Table A4.1: All models from the G-ASIS framework and their properties. YES* does not mean the metastable state is always stable, only that it is not proven it is unstable. This table assumes $\delta = 1$.

Rules (link-breaking) (link-creation)	Model name and appearance in literature	Always metastable	Lower bound on epidemic threshold	Upper bound on epidemic threshold
X_iX_j X_iX_j		YES*	$\frac{1}{\rho}$	Linear
X_iX_j $1-X_iX_j$		NO	$\frac{1}{\rho}$	Constant
X_iX_j $(1-X_i)(1-X_j)$	ABN model [19]	YES*	$\frac{1}{\rho}$	Linear
X_iX_j $1-(1-X_i)(1-X_j)$		NO	$\frac{1}{\rho}$	Linear
X_iX_j $(X_i-X_j)^2$		NO	$\frac{1}{\rho}$	Linear
$1-X_iX_j$ $1-(X_i-X_j)^2$		YES*	$\frac{1}{\rho}$	Linear
$1-X_iX_j$ X_iX_j		YES*	$\frac{1+\omega\xi}{\rho}$	Linear
$1-X_iX_j$ $1-X_iX_j$		YES*	$\frac{1+\frac{\xi\omega}{\xi+1}}{\rho}$	Linear
$1-X_iX_j$ $(1-X_i)(1-X_j)$		YES*	$\frac{1+\omega\xi}{\rho}$	Linear
$1-X_iX_j$ $1-(1-X_i)(1-X_j)$		YES*	$\frac{1+\frac{\xi\omega}{\xi+1}}{\rho}$	Linear
$1-X_iX_j$ $(X_i-X_j)^2$	AFND model [Example 5, p. 49]	YES*	$\frac{1+\frac{\xi\omega}{\xi+1}}{\rho}$	Linear
$1-X_iX_j$ $1-(X_i-X_j)^2$		YES*	$\frac{1+\omega\xi}{\rho}$	Linear
$(1-X_i)(1-X_j)$ X_iX_j		YES*	$\frac{1}{\rho}$	Linear
$(1-X_i)(1-X_j)$ $1-X_iX_j$		NO	$\frac{1}{\rho}$	Constant

(Continues on next page)

Rules (link-breaking) (link-creation)	Model name and appearance in literature	Always metastable	Lower bound on epidemic threshold	Upper bound on epidemic threshold
$(1-X_i)(1-X_j)$ $(1-X_i)(1-X_j)$		YES*	$\frac{1}{\rho}$	Linear
$(1-X_i)(1-X_j)$ $1-(1-X_i)(1-X_j)$	AID* model [Example 4, p. 48]	NO	$\frac{1}{\rho}$	Constant
$(1-X_i)(1-X_j)$ $(X_i-X_j)^2$	AID model [17]	NO	$\frac{1}{\rho}$	Constant
$(1-X_i)(1-X_j)$ $1-(X_i-X_j)^2$		YES*	$\frac{1}{\rho}$	Linear
$1-(1-X_i)(1-X_j)$ X_iX_j		YES*	$\frac{1+\omega\xi}{\rho}$	Linear
$1-(1-X_i)(1-X_j)$ $1-X_iX_j$		YES*	$\frac{1+\frac{\xi\omega}{\xi+1}}{\rho}$	Linear
$1-(1-X_i)(1-X_j)$ $(1-X_i)(1-X_j)$	ASIS* model [Example 2, p. 46]	YES*	$\frac{1+\omega\xi}{\rho}$	Linear
$1-(1-X_i)(1-X_j)$ $1-(1-X_i)(1-X_j)$		YES*	$\frac{1+\frac{\xi\omega}{\xi+1}}{\rho}$	Linear
$1-(1-X_i)(1-X_j)$ $(X_i-X_j)^2$		YES*	$\frac{1+\frac{\xi\omega}{\xi+1}}{\rho}$	Linear
$1-(1-X_i)(1-X_j)$ $1-(X_i-X_j)^2$		YES*	$\frac{1+\omega\xi}{\rho}$	Linear
$(X_i-X_j)^2$ X_iX_j		YES*	$\frac{1+\omega\xi}{\rho}$	Linear
$(X_i-X_j)^2$ $1-X_iX_j$		YES*	$\frac{1+\frac{\xi\omega}{\xi+1}}{\rho}$	Linear
$(X_i-X_j)^2$ $(1-X_i)(1-X_j)$	ASIS model [9, 11, 17, 20]	YES*	$\frac{1+\omega\xi}{\rho}$	Linear
$(X_i-X_j)^2$ $1-(1-X_i)(1-X_j)$		YES*	$\frac{1+\frac{\xi\omega}{\xi+1}}{\rho}$	Linear
$(X_i-X_j)^2$ $(X_i-X_j)^2$		YES*	$\frac{1+\frac{\xi\omega}{\xi+1}}{\rho}$	Linear
$(X_i-X_j)^2$ $1-(X_i-X_j)^2$		YES*	$\frac{1+\omega\xi}{\rho}$	Linear

(Continues on next page)

Rules (link-breaking) (link-creation)	Model name and appearance in literature	Always metastable	Lower bound on epidemic threshold	Upper bound on epidemic threshold
$1-(X_i-X_j)^2$ X_iX_j		YES*	$\frac{1}{\rho}$	Linear
$1-(X_i-X_j)^2$ $1-X_iX_j$		NO	$\frac{1}{\rho}$	Constant
$1-(X_i-X_j)^2$ $(1-X_i)(1-X_j)$		YES*	$\frac{1}{\rho}$	Linear
$1-(X_i-X_j)^2$ $1-(1-X_i)(1-X_j)$		NO	$\frac{1}{\rho}$	Linear
$1-(X_i-X_j)^2$ $(X_i-X_j)^2$		NO	$\frac{1}{\rho}$	Linear
$1-(X_i-X_j)^2$ $1-(X_i-X_j)^2$		YES*	$\frac{1}{\rho}$	Linear